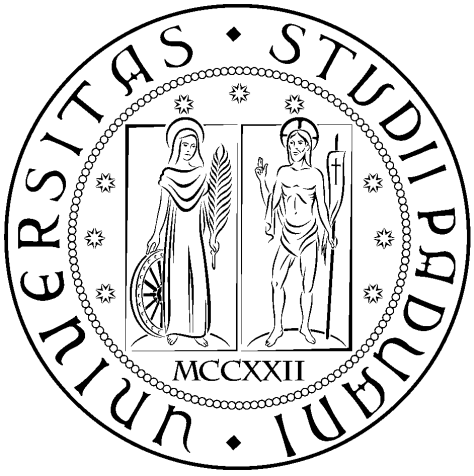

University of Padua
INDUSTRIAL ENGINEERING
DEPARTMENT

Master Level Degree Thesis

in Mechanical Engineering

EXPERIMENTAL EVALUATION OF THE STRUCTURAL PROPERTIES OF INNOVATIVE BIOMATERIALS

Supervisor: ***Prof. Eng. Nicola Petrone***

Co-supervisors: ***Tiziana Martinello***

Prof. Roberto Meneghello

Student: Giacomo Cavazzano

ACADEMIC YEAR 2013-2014

INDEX

Alla mia famiglia...

PART ONE

CHAPTER 1

Tendons: structure and decellularization treatments.

1.1-Introduction.

Tendons possess a poor capacity of regeneration and the scar that forms at the site of the injury causes an alteration in the mechanical properties due to the non-alignment of collagen fibers and to an alteration of the composition of the extracellular matrix.

Tendon lesions often become debilitating injuries affecting the quality of life of patients since they do not lead to a restitutio ad integrum; infact, it is important to note that current repair techniques have a number of limitations and do not provide a functional recover of the damaged tendon.

One answer to these problems may be given from tissue engineering that offers innovative high therapeutic potential in replacement of the classical techniques.

The aim of tissue engineering, in this case, is to substitute the completely damaged tendon through a bioscaffold, obteined from cadaveric tendon tissue the production of extracellular matrix and its organization into a functional tendon tissue.

The use of human biological scaffold is more interesting than synthetic ones, as far as the former has can't still maintains the native tendon mechanical properties, biocompatibility and biofunctionality.

An in vitro tendon scaffold was obtained from human tendon using a technique that eliminates the cells present in the native tissue, and this is essential to avoid problems of antigenicity in future clinical application. The decellularization technique, which will be later described, however, should not damage the structure of the matrix will change orientation of the collagen fibers.

To increase the regeneration of tendon, stimulating cellular migration and production of endogenous growth factors endogenous growth factors, it is important that the scaffold is injected with autologous mesenchymal stem cells.

The recellularization is used to recreate a healthy tissue and similar to initial conditions and suitable for eventual transplantation into a recipient, where the essential

problem is the rejection due to the presence of non-autologous cells.

A rich and readily available source of stem cells is adipose tissue, and these adult mesenchymal stem cells isolated from patients, are used to recellularize the decellularized scaffolds tendon. After the recellularization the structure of the tendon is not compromised, and that it is therefore a good starting point for obtaining a natural biocompatible scaffolds.

The overall aim of this thesis is to mechanically test the healthy tendons and tendons subjected to a decellularization process. In other words, the study has verified if the treatments reduces UTS or elastic module, and thus if there is a inevitable impairment of the scaffold.

The study might be extended in a second time step in order to check mechanical properties after the ricellularization process.

1.2-Macroscopic structure of tendons.

Tendons are an important part of a joint and their position is usually between muscles and bones. The force created by the muscle is transmitted through tendons to the bones, making joint movement possible. A muscle has regularly an origin and an insertion, that indicate respectively the proximal and the distal points; and because muscles basically have two tendons, the latter occupy these two points. The point of union with a muscle is called a myotendinous junction (MTJ) and the point of union with a bone an osteotendinous junction (OTJ).

Healthy tendons are brilliant and have a pearl color; to a closer it can be seen the fibrous structure of the scaffold, which is the structural part of tendons and has a great resistance to mechanical loads. The shape and the way they are attached to the bone may vary considerably; in fact, depending on the function and on the body position, tendons can range from wide and flat to cylindrical, fan-shaped and ribbon-shaped tendons.

Muscles designed to create powerful and resistive forces, like the quadriceps and triceps brachii muscles, have short and broad tendons; instead those that have to perform subtle and delicate movements, like the finger flexors, have long and thin tendons.

Friction is reduced by the surrounding structures which guide the tendon during its gliding, also avoiding tendons impairment. Five categories can be distinguished.

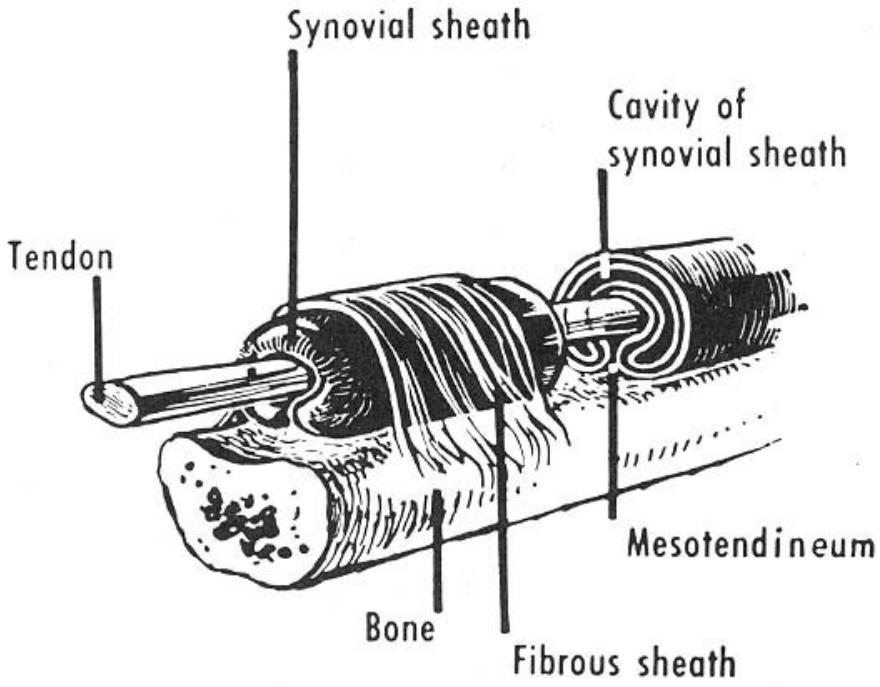

Figure 1.1: External layer of a tendon.

The *fibrous sheaths* or retinacula are the external layer of the canals through which the tendons glide, especially the longest ones. The grooves and the notches are usually lined with a fibrocartilaginous floor and covered with the fibrous sheath or retinaculum. Where the tendons curve, due to the joint shape, the fibrous sheaths have a reinforcement structure named *reflection pulley.*

The *synovial sheaths* are access tunnels for tendons to bone surfaces or other anatomic structures that might cause friction, wrapped mostly around the tendons of hands and feet. Under a fibrous layer, there are two thin and serous sheets, the parietal and visceral sheets. These sheets form a closed duct including peritendinous fluid for lubrication. In some tendons, for instance Achilles tendon, which do not have a true synovial sheath, there can be a *peritendinous sheet* (paratenon) to reduce friction. It is composed of loose fibrillar tissue and it works as an elastic sleeve permitting free movement of the tendon against surrounding tissues. The *tendon bursae* are the fifth extratendinous structure playing an important role in the reduction of friction. They are located in those anatomic sites where a bony prominence might otherwise compress and wear the gliding tendon.

1.3-Paratenon, epitenon and endotenon.

Except for some places in feet and hands, tendons are mostly surrounded by loose areolar connective tissue called paratenon. The above-described double-layered tendon sheaths can only be found in the areas where a change of direction and increase in friction necessitate very efficient lubrication.

Paratenon works as an elastic lubrificating sleeve, but less than a true tendon sheath.

Under the paratenon, the entire tendon is wrapped in a fine connective tissue sheath called epitenon.

On its outer surface, the epitenon is contiguous with paratenon, together forming the peritendon. The next inner layer is called endotendon, that wraps each tendon fiber and binds individual fibers in larger units of fiber bundles.

Along with its important function of binding, the endotenon network allows the fiber groups to glide on each other and carries blood and lymphatics vessels and nerves, to the deeper portion of the tendon.

1.4-Microscopic structure of tendons.

As in Figure 1.2, collagen (mostly type I) and elastin, that are embedded in a proteoglycan-water matrix, are the main components of tendons. Collagen is about the 65–80% and elastin approximately 1–2% of the dry mass of the tendon. These two elements are produced by tenoblasts and tenocytes, which are the elongated fibroblasts and fibrocytes that lie between the collagen fibers and are organized in a complex hierarchical scheme.

Soluble tropocollagen molecules form cross-links to create insoluble collagen molecules, which then aggregate progressively into microfibrils units clearly visible to a electronmicroscope, called collagen fibrils. The basic unit of a tendon is the primary fiber bundle, which is a bunch of collagen micro fibrils. A collagen fiber is the smallest tendon unit visible using light microscopy and is aligned from end to end in a tendon. A fiber also represents the smallest collagenous structure that can be tested mechanically, although a larger fiber bundle makes the testing more reliable.

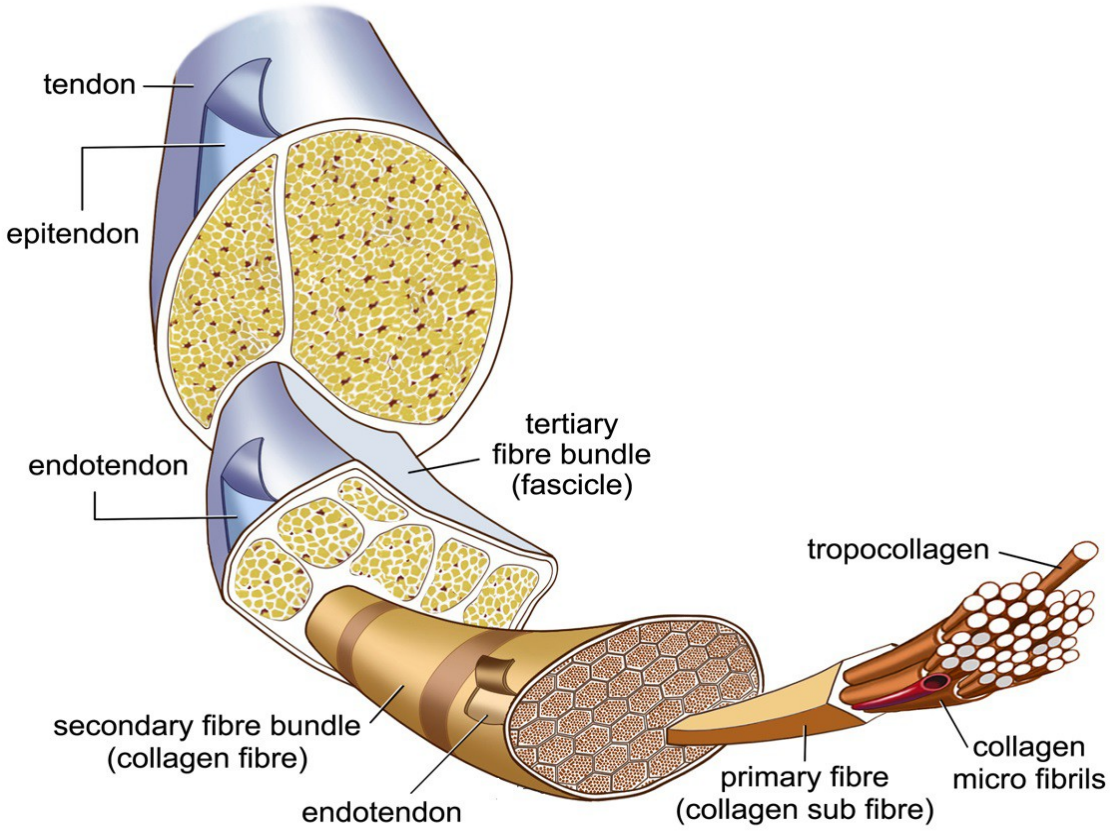

Figure 1.2: Structural organization of the fibers.

A bundle of collagen fibrils, that have a diameter that varies from 20 nm to 150 nm, forms a collagen fiber. A fine sheath of endotenon connective tissue invests each collagen fiber and binds fibers together. A bunch of collagen fibers forms a primary fiber bundle (subfascicle), and a group of primary fiber bundles forms a secondary fiber bundle (fascicle). As before, a group of secondary fascicles forms a tertiary bundle and then at last the tertiary bundles make up the tendon surrounded by the epitenon. In human tendons, the diameter of the tertiary bundles varies from 1000 μm to 3000 μm. The diameter of the secondary bundles ranges from 150 μm to 1000 μm.

Subfascicles has instead a diameter between 15 and 400 μm.

1.5-Tendon decellularization treament.

The tendon samples stored in sterile tubes and kept in saline solution are cleaned under

the aspirator, in a sterile environment, from the possible presence of tendon sheath, connective muscle insertions or excerpts.

Then the samples are subjected to 5 cycles of freezing and thawing, respectively, in liquid nitrogen and 37 ° C.

Subsequently whole tendons were immersed in hypotinic solution (10 mM TRIS pH 8) with two proteases inhibitor: leupeptin (1mg/ml), phenylmethylsulfonyl fluoride (100 mM) and EDTA (Ethylenediaminetetraacetic acid) 0.1% for 48 hours at a constant temperature of 37 ° C and under stirring.

After the inactivation of endogenous protease sample tendon is decellularized using a hypotonic solution with 1% SDS (Sodium Dodecyl Sulphate) for 48 hours at constant temperature of 37 ° C under stirring.

After 3 washes in PBS 1X (Phospate buffered saline), to eliminate the presence of SDS, the tendon is sterilized for 5 hours by UV rays.

The scaffold thus prepared may be kept at a constant temperature of 4 ° C in saline.

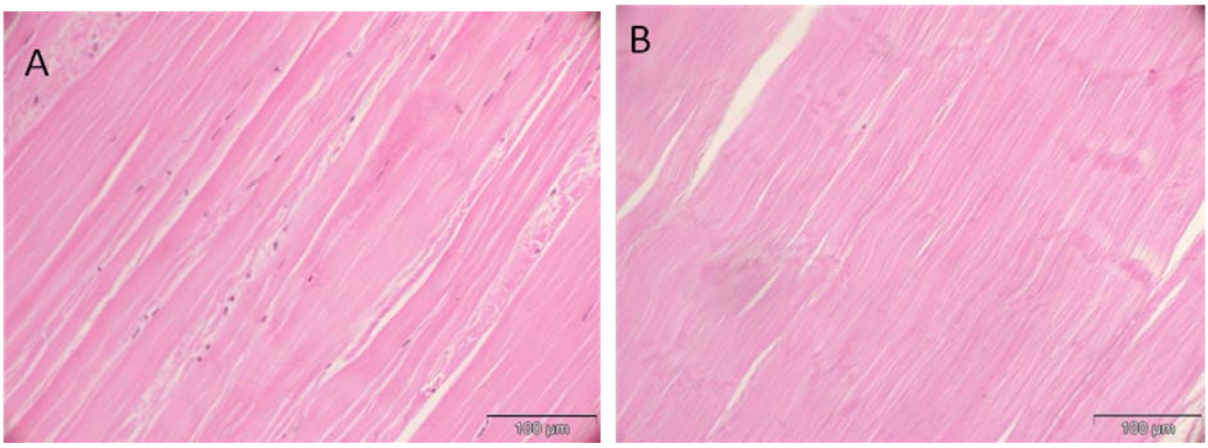

Figure 1.3: In the two figure can be notice the tendon matrix of a normal tendon (A) and of a decellularized one (B). The matrix in the second image is still compact.

1.6-Rational of the project.

The study has the aim to quantify the variation of the biomechanical characteristics such as strength and stiffness of human tendon scaffold first thawed, then decellularized and finally recellularized to allow compatibility with a receiving body in an eventual transplantation.

The determination of the characteristics will be made through axial tensile tests and repeated for different scaffolds. The scaffold must be done by comparing between them, especially to determine if substantial changes are recorded on those who suffer decellularization and reengagement.

1.7-Overview.

INDEPENDENT VARIABLES

The main variable of the study will be the type of scaffold to study, in fact, it undergoes several treatments, so you will have to figure out how to change the mechanical properties of the scaffold at various stages of the process.

The stages involved are:

- freshly drawn;
- thawed;
- decellularized;
- recellularized;

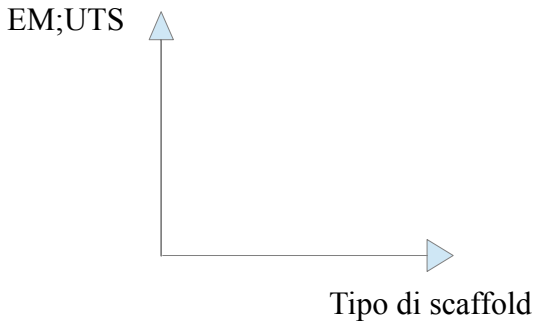

DEPENDENT VARIABLE

The main variables to be quantified are the elastic modulus (EM) and the ultimate tensile strength (UTS). These must be calculated from the experimental curves but using force diagrams (measured in Newtons)/displacement (in mm), but since the elastic modulus is obtained from the curve stress-strain, will be measured the net section of the tendon and tis length.

The relations are used:

$$\sigma = F / A \quad ;$$
$$\varepsilon = \Delta L / L_0 \quad ;$$

In the case of perfect linearity the calculation of the stiffness is simple and immediate, it coincides with the slope of the line on the graph stress-strain, in this case, the tendons have not ideal behavior, therefore the calculated curves have trend almost straight but will be implement the calculation of the module via alternative methods, such have the point of null second derivative.

CHAPTER 2

Mechanical properties of a generic material and tendon tissue.

2.1 Introduction.

While talking about properties of a material, is interesting to define the response to a certain kind of solicitation: electrical properties for electric inputs, chemical propieties for chemical reagents, etc...

Mechanical proprieties of a material means the response to a mechanical stress (concentrated forces, pressures, displacement, etc...). Two samples of different material but with same geometry, will respond differently if they undergo to the same loads and the same way of application.

Hence, will be generated stresses and strains along all the samples, but their magnitude will be different for each sample. The material plays a big role in defining the level of displacements of a body that is loaded with given forces, and vice versa.

Material can be classified in five categories:

- INHOMOGENEOUS: if these properties vary from point to point;
- HOMOGENEOUS: if mechanical properties don't depend on the location;
- ANISOTROPIC: if, focusing on a single point, material properties change depending on the direction considered;
- ORTOTROPIC: if , referring to the previous situation, three axes of symmetry can be individuated;
- ISOTROPIC: if the properties do not vary with the direction.

2.2 Elastic and elastoplastic behaviour.

Forces are absolute quantity, in fact they don't depend on bodies geometry or mechanical properties, but on an external action.

The force-displacement or the stress-strain curves can both be plotted, but only the latter expresses an unique relationship between samples that have different dimensions.

The law used while studing a stress-strain diagram are:

$$\sigma = F / A = Stress \quad ;$$
$$\varepsilon = \Delta L / L_0 = Strain \quad ;$$
$$\Delta L = L - L_0 = Displacement \quad ;$$

where F is the force applied to the sample tips, L_0 is its initial length and A is its section.

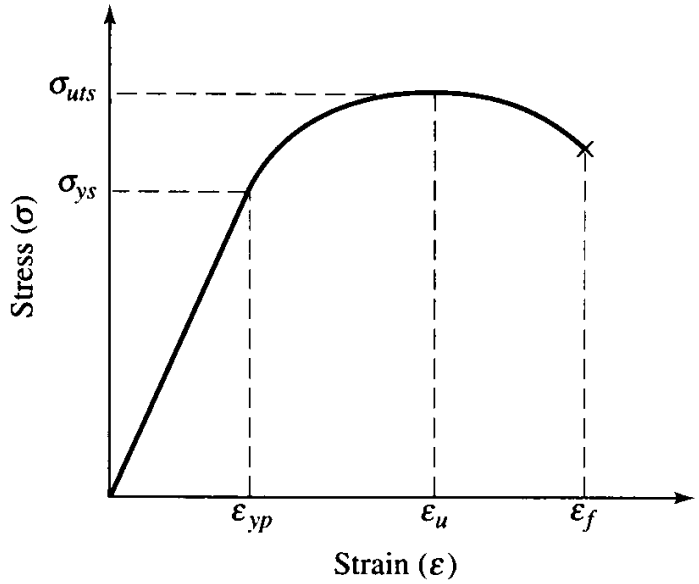

Figure 2.1: Example for stress-strain curve for an elasto-plastic material, during a traction test.

Hence, while the force is constant, a section increment implies a stress decrement and vice versa. This means that a bigger section can undergo to a bigger force before the sample rupture.

A typical traction diagram for elasto-plastic materials, such as for quite all metals, is represented in Figure 2.1; while stresses are under a certain value, the sample behaviour is strictly elastic. This implies a perfect return to the initial geometry conditions and a linear relationship between stress and strain, given by the law:

$$\sigma = E \cdot \varepsilon \quad ;$$

where E is called Young (or elastic) module, graphically it can be individuated as the curve first part slope.

Over a certain stress value, the yield stress (σ_{ys}), the deformation is no more reversible; the sample is deformed definitively, except for the elastic component that disappear once the force is removed. This is called plastic behaviour and microscopically it is due to internal infinitesimal damages.

Another important stress value is the ultimate tensile strength's stress (σ_{uts}), which is the maximum stress bearable by the sample. Though the rupture occurs for a determined value of strain (ε_f = final strain) to which correspond a σ_f (final stress), the latter is smaller than σ_{uts}. This happens because during the traction and for strains over ε_{uts} the behaviour is still plastic but occurs the necking, in which the section becomes smaller and smaller.

The fragile materials behaviour is just linearly elastic, it doesn't present a yield point and has no plastic region; this means that the rupture occurs after a certain value of stress, suddenly and without forewarning. In this case σ_{uts} and σ_{ys} coincide.

2.3 Viscoelastic behaviour of a material.

In some case, the response of a material depends on how an applied force varies in time; this is a viscous behaviour. Particularly interest is given to the viscoelastic behaviour.

To show the characteristic, can be useful a comparison between a behaviour elastic and the viscoelastic one, for hypothetical condition of stress application.

When $t = t_{0,}$ the same stress σ_0 is generated to both the samples and hold constant until $t = t_1$; then the stress is removed. For an elastic sample the response is well-known: instantaneous strain to ε_0, constant from t_0 to t_1, then complete restoration of initial conditions.

For the viscoelastic material after an initial strain of ε_0, the sample continue to elongate (ε increase with time) until the stress is applied; when $t = t_1$, there will be a partial return of ε_0; but the complete restore occurs only trough time.

A daily life example could be the behaviour of a plastic wire that, loaded with a

constant force, elongates continously, excpecially if the temperature is high.

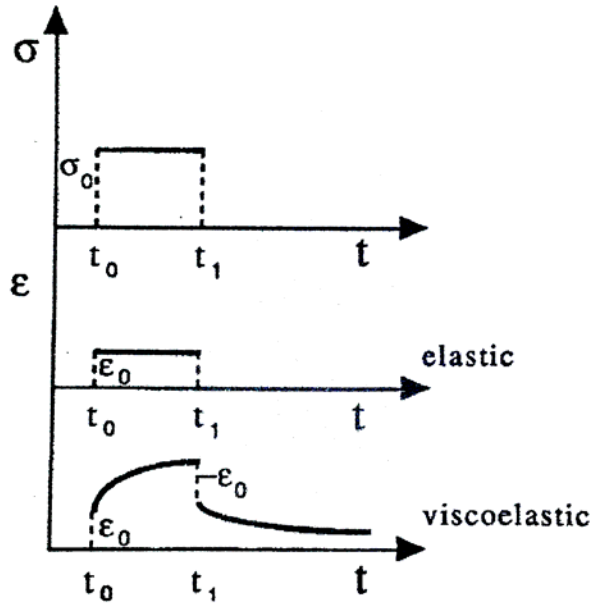

Figure 2.2: Viscoelastic response to a single stress.

An observation is needed: the response of a viscoelastic system depends both on time and stress history. This means that, for instance, if are applied two stress consequentially, one (σ_0) between t_0 - t_1 and a twofold stress in the time lapse $t_2 – t_3$, then:

- if the first elongation is not totally restored, the new elongation will start instantly as a sum of the initial position plus the elongation $2\varepsilon_0$ due to the second stress ($2\sigma_0$). Then the sample continues with its natural course as former described;
- if the second stress is given while the first strain is completely recovered, then the behavior is identical to the first case except for the module that is twice ε_0, because of the second stress $2\sigma_0$.

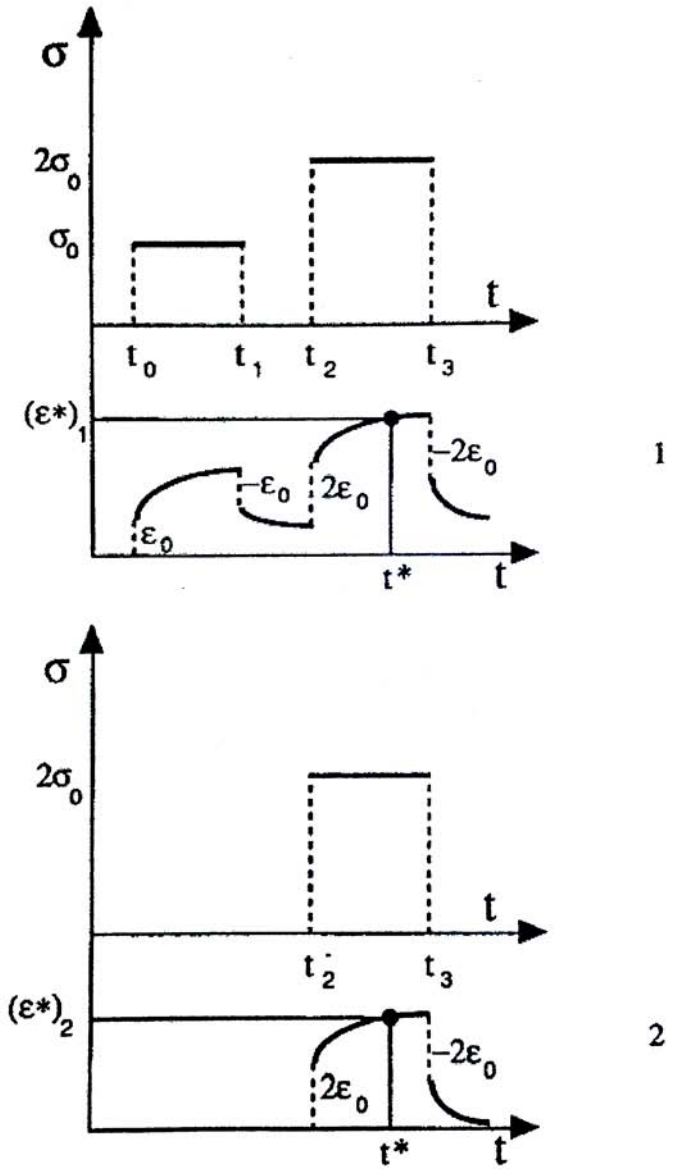

Figure 2.3: History dependency of viscoelastic behaviour.

The strain induced on the sample can be briefed by the law:

$$\varepsilon = function(\sigma, time) \quad ;$$

Linear viscoelasticity happens when there's a direct proportion between ε_0 and σ_0, expressed by:

$$\varepsilon = \sigma \cdot function(time) \quad ;$$

In this case can be defined the creep compliance (C(t)), characterizing the viscoelasticity.

Creep test consists in a load application to a sample, recording the elongation trough

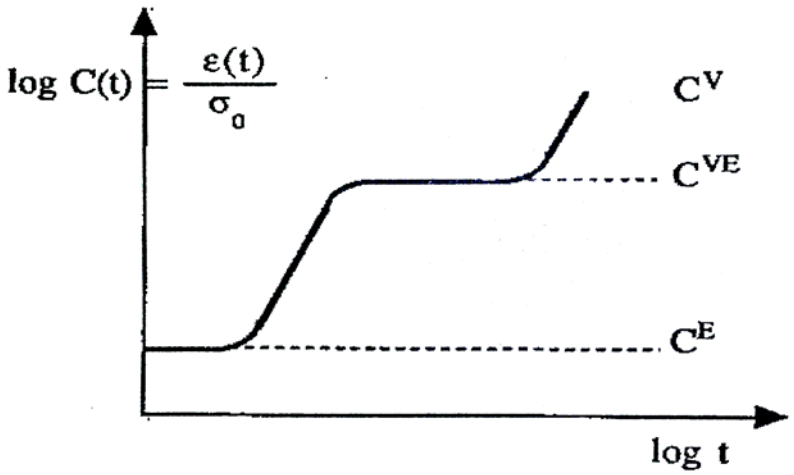

Figure 2.4: Creep compliance; C^E : elastic component; C^{VE} : viscoelastic component; C^V : viscous component.

time (then ε). Creep compliance is the ratio between measured strain and stress applied, intrinsic characteristic of the material.

To understand how, under a constant load, the sample can elongate progressively trough time, is useful to individuate the microstructural mechanism responsible of this undefined deformation (always referring to plastic materials).

An amorphous polymer can be represented as a tangle of macromolecules; a stress in elastic range causes a relative displacement of macromolecules, that is recovered the once the load is eliminated (elastic ε).

If temperature is high enough, some wider movements are possible; they can show themselves as the time passes by: macromolecules, in a lapse of time, tend to reach a new stable configuration (viscoelastic ε); in another time period they return to initial situation once the system is unload. Furthermore in some conditions of material and temperature, relative movement can indefinitely proceed, as if macromolecules glide one near each other under stress application.

The mathematical model of a viscoelastic behaviour can be represented as a

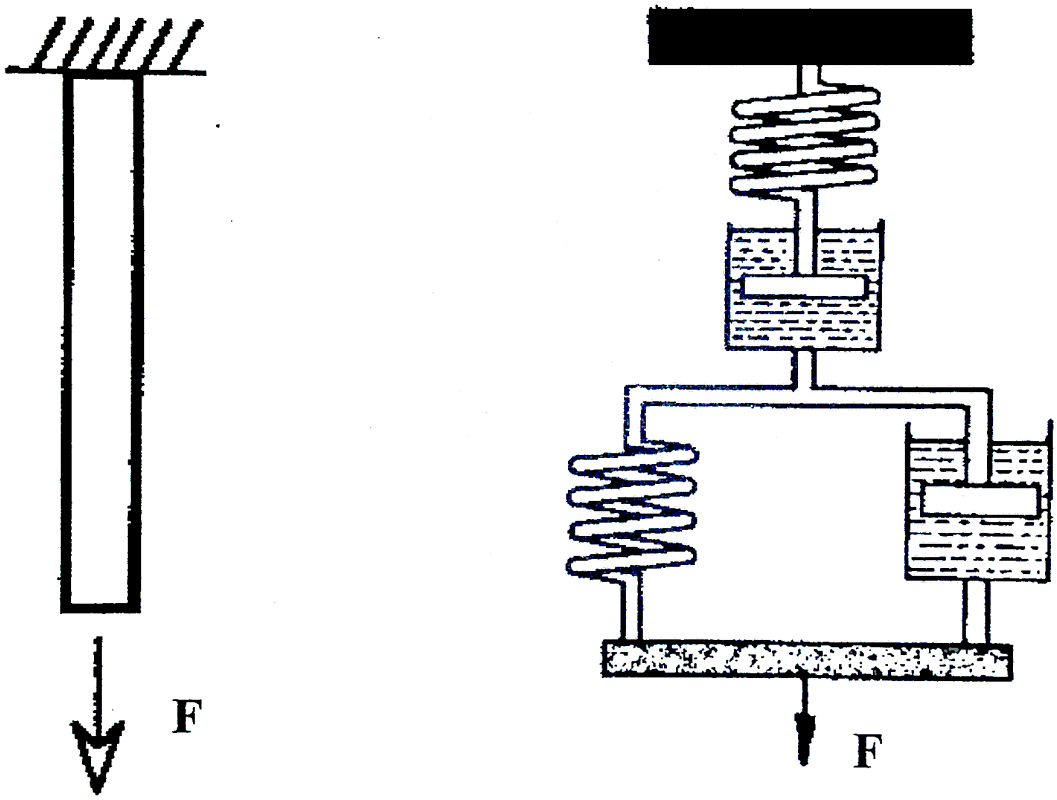

Figure 2.5: Sample which undergoes to a load F and rheological model.

rheological model.

It's a combination of mechanical impedances (springs and newtonian dashpots); thay can be placed differently and in several combinations, using parallel and serial configurations. This particular rheological model integrates both Maxwell and Kelvin-Voigt models.

If a solicitation (τ) is applied, both models are affected equally. Deformation of rheological model, instead, is given by the sum of the deformation of both models.

Then:

$$\gamma = \gamma_e + \gamma_v + \gamma_r \quad ;$$

where $\gamma_e + \gamma_v$ is given by $\tau \cdot (\frac{1}{G} + \frac{t}{\eta})$ (G is shear modulus; η is the viscosity); γ_r is

the delayed deformation of the Kelvin-Voigt model $\gamma_r = \frac{\tau}{G} \cdot \left(1 - e^{-(t \cdot (\frac{G}{\eta}))}\right)$; finally:

$$\gamma_{tot} = \frac{\tau}{G} + \frac{\tau}{\eta} \cdot t + \left[1 - e^{-(t \cdot (\frac{G}{\eta}))}\right] \quad ;$$

2.4 Load curve model for tendon and ligament tissue.

The tendons are tissue with anisotropic behaviour; analysis of the load-elongation curve can highlight characteristics of non-linear viscoelasticity, however markedly influence by the speed of deformation. The detailed examination of the structural properties of tendon and ligament tissues is conducted through tensile tests, usually at constant speed.

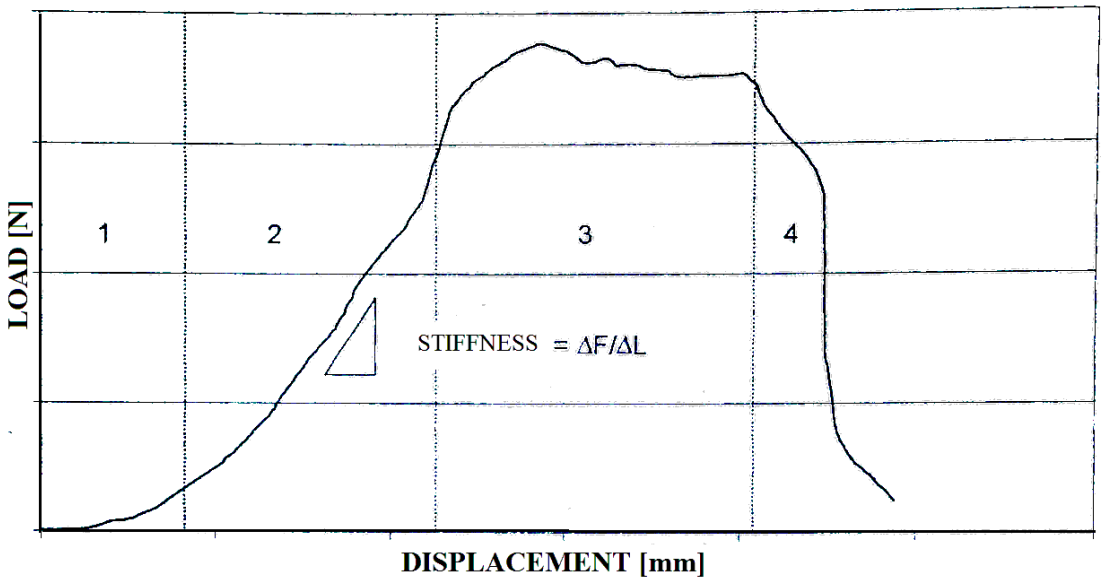

Figure 2.6: Qualitative trend of the Load-Displacement curve for a tendon tissue.

Conventionally, the structural properties refer to the load-elongation curve, while the mechanical properties of the curve taken as reference is the one that shows the trend of the stress in function of the strain.

The trend of a typical load-d curve for a tendon tissue is shown in Figure 2.6. Four zones can be recognized. The first portion of the curve is usually called the "toe region", where there is a trend highly non-linear, due, on a microscopic scale, to the stretching of the wavy pattern in which the fibers are originally arranged. As the applied load increases, the number of fibers, which have become almost straight, while they all have completely lost the wavy pattern, the response becomes more linear (second part of the curve). For higher loads involved there are microstructural damage (third section) until reaching the last portion of the curve when the tendon rupture occurs.

Figure 2.7 shows the stress-strain curve with the qualitative indication of the region of physiological functioning. In most cases, the interest is directed to the first two sections of the load-elongation curve, though the physiological functioning rarely carries the load level over the second part.

Furthermore, the value of stiffness of the tendon is obtained by examining the second portion of the curve.

The above described events can explain perfectly why the tendon tissue (or any other biological tissue) has a viscoelastic behaviour. This is manifest in the time dependent aspect

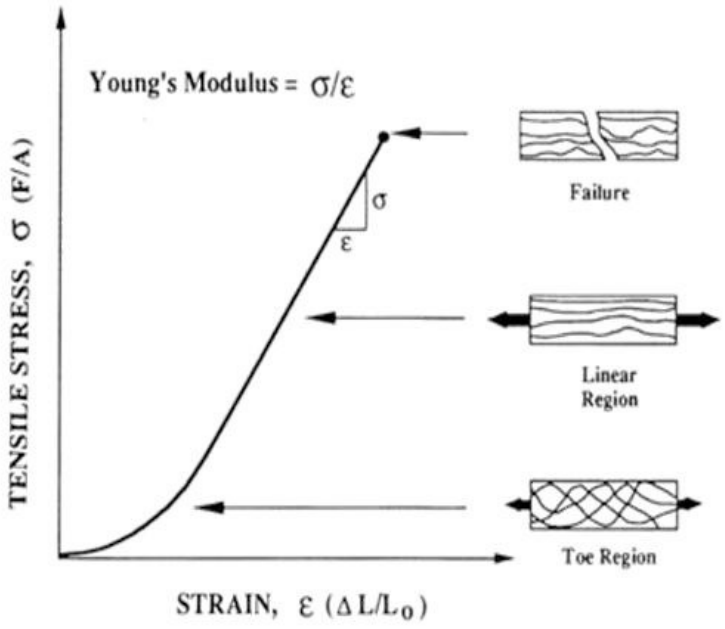

Figure 2.7: Results of the stress-strain curve for a tendon tissue; note how the micro-structural damage affecting gradually more and a greater number of fibers up to the complete breakdown of the structures.

of the material response, in damping of vibrations and in the attenuation of waves including those used in clinical diagnostic ultrasound. The viscoelastic behaviour of biological materials is due to various interactions of collagen with the proteins, water, and ground substance when it is loaded. As this is a rate dependent phenomenon, a material will respond differently if quickly loaded as opposed to a slower loading.

The slope of the stress–strain curve will increase with an increasing strain rate (Fig. 5), and the apparent elastic modulus, the constant of proportionality relating the strain to the stress, will increase accordingly. If a viscoelastic material is stretched to a constant deformation, it will slowly relax, with the stress in the material decreasing. A relaxation curve

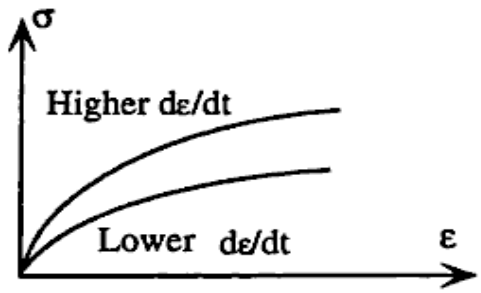

Figure 2.8: Dependence of the stress-strain curve on the rate of deformation of a viscoelastic test specimen.

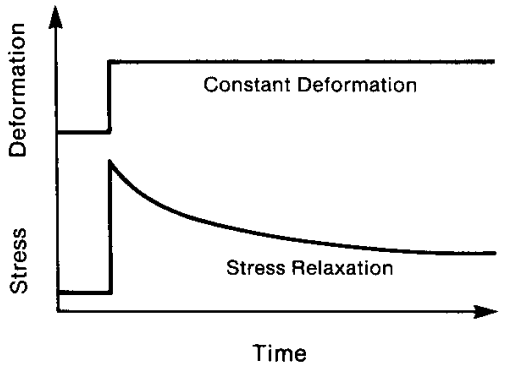

Figure 2.9: Trend of the stress subjected to a constant and impulsive deformation.

is a plot of the viscoelastic stress versus time response (Fig. 2.9).

CHAPTER 3
Experimental Equipment.

3.1 Introduction.

In the study of samples of tendons must ensure a good grip of the scaffold on the machine. To do this it was necessary to design a new system of aluminium grips that acts as an interface between the soft tissue of the tendon and the machine for axial test.

This is precisely the delicate point of the project, as the system has been designed with two pairs of notched plates so that the specimen could be hold tight by the tips.

A too high clamping pressure may cause the cutting of the sample; if it is too low, the specimen is likely to slip between the two plates. In both cases, the test is invalid and the greatest risk is that the specimen is damaged.

Also the availability of samples is definitely another weakness of the project, as they come from human donors.

With these assumptions, it becomes peremptory, then, make sure to develop a good technique before proceeding with the study of the human scaffold specimens to avoid invalidation of the tests and increasing the infallibility of the method.

This chapter aims to describe the equipment used in performing the test and the method used, as well as illustrating the result of design that led to the creation of two grips to be used on the traction machine MTS 858 MiniBionix II at the DIM - University of Padua, or any similar machine that uses a pair of hydraulic clamps.

3.2 Specimens section instrument.

The cross section of the tendon is measured using a system of movable cursor. It has a rectangular slot 4.1 x 7.25 mm and provided with a dial test indicator in contact with the plate of the load. The principle of the operation is similar to that for the tool shown in Figure 3.1. The plate is loaded in such a way as to develop a constant pressure of 0.12 MPa sufficient to

produce the squashing of the scaffold. The degree of the squashing tends to increase over time due to the viscoelasticity of the collagen tissue. Conventionally it need to pass two minutes, after which there is an indication of the dial gauge, representative of the tendon thickness less than an offset of zero. The multiplication of the measurement made for the width of the slot gives the value of the cross section.

The measurement is performed over the entire length (head gripping excluded) of the specimen, that is the central 15 mm of the sample. It must be calculated an average of the measurements thus obtaining the final value of the cross section that shall be used for the calculation of rated stresses.

The dial indicator (Mitutoyo IDU 25) is placed above the plate. The cursor of the indicator, which has a internal spring, need to be placed on the center of the section measurement system plate (Figure 3.2).

Figure 3.1: Plunger system that allows to calculate the cross section of the sample.

Figure 3.2: It can be noticed the positioning of the dial indicator, which must measure the displacement at the center of the plate.

The detailed description of the measurement procedure is postponed to the next chapter.

3.3 Clamping system.

A similar study of the cruciate ligaments has already been done in the laboratories of the University of Padova. However, it was performed the redesign of the entire functional test equipment, according to the requirements of repeatability, because the instrumentation already designed could be partially reused.

While in the older project the specimens length were much more higher, the new gripping system has been completely redesigned to be able to measure the biomechanical

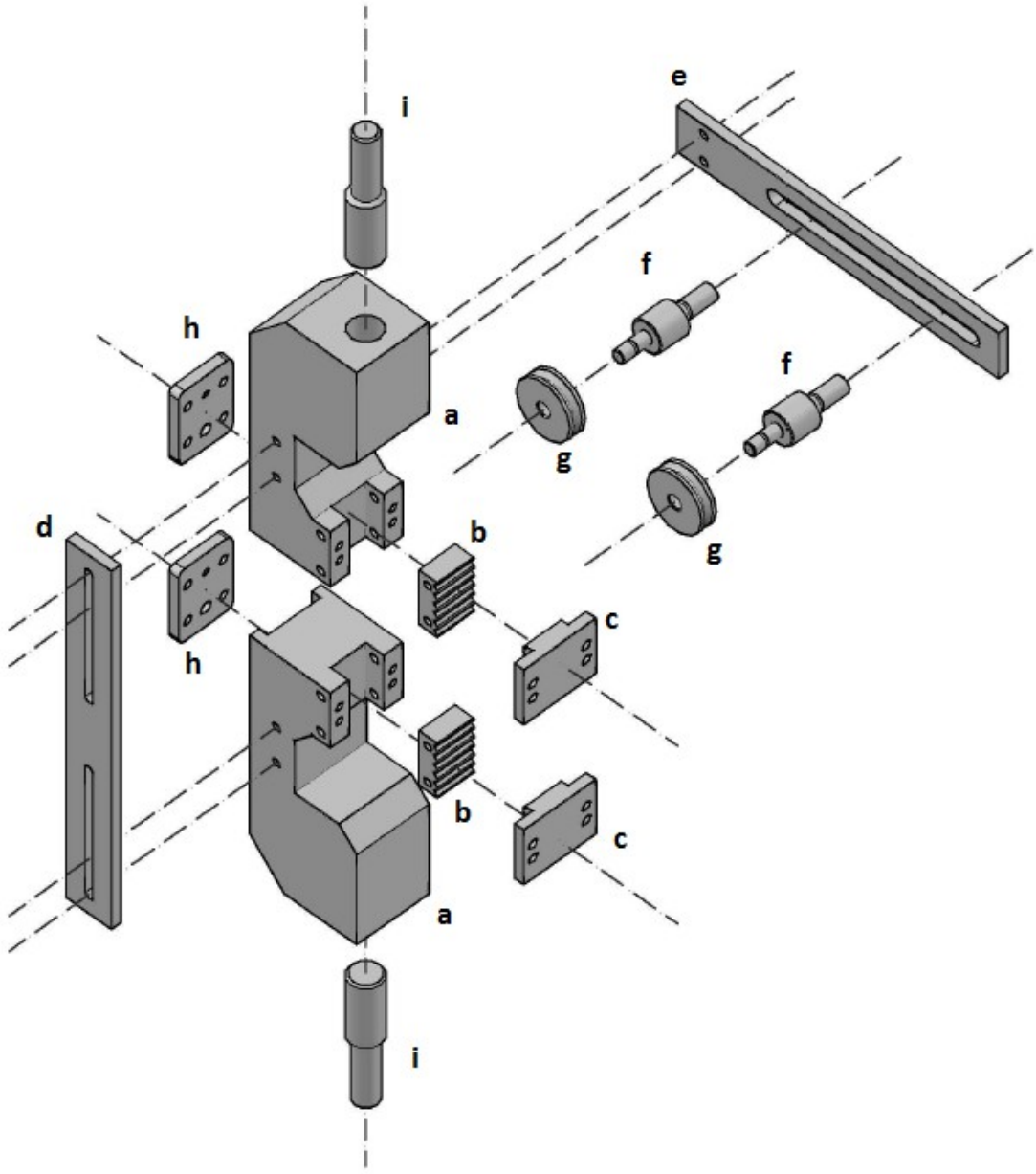

Figure 3.3: Exploded view of the clamping system.

properties of shorter tendons.

Keeping the design criteria previously used, the system looks like in figure 3.3.

The clamps consist of two main bodies (a), that present a C-shape to maintain aligned the machine and the specimen axes. On the front face they have a cavity in which will be located the fixed plates (b); these are interfaced with a removable couple (c), which clamps the scaffold. Both pairs of plates are notched to allow the increase the grip.

On the back of the main body, is hollowed the coolant chamber (Fig. 3.4), in which the liquid nitrogen will flow. To allow a constant flow of nitrogen, the chamber is covered with a double hole lid (h); trough brass fittings it is possible to connect clamps to the nitrogen

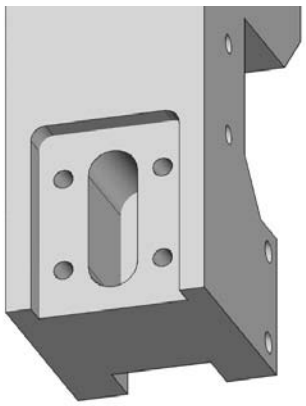

Figure 3.4: Particular of the cooling chamber at the rear of the main body.

cylinder.

Obviously the nitrogen flow will be regulated using the valve of the cylinder and it is expected that it will not be exaggerated in order to avoid the whole freezing of the tendon.

Particular care has been paid to the problem of the tendon alignment to the action axis of the machine, in order to avoid the interfering non-tensile components that are useless for the purposes of the study. In this regard the main body has been shaped so that the axis of the pins (i), which will be gripped by the machine, is alligned with the axis of the sample; also was prepared an aligner rod (d) that will allow comfortably and in total safety tendons fixation between the plates when the system is already mounted on MiniBionix. The pulleys formed by rollers (g), pins (f) and rod spacer (s) will allow the pre-tensioning of the tendon in order to stretch the fibers before. This shrewdness eliminates the initial toe region on the stress-strain graph.

Please refer to the next chapter for the placing procedure of the specimen and the mounting on MiniBionix.

3.4 Equipment made in the DIM - University of Padua.

Following the project described above, has been reproduced ex novo the clamping system for the study on tendons.

The figure shows how the pieces are assembled and which kind of precautions have been taken, all the details are listed in the captions. Note that the figure show only one main body with its adjacent pieces. The whole assembled system is shown once putted on the MiniBionix.

The system is made of aluminum with a variable height of about 45 cm and a weight of about 2 kg. The choice of material has been conditioned by the need to keep the system as clean as possible and easy to handle.

The used screws are made of stainless steel that combine resistance to loads and corrosion.

Figure 3.5: Rear, front and left views of the main body. Note, in the rear view, the chamber for nitrogen.

Figure 3.6: On the back of the main body is first cut and then is put a sheet of insulating material; in the right photo is subsequently added the lid. A hole is used to the liquid nitrogen entry and the other to vent.

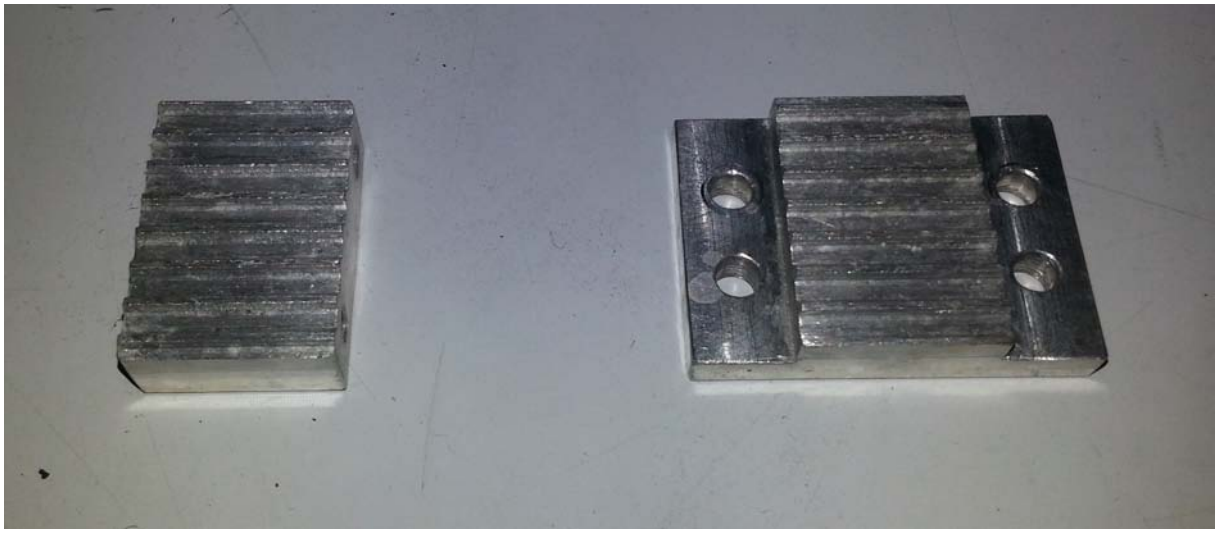

Figure 3.7: Notched plates; the left goes in front of the main body and the right one is removable.

Figure 3.8: Pulley system; used to align the tendon and for the pre-tensioning.

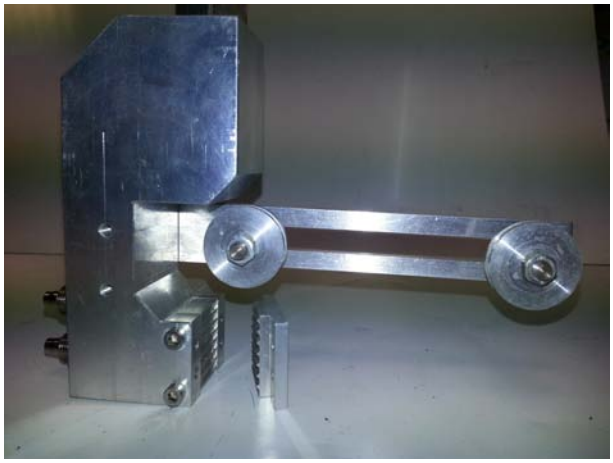

Figure 3.9: Upper assembled system. The removable plate is detached. The left pulley can move sideways to improve alignment.

3.5 - Refrigeration implant.

The clamps have been provided with a system for the nitrogen refrigeration. It has been used a Dewar (which is a typical insulated vase, often used for maintaining under a pressure of about 0.5 bar of nitrogen; approved by AirLiquide Italy).

The connection has been made with copper and brass fittings. Due to time constraints it was not possible to find flexible pipes, so the ducts used are made in Teflon that have a

good resistance at low temperatures. However because of the stiffness increase of the pipes, some precautions must be taken.

The fittings and ducts were covered with insulating material to prevent loss of refrigeration as shown in Figure 3.10.

Figure 3.10: Refrigeration plant. The white cylinder on the right is the nitrogen Dewar; on the bottom left there are the ducts; on the left upper corner the clamp system is connected to the Teflon insulated pipes.

When the structure is still at ambient temperature is necessary to wait about ten minutes to have an effective sub zero temperature on the plates. From that moment on, the system becomes operative.

Figure 3.11: Detail of the rear of the clamp; the insulated pipelines in Teflon bring the liquid nitrogen in the refrigeration chambers in which the vaporization occurs. Locally, the temperature is maintained around -6°C using the valve of the Dewar. Note the vent holes on the upper side of the lids.

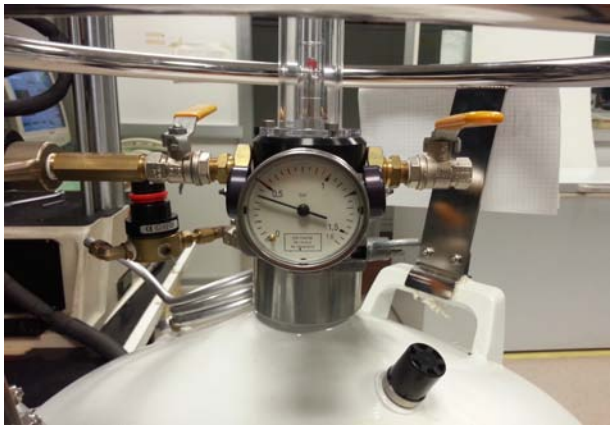

Figure 3.12: Particular of the valves and of the pressure (0,5 bar) gauge of the Dewar vase. The valve on the left allows the flow of liquid nitrogen, while the left (unused) allows the escape of vapours of nitrogen (warmer).

CHAPTER 4
Measuring methods.

4.1 Introduction.

This study tries to define a limit of stress sustainable by a connective tissue such as tendon, but can also be extended to other biological tissues and ligaments. In the literature, there are few sources that describe a standardized and precise method of measurement of the biomechanical properties of the tendons.

Here an attempt was to define a method that stresses tendons, describing aspects as much as possible. Considering that the mode of stress on the tendons of the human body in the everyday life, it is easy to understand that there is no unique method. Furthermore, the viscoelastic nature of the tendons adds more variables to the study, such as the speed of deformation.

However, there is still poor availability of human tendons, and the study has been simplified to slow deformations and probably unlikely (also because most of the ruptures occurs by high strain rate), but certainly more burdensome for the sample.

In these conditions are therefore considered almost exclusively the elastic properties of the tissues, thus being able to define simple but precise characteristics

The experimental procedure comprises basically two stages: preparation of the specimen in a first time and subsequently positioning on the machine that has already got the grips mounted on.

The first phase consists in defrosting and suturing the tendon samples that have a length of about 40 mm; the positioning is done through the pulley system. The suture made previously allows to be very accurate and to pre-tension the specimen before closing both clamps.

At the end of the preparatory stages, we will proceed with the static traction test. From the elaboration of experimental data, it will be possible to calculate maximum stress and elastic modulus and compare the data with those found in literature.

4.2 Suture on the tendon.

- Thaw the specimens given, that are stored at a temperature of -20°C. Wait until their temperature reaches a balance with the environment.
- Prepare the needle and the thread, they must not be absorbable by the organic tissues.
- Suture the sample. The suture should not be too invasive and can be done with the common sewing needle and thread. It is easy to pierce the tendon with the needle, then run a lap around to secure the thread at one end of the sample. Be sure to sew the wire so that when pulled straightens the specimen. Suture the specimen at a distance of about 5 mm from the head.

Figure 4.1: Sample sutured on a tip. The suture is useful for positioning on the clamps and eventually for pre-tensioning.

4.3 Section measurement.

- Put in a row the sutured samples and keep them under saline.
- Place the sutured tendons under the movable cursor, apply a load equal to a pressure on the tendon approximately 0.12 MPa. The magnitude of the load is variable in relation to the weight of the plate, the size of the slot and the action exerted by the indicator. After two minutes, read the value measured by the dial indicator.

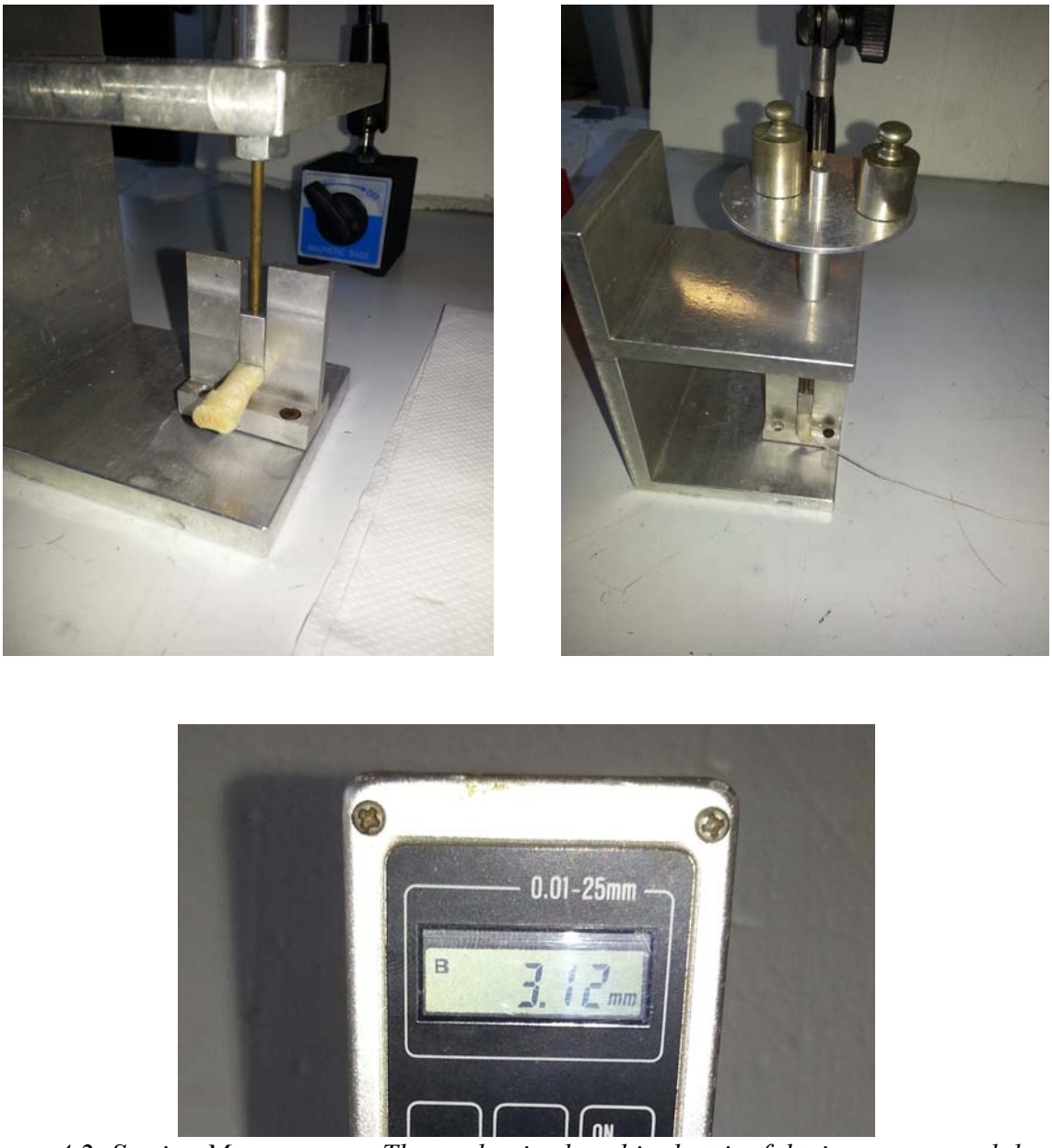

Figure 4.2: Section Measurement: The tendon is placed in the pit of the instrument and then is put on the plate light weight. On the dial indicator is shown the difference of height of the cursor (previously offset).

- Calculate the cross section by multiplying the width of the slot for the lowering of the indicator slider. Repeat the detection on length of the specimen. The cross section (CSA) of reference for the calculation and for the operations of grouping is the result of the average of the measurements performed.
- Replace the samples, in order of size, always in saline, making sure to keep them at room temperature before proceeding with the placement.

4.4 Positioning and refrigeration of the specimen.

- With the plates at room temperature, proceed with the positioning of the sample. The clamps are still open and the two main bodies spaced at 15mm. Via the pulley system, lower the sample, holding the suture, so as to place it at the center of the assembly. Place the movable bottom plate and screw it to the main body. Assure that the lower sample tip is alligned with the MTS action axis. The tightening torque must not exceed 4Nm for each screw, in order to avoid that the specimen is damaged.
- Apply to the thread, which was passed over the pulley, a weight of magnitude irrelevant but enough to stretch the specimen. Keep in mind that a greater weight would eliminate the toe region from the stress-strain diagram.
- Close the upper plate with the same criterion used for the lower one.
- If the clamps are still at ambient temperature, the nitrogen takes about ten minutes to bring the temperature of the plates below zero. Is eventually better to open the valve of the Dewar before, to optimize the time. With a digital thermometer check if the temperature to the plates is constant and don't make it drops too much. Because of the power of the nitrogen refrigerator, it should in fact prevent that the entire sample ices. To avoid test invalidation, use the valve as a flow regulator.
- Wait for the freezing of the tendon tips and then start the test.

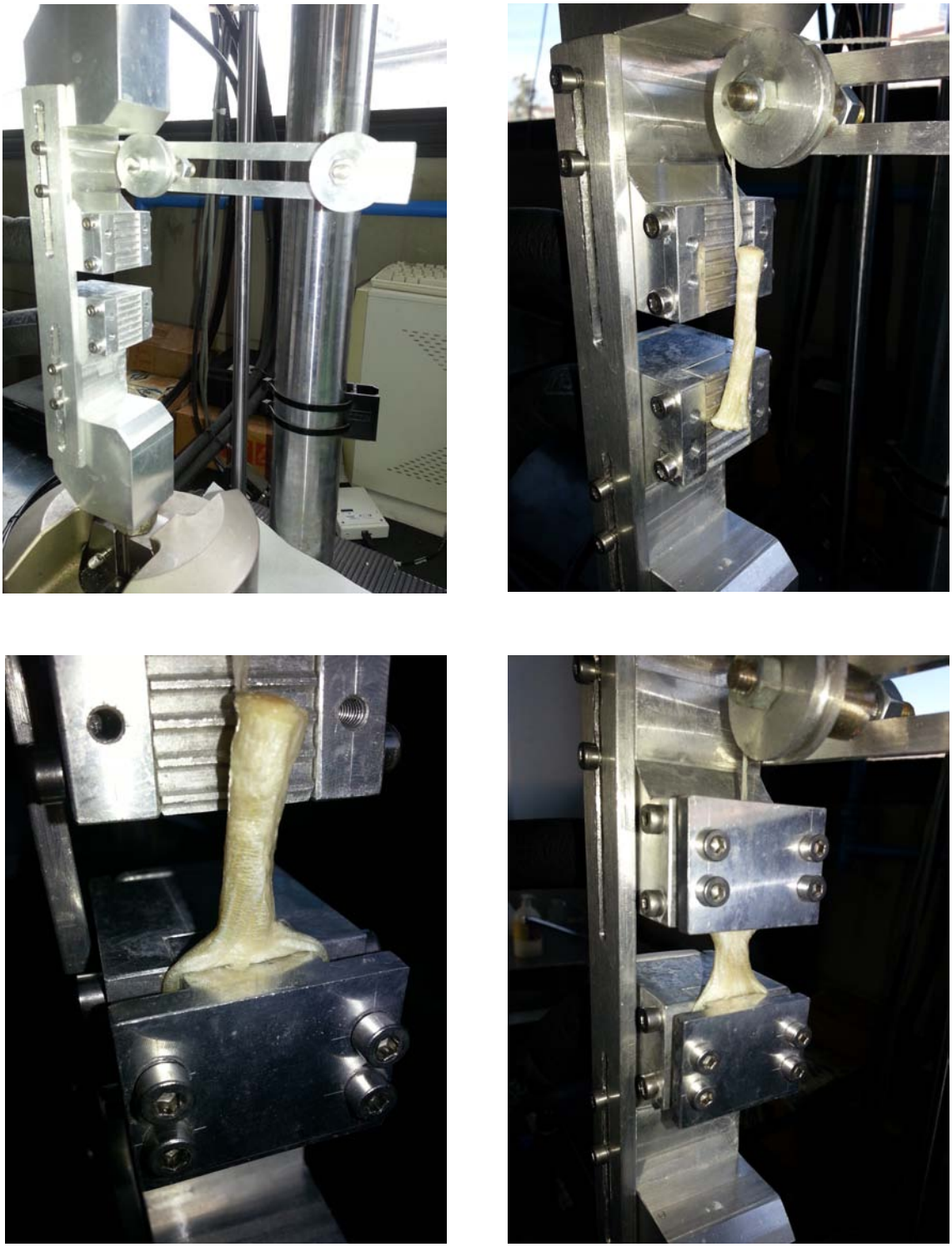

Figure 4.3: Placing procedure. First is close the bottom clamp and then the upper one.

4.5 Static traction test procedure.

For the definition of static program cycle hs been defined as a MPT procedure:

- Initial preload, made by machine, with a rate of 50 N to 2.5 N/s. Total duration of about 20 s.
- Application of a load in deformation control with a strain rate of 0.25 mm/s until rupture.
- Return to the starting position.
- Acquisition of data with a frequency of 200 Hz, rounded up to 204 Hz because of the MTS MiniBionix 858 acquisition system clock.

CHAPTER 5
Results and data analysis.

5.1 Introduction.

Is well known that organic tissues in question are difficult to grip due to their soft consistency and slippery surface. Various attempts have been carried out step by step integrating different solutions, starting from a ambient temperature configuration and adding subsequently factors act to increase the friction.

The first data collected were not representative of an in vivo situation, that is, with tendon attached to the bone. The reason for this discrepancy is due to the fact that occurred situations in which the notches cut the specimens or the tendons, because the lack of grip, slip away, impairing the samples and invalidating the test.

During the development of the clamping system, occurred two main events:

- a too tight grip causes local stresses on the part of tissue squeezed; the specimen gone to break close to first notch of the upper or lower plates;
- with a too low grip the specimen may slide due to the scarcity of friction between aluminium and tissue, causing the tips impairment.

These two situations are to prevent; in fact a traction test to be reliable, whatever the nature and consistency of the sample (whether organic or inorganic, solid or soft), needs to make the break point in a central section away from the grips, point in which the stress are exclusively alligned with the traction axis.

To accomplish this target a general specimen is dimensioned so as to determine the location of the break, then you increase the stiffness of the samples extremes.

In the case of tendons a good solution has been developed using the particular clamps cooled with liquid nitrogen. By freezing the heads of the tendons creates two zones that locally have a greater stiffness.The analysis was performed for 6 flexor digital tendons, 4 isolated from lama (A, B) and 2 from dog (C). Two lama's tendon and one of dog were

decullarized.

5.2-Specimens section values.

As reported previously, after the thawing and the suture, the section of the samples were measured. The estimation was made by adding a weight of about 100g on the plate of the measuring instrument of the sections, to facilitate the escape of water from the sample.

The acquired data are shown in the following table (Figure 5.1).

	NORMAL			DECELLULARIZED		
Measure number	A	B	C	A	B	C
1	5,2	3,02	2,52	5,23	2	2,83
2	5,15	3,01	2,46	5,16	3,47	2,84
3	5,2	3,05	2,51	5,22	3,68	2,9
4	5,15	3,1	2,44	5,15	3,7	2,86
Average [mm]	5,175	3,045	2,4825	5,19	3,2125	2,8575
Notch width [mm]	7,15	7,15	4,15	7,15	7,15	4,15
Section [mm^2]	37,00125	21,77175	10,302375	37,1085	22,969375	11,858625

Figure 5.1: Section estimation.

After the four measurement has been done an average. The notch width is constant for the samples A and B; C needed to be measured in a smaller notch. In the table are listed also the notches and multiplying them for the average it gives the section estimation.

The sections for same types does not have great changes. The sections for decellularized samples seem to be slightly bigger.

5.3-Strength and stiffness evaluation.

With the laws expressed in the above chapters, it is easy to calculate for each specimen the ultimate stress beared by the tendon. Once is plotted the Load-Displacement curve and converted load in stress, dividing the first by the section early measured, the σ_{UTS} is the stress the UTS load.

Regarding the elastic modulus, it is more complex its calculation; the data acquired

present in fact some noise which amplifies exponentially while searching the best point for the slope interpolation.

The criterion used is that of the second derivative, it intends to calculate the first and second derivatives of all the acquired curves and the point where the second derivative is zero (or remains constant) is the point where must be taken the slope of the curve stress-strain.

Though, because the specimens are made of organic tissue, not all of them have an ideal trend. This implies that the second derivative doesn't always have a solution for zero.

In these cases are taken the point where the second derivative is constant and nearest to zero value.

The stress and strain, calculated starting from load, displacement, section and length, are filtered using the moving average, which is a low-pass filter. This dumps high frequency noises and makes a clearer curve.

Now the calculation of the first and the second derivatives becomes cleaner and the curve that comes out is more acceptable than those calculated from the raw data. To complete the calculation of the points and make reading easier, is executed another moving average of first and second derivatives.

An example of first and second derivatives calculation is displayed in the next paragraph.

5.4-Stress-strain diagrams.

The samples tested presented similar length (between 60 and 70 mm).

A and B stands for llama tendons, but compared to A, B was obtained by splitting longitudinally a tendon from a one more thick; the cutting damages the outer structure (epitenon), that normally holds together the fibers. So "A normal" stands for llama tendon which preserves its original structure, “A decellularized” means llama tendon which has integral structure and without cells, “B normal” has damaged epitenon and integral cells, and last “B decellularized” is for llama tendon but with structure partially damaged. A and B has similar geometry both for length and section size

C stands for dog tendon which, compared to A and B, has same length but smaller section area. Even for C there were two samples one with cells and the other not.

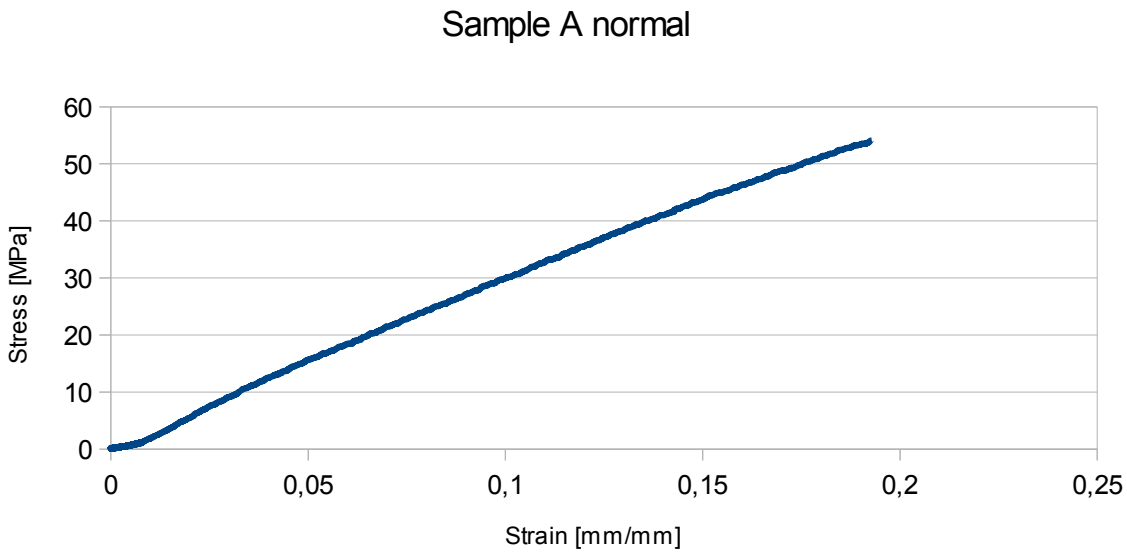

Figure 5.2: A normal sample stress-strain curve. This sample has not reached the UTS, but is evident the linear behavior of the tendon.

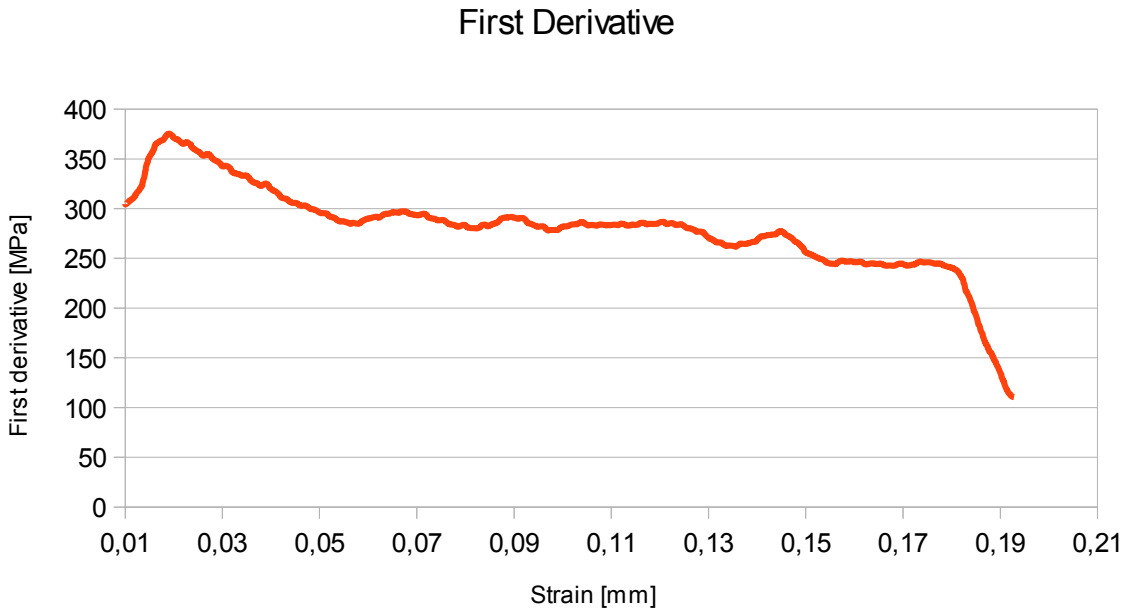

Figure 5.3: First derivative. In the zone between 0,06 and 0,11 mm/mm (strain) the derivative has a value quite constant. That is the point of slope determination.

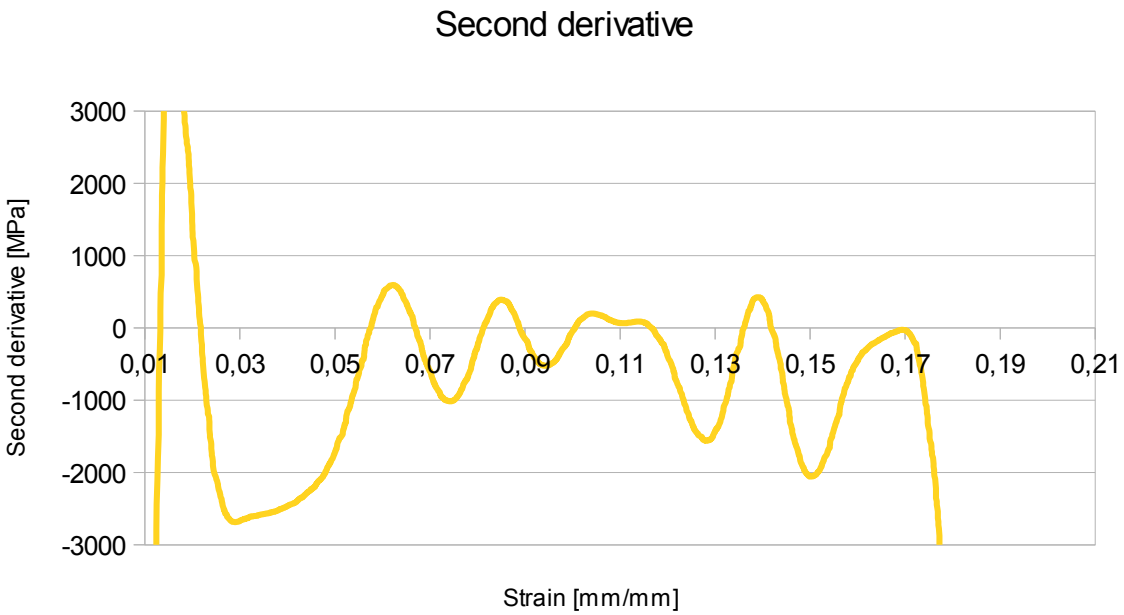

Figure 5.4: The second derivative has a average value about zero between 0,06 and 0,11, which is the slope determination zone.

A problem occurred while testing the A normal specimen, because of the limit detectors that where set to 2 kN; an overcoming of these limits make the test machine shut down. The specimen gone broken without reaching its UTS. The only value that can be measure is the elastic modulus that is approximatively 285 MPa.

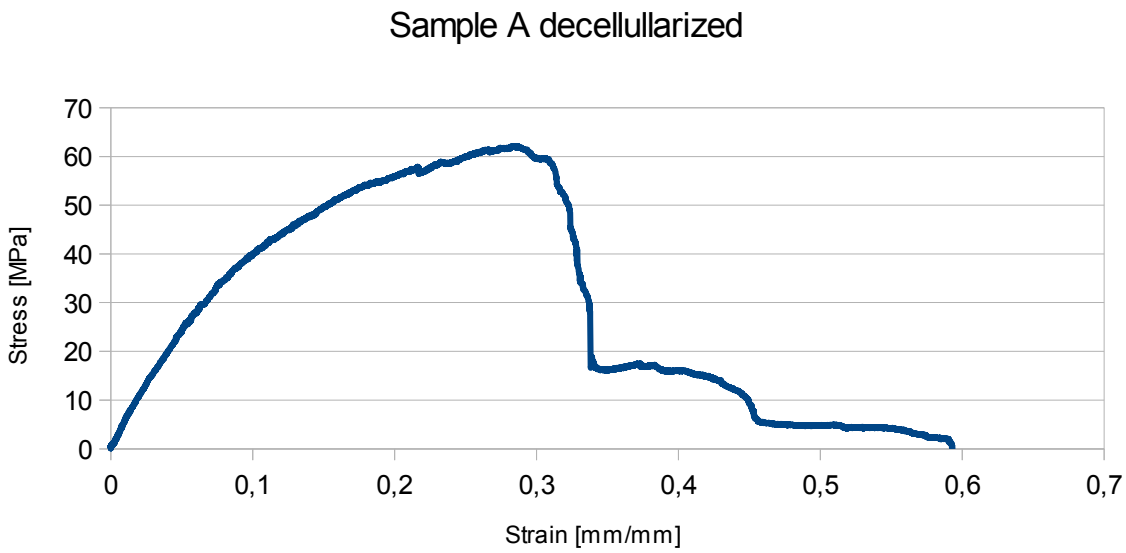

Figure 5.5: This curve has a typical trend of a tendon. The toe region is not so evident, probably because tendon goes inadvertently pre-tensioned.

The A decellularized sample has reached a σ_{UTS} = 61 MPa and a Young modulus of about 460 MPa. Is also noticeable a progressive rupture of the tendon.

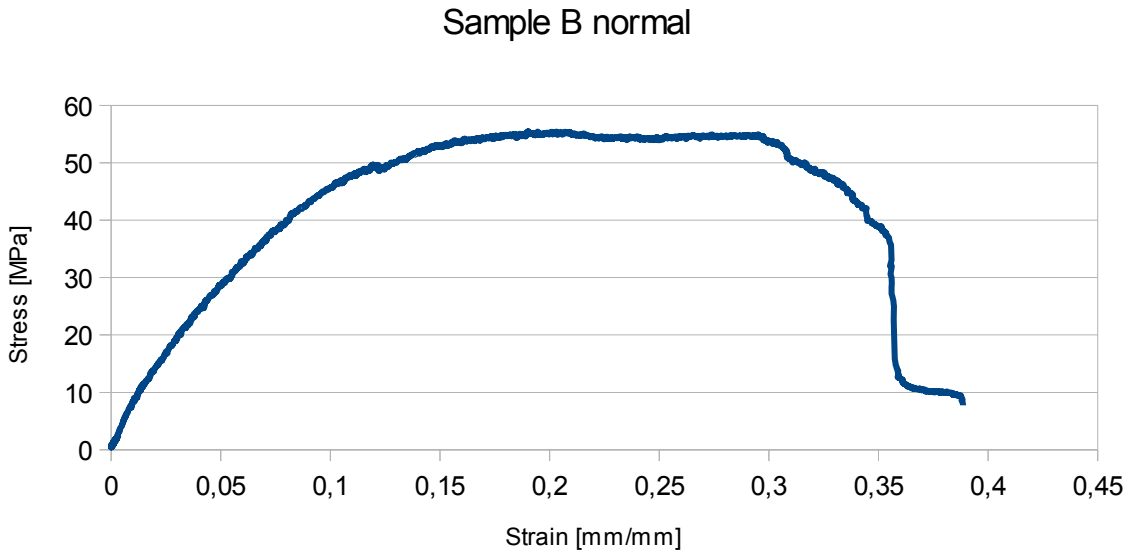

Figure 5.6: This specimen has a extended plateau where the fiber rupture occurs.

The values of this sample are : σ_{UTS} = 55 MPa and ε = 401 MPa.

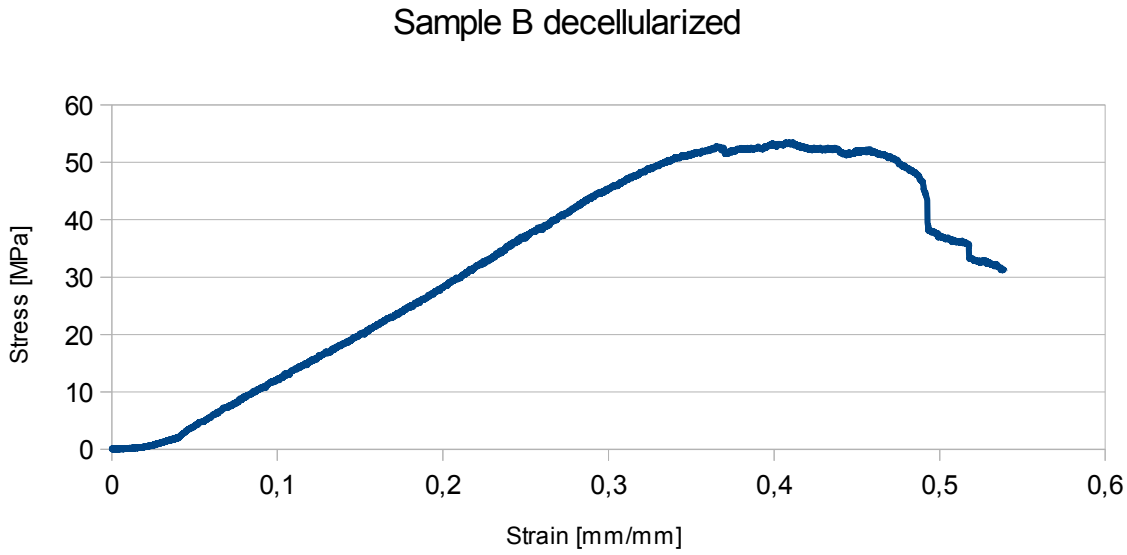

Figure 5.7: In this case is highlighted the toe region at the beginning of the test. Then there is a good linear trend until yield and rupture.

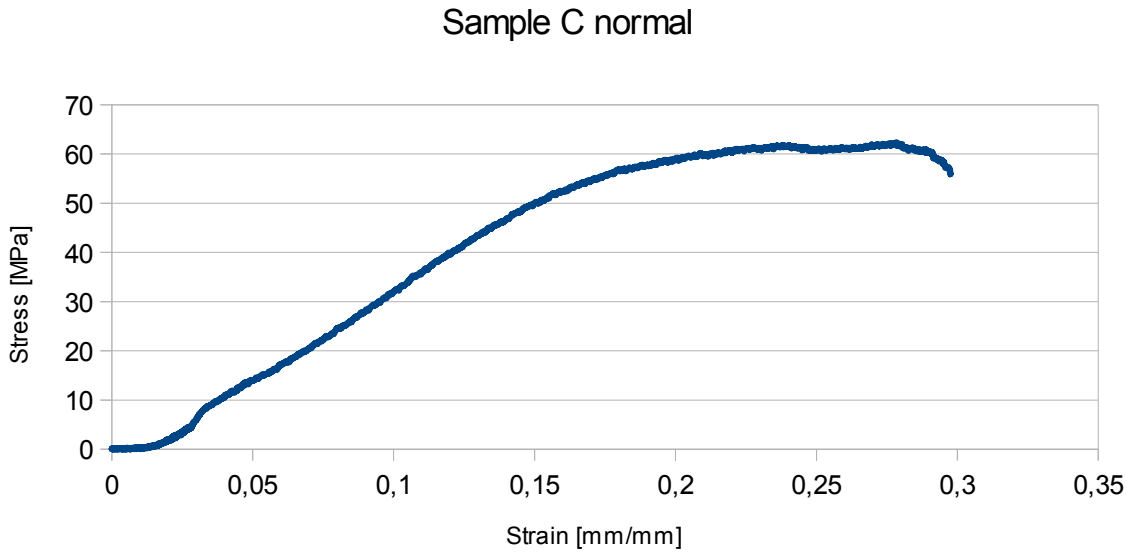

Figure 5.8: This specimen has a thinner section but the strain stress curve trend is still as expected.

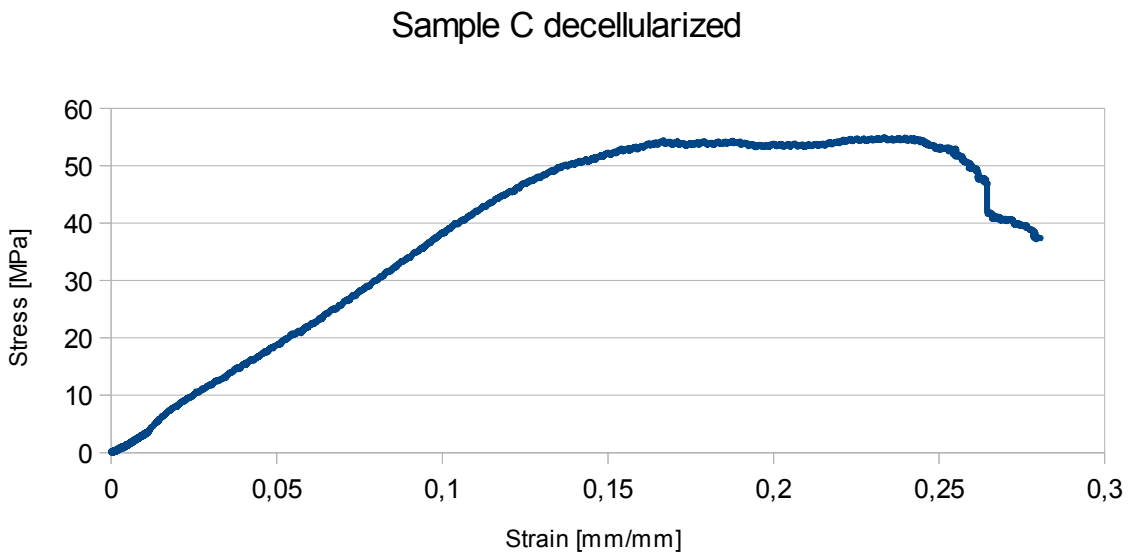

Figure 5.9: This is the most interesting sample, in fact it has undamaged epitenon and compared to its non-decellularized twin it does not show important changes of modulus and σ_{UTS}.

5.5-Strength and stiffness comparison.

In the next table (Figure 5.10) are displayed the result in order to compare the biomechanics of each sample.

	A	B	C	A	B	C
σUTS [MPa]	>54	55	62	61	47	55
stic Modulus [MPa]	285	401	400	460	161	405

Figure 5.10: Stiffness and strength comparison table.

The σ_{UTS} doesn't seem to change consistently between the normal and the decellularized tendons. The decellularized sample though have lower σ_{UTS} value, and the B sample registers, in the case of decellularization, a big change of Elastic modulus, which means lower stiffness.

CONCLUSIONS

From the point of view of data analysis, this study does not allow for a statistical survey. The six samples studied show slight variations in strength and stiffness, except for those who have suffered damage of the epitenon.

In fact, unlike the specimens A and C, B specimens have no validity in case of deepen study of the biomechanical variations of decellularized tissues, as they represent a unlikely situation in the case of homologous transplantation of recellularized tendon on patient which has undergone a complete lesion.

The most important part of the study was the development of the gripping system. As mentioned above, the consistency of the tendons is soft and slippery, hence the problems encountered were all about grip. Were examined more possible solutions, balancing cost of the system, operational simplicity, repeatability of the tests and, last but the most important, the effectiveness of the grip.

Starting from a situation at room temperature, in which the specimen was cut from the teeth of the plates and measured values of UTS and stiffness too low or slid away, ruining the tips of the sample; were evaluated solutions in which it was increased, through the use of materials located between tendon and plates (gauze, paper, balsa wood, ...).

The final solution (liquid nitrogen) has given excellent results, comparing them with the values found in the literature that provide values of ultimate stress above 40 MPa up to 100MPa (depending on the type of animal), and above 400 MPa for the stiffness.

The study need to be surely improved and deepened, making a cross research and including more variables. Aiming as far as possible to a perfect solution.

PART TWO

CHAPTER 1
The fixed prosthesis and its alternatives.

1.1-Introduction.

The prosthetic rehabilitation of a dental patient implies the introduction of an artificial object in a highly dynamic system such as the stomatognathic apparatus, becoming an integral part or replacement both anatomical and functional.

All the materials and restoration existing techniques have limitations and do not have exactly the same characteristics of natural tooth tissue, the clinician must therefore choose the appropriate procedure for each clinical case, taking into account the preferences and needs of patients.

On the one hand, the professional will have to choose a solution that can withstand the loads of the occlusal surface of the dental arch in the area concerned, on the other hand will try to meet the aesthetic needs of the patient. The knowledge of the characteristics of the different solutions is a prerequisite for the satisfaction of these two aspects.

The alternatives that are likely to emerge for the prosthetic fitting of a single tooth implant are numerous, from the type of material to construction geometry, especially at this time when technology allows to create studio entire production processes, without resorting to the technician's work.

The prosthetic product in fact can be designed and built using the CAD CAM technology that, thanks to dedicated software, is capable of starting from the scan of the titanium abutment to design the interface between titanium and prosthetic superstructure, be it an abutment on which then will be cemented a crown or a dedicated one-piece materials.

The fact of choosing one or the other possibility depends on a number of variables, the coupling of more materials in fact leads to the pros and cons that the use of a single material has not.

The purpose of this thesis is to analyze the mechanical behavior of two prosthetic solutions.

The first in Lava Zirconia abutment (sub) adhesively cemented to a crown

(superstructure) always built with technical and Cad Cam and made of an innovative material, the nano-ceramic resin (3M- ESPE Lava Ultimate).

For the second solution has been used the same nanoceramic material, but adhesively coupled directly on the abutment. The support structure of both solutions consists of a zirconia abutment to the implant Aon Not Rot. H. 8 EI fixed on an implant of the same company with a diameter of 4 L. 11.5 nPOP E-INT, inserted inside a cylindrical support made of the Palapress resin.

The two solutions will be tested from different points of view, on the one hand will be analyzed the characteristics of resistance to fatigue, on the other hand will evaluate the average value of breakage of the article with a static compression load test and finally will be analyzed, with the help of an industrial tomograph Wenzel Exact-XS Workstation, differences detected before and after the test load so as to identify failures or changes to a non-destructive examination of the sample.

Subsequently, the alternatives will be listed among the most common solutions adopted for a fixed prosthetic, specifying what are the qualities of each.

The fixed prosthesis is able to successfully restore the health of the oral tissues with aesthetics and functionality stable over time, the type of materials and manufacturing processes have undergone major changes over the years, it has grown from metal implants to digital technology within few decades; making an analysis of the solutions available now in the dental world it is appropriate to brief a historical overview to understand how it has arrived at the current scenery.

1.2-The Metal-Ceramic.

The caramic, of which must be mentioned the importance and characteristics, having regard to the diffusion in the dental field, was introduced more than two centuries and with its application in metal-ceramic technique occupies fifty years a major part of prosthetic dentistry.

The ceramic materials have become synonym of aesthetics, oral strength and biocompatibility and their inherent fragility has been overcome thanks to the development of substructures support with appropriate mechanical properties, such as those of the metal

alloys.

The metal-ceramic restorations are constituted by a metallic substructure of

Figure 1.1: Metal-caramic implant.

reinforcement suitable for supporting the ceramic layer: the combination of a hard and fragile material with one more elastic allows to obtain a product with physical characteristics more satisfactory; so it is used the good mechanical properties of specific dental alloys, the precision obtainable from the proceedings of lost wax casting and aesthetics, durability and biocompatibility of ceramics.

The metals, however, have always been a limit in the nature of the aesthetic, therefore, parallel to the great and proven clinical success of metal-ceramic, have followed through time proposals for various totally-ceramic systems.

Currently, prosthetic dentistry has received a strong boost to the ceramic restorations called "metal-free" or "full ceramic".

Although this type of reconstruction is clearly advantageous in certain clinical situations and can provide excellent aesthetics, common in use does not replace the metal-ceramic which still represents the majority of restorations products, enjoying a non-clinical use surpassed by any other system in this particular field of aesthetic dentistry.

For all of these restorations, whether they are with supports of metal alloys or ceramics, the success is due not only to the clinic design, but also to the correct combination

of materials and appropriate construction techniques assigned to the dexterity and creativity of the craft workshops that produce them.

The glass-ceramic coating delamination in fact is a not rare occurrence that interests all types of substrates. These fractures affect the function and compromise the aesthetic and are definitive solution only with the replacement of the product.

The metal ceramic technique has a long and documented clinical success together with the aesthetic satisfaction and is applicable in a variety of therapeutic solutions (single crowns and bridges both in the anterior and posterior arches), proving that it is still irreplaceable in the current proposals: long-term studies show how, in particular in the posterior metal ceramic restorations, it reduces the risk of coronal fractures of teeth, widely compromised while maintaining the functions and morphology of the occlusal tooth for longer periods of time than other reconstruction systems.

Many types of alloys are commercially avaible and dental ceramics that rely on different technologies of construction and which must meet specific requirements in order to be combined in a manufactured metal-ceramic: the alloy must have a melting temperature higher than the cooking temperature ceramics, must possess high modulus of elasticity and mechanical resistance and an appropriate coefficient of thermal expansion that is only slightly higher than that of the ceramic.

The problems of compatibility between the materials is transmitted to the gap between metal and ceramic and there are countless factors and combinations of them that affect the strength of the bond and then in general the finished product.

One of the primary requirements for the success of a metal ceramic restoration is therefore the development of a lasting bond between porcelain and metal; historically theories of bonding forces have focused on micromechanical retention and chemical bonding across the interface due to formation of an oxide layer interposed.

The oxidation behavior of these alloys significantly determines their potential for binding with ceramics. The adhesion and consistency of the oxide layer on the metal surface is essential for a good match with the ceramic: if the oxide has poor adhesion with the metal the metal-ceramic bond will be weak.

The requirements described have been extensively documented, but today the great heterogeneity of materials available puts dental labs first of innumerable difficult to standardize work procedures and able to influence clinical outcomes.

The overall survival of these restorations is estimated around 85% at 15 years of operation. Despite the improvement of the existing glass-ceramic bond with the metal substrates it happens that the function has the clinical detachment of the coating. The fracture of the ceramic is a major problem and it costs for both the clinician and the patient.

Clinical studies indicate that the incidence of fracture of ceramics varies 1-3% at 5 years and 5-10% after ten years of operation but these percentages may increase under important and repeated stresses: the failures are conditioned by where it is introduced, but on the other hand, in clinical practice, is difficult to control the strength and direction of the masticatory loads.

However, these fractures have a multifactorial origin. A common cause are microcracks present in the ceramic, and especially in the bridges more extended in the anteroposterior level, the slightest bending of the substructure promotes propagation with catastrophic failures of restorations.

Many studies demonstrate the importance of microcracks in the ceramic, they may originate from the processes of condensation and sintering of the ceramic on the metal support and from the difference in the coefficients of thermal expansion; in order to minimize their formation, in addition to compliance of the appropriate pair of materials, an uniform layer of the materials need to be produced in the piece.

Another major cause of failure are technical errors and the manual application of ceramics can produce noticeable porosity and weak sites which are cause of fracture; every effort must therefore be applied by operators to prevent their formation. A poor design of the substructure, the thermal incompatibility between materials, excessive thickness of ceramic with inadequate support or vice versa too thin thickness of the coating, the non-registration of occlusal forces or trauma will inevitably produce the clinical failure.

Although various methods are proposed for direct repair through the use of composite resins, they offer adhesion values much lower (18 to 25 MPa) and constitute the only remedies to postpone the ultimate resolution that is the only replacement of the prosthetic.

In the case of a single tooth restorations, particularly in the rear, the solution metal-ceramic based was the one preferred by the majority of clinicians at the present. Instead the aesthetic needs and characteristics of the materials, have led to an increasing demand for different solutions, the all-ceramic crowns have become of common use and represent an obvious choice in some situations.

1.3-The fully ceramic prosthesis.

Figure 1.2: Fully ceramic prosthesis.

The success of ceramic restorations, thanks to the naturalness of the aesthetic results and consequent patients demand of metal-free restorations have pushed the introduction and development of fully ceramic restorative systems in fixed prosthesis. These systems are currently the subject of numerous evaluations for their predictability and success over time.
The idea of this type of treatment dates back in 1967 thanks to Mc Lean and arrives to our days with a series of ceramic materials of which the zirconia is the most recent and innovative applications in dentistry.

Among the systems defined "high resistance" the glass-ceramic structures reinforced with lithium disilicate (Empress II), with a flexural strength of between 300 and 400 MPa, thanks to the glass component, provide good translucency, but it is recommended for adhesive cementation, to promote the strength and durability (which requires great care and clinical precision) and also remain indicated for bridges of up to three element for anterior losses or at least in the premolar area; remains controversial also their biocompatibility.

The system In-Ceram Alumina (alumina infiltrated with glass) was introduced for the first bridge systems of three elements in the anterior with a resistance to bending that varies in a range between 236 and 600 MPa according to the method of production adopted by the laboratory: "slip-casting", sintering at 1120°C of the cap in pure alumina mixed and applied

on an special plaster abutment and subsequent infiltred with glass,or prefabricated and partially sintered blocks milling.

The same manufacturer proposes variants In-Ceram Spinell (alumina and magnesium oxide) more translucent but less resistant and In-Ceram Zirconia, that combines the alumina infiltrated with glass with a 35% of partially stabilized zirconia to achieve a resistance to flexion up to 800 MPa, and this solution has a high opacity comparable to a metal alloy that does not have aesthetic advantages in the anterior sectors.

Only the restorations with a zirconia core can be considered today the main alternative to main metal-ceramic restorations, for the support of reconstructions extended in the posterior and also anterior, on pillars of both natural and implants with different designs of preparation.

The zirconia presents values of tensile strength of 900-1200 MPa and a compressive strength of about 2000 MPa.

Regarding these systems are available retrospective clinical studies of up to five years demonstrating an overall survival of 73.9% of the restorations considered a failure due to delamination of the coating in 15% of cases at 36 ± 13.8 months.

Several investigations are underway to study the problems that gradually emerge from the clinic: potential structural damage resulting from the processing of zirconia surface, aging, adhesion of ceramic glass coating. But there is a problem that must be taken into careful consideration, for any prosthetic solution: biocompatibility. As described, a number of new ceramic products have been introduced in dentistry.

The improvement of the mechanical properties today promotes the elimination of metal substructures and consequently these materials remain in direct contact with the natural dental and periodontal tissues for long periods of time.

Biocompatibility of feldspathic ceramics in general has been widely proven by long clinical use.

Regarding the most modern glass-ceramics is shown the potential cytotoxicity of ceramic lithium disilicate Empress II.

For the zirconia and alumina are reported instead absolutely favorable opinions regarding the biocompatibility already evaluated for orthopedic implants.

The fine particle size and the absence of porosity of the zirconia-yttria make it suitable for biomedical applications and are excluded the carcinogenic effects also postulated for

impurities that may be present in the zirconia deriving from radioactive elements (uranium and associated radio zirconium) both on purified zirconia and which is not. It was confirmed low cytotoxicity of the zirconia-yttria both white and colored for dental applications.

The bacterial adhesion, which is an important aspect to consider in the restorations to avoid marginal leakage or periodontal alterations, seems to be irrelevant on zirconia and different studies agree that it is lower than titanium.

Thanks to today's technology CAD-CAM abutments for implants are also offered in zirconia and alumina to provide emergency items replaced highly aesthetic and integrated with the natural elements contiguous especially in the earlier losses.

The use of ceramic zirconia abutments reduces the risk of bluish coloration that can transpire through the gingival tissues.

In particular the aesthetic restorations in the maxillary anterior region have always been a challenge for the dental team, it is precisely in this field that the metal-free restorations make it appear their positive characteristics.

There is the ceramic oxide, used as a building material; it has been shown to have superior mechanical properties to the glass ceramic materials, but put the bulk limit can be used in restoration in areas where the aesthetic demand was not as important as translucency characteristics lower compared to the other alternatives present.

The lithium disilicate glass ceramic is a material capable of satisfying both the mechanical characteristics and the aesthetic ones, in fact it presents mechanical resistance and a sufficiently high value of translucency combined with the possibility of characterization definitely better than the material above; its use remains limited, however, according to some studies, to the anterior sectors, as the mechanical needs on the posterior under certain parafunctional conditions would not be satisfied by prosthetic restorations fabricated with this technology.

The response characteristics of mechanical prostheses made of this material can be greatly enhanced thanks to CAD CAM technology combined with the heat pressing technique, with the digital design in fact it will improve the value of accuracy of the prosthetic; the abutment made following the initial scan will perform a series of steps in which the constructive addition of material is carried out together with a thermal treatment at high pressure.

1.4 The Zirconia.

Figure 1.3: Zirconium dioxide.

Zirconia is known as gemstone since ancient times, its name comes from arabic Zargon and means gold-colored (zar = gold, and gun = color). The zirconia (zirconium dioxide, ZrO_2) was identified by the German chemist Martin Heinrich Klaproth in 1789 and its use as a biomaterial began in 1960.

The pure zirconia exists in three different crystal structures: monoclinic from ambient temperature up to 1170 ° C, the tetragonal 1170 ° C to 2370 ° C and cubic over 2370 ° C.

The sintering temperature of pure zirconia is between 1500 and 1700 ° C, and during cooling, there is the transformation from the tetragonal to the monoclinic structure at about 1170 ° C with a volumetric expansion of about 3-4%. This means the establishment of residual stresses leads to fragmentation of the piece.

By the addition of other refractory oxides such as CaO, MgO, Y_2O_3 and CeO_2 is possible to stabilize the cubic structure and the tetragonal zirconia at room temperature in a metastable state, and therefore, produce materials for which have been found many applications.

The zirconia combined with oxides stabilizers so that it retains the tetragonal structure at room temperature is called fully stabilized zirconia or Tetragonal Zirconia Policrystal (TZP).

Have recently been developed ceramic materials composed of zirconia and refractory

oxides with high mechanical strength and toughness by exploiting the phase transformation.

One of the most important is the partially stabilized zirconia (PSZ), which is obtained by combining with 9% MgO and using special heat treatments.

MgO is sintered at about 1800 ° C and if it is rapidly cooled to room temperature will have a completely metastable cubic structure .

However, if this material is heated again to 1400°C and held at this temperature for a sufficient period, creating a fine submicroscopic precipitate with metastable tetragonal structure.

Under the action of stresses that cause small cracks in the ceramic material the tetragonal phase is transformed into the monoclinic phase causing volumetric expansion of the material at the apex of the crack which delays the propagation of cracks, absorbing the energy (via structure transformation) and closing the clique (via volumetric expansion).

Hindering the advancement of cracks the ceramic material is then "toughened" .The PSZ has a fracture toughness among the highest of advanced ceramic materials. The Mg - PSZ has been tested and introduced for biomedical applications but its use has stopped in the 90s, due to the residual porosity and technological difficulties of production including the high sintering temperature required (1800°C, against 1400°C for TPZ). The PSZ can also be achieved with other systems including the yttria-zirconia .

The tetragonal zirconia TZP is among the most studied ceramic materials because of its prerogative of “auto-toughnessing” due to the transformation of monoclinic tetragonal phase following the application of a load .

The necessary condition for this to happen is to stabilize at room temperature through the stabilizing oxide (yttria ,shoots, ceria or magnesia) and also from the literature it is known that there are two critical dimensions of the crystal grain: a higher (~1 micron) over which the tetragonal phase is spontaneously transformed into monoclinic affecting the mechanical properties of the material, and a lower, below which there is no strain induced transformation (~0,1 to 0,2μm) it is important to control the grain size. The good dimensional and chemical stability , mechanical strength and toughness , combined with an elastic modulus of the same order of magnitude of a steel alloy (~ 220 GPa) were the origin of the interest on the use of zirconia ceramic as a biomaterial .

Today, this TZP ceramics, whose requirements for surgical implants are described in ISO 13356, is a material widely used in orthopedics and since 2000 also in dentistry.

The TPZ containing approximately 2-3 mol% of yttria (Y_2O_3) is entirely composed of tetragonal grains. It is very important to consider the nature of the metastable tetragonal grains. As already said, there is a critical dimension, also linked to the concentration of yttria, above which the grains transformation T-M takes place spontaneous, while this transformation will be inhibited in a fine grain structure. An interesting feature of the transformation of zirconia toughened ceramic is the formation of layers of compression on their surface. The tetragonal grains surface can transform spontaneously into monoclinic due to abrasive procedures, and this produces compressive stress to a depth of several microns below the surface. While this phase transition surface may have an important role in the improvement of the mechanical properties, on the other hand the thickness of the layer of processing may constitute a limit: the progression of the tetragonal-monoclinic transformation can cause surface cracks followed by the detachment of the grains from the surface, with deleterious effects on the mechanical behaviour and wear.

In this experimental work was considered a particular type of zirconia, which is proposed in commercially blocks ready for milling, which is the commercial most representative products of the "soft machining" systems, i.e., those that allow the creation of the prosthetic to work of special equipment for multi-axis milling :

- Cercon ® (Dentsply Int)
- Lava ® (3M Espe)
- Procera ® Zirconia (Nobel Biocare)
- YZ cubes for Cerec inLab ® (Vident) ZirCAD IPS e.max ® (Ivoclar Vivadent)
- Zirkonzahn ® .

The abutments, derived from the impression or a wax pattern, are scanned; then the structure is designed with a software (CAD, computer aided design) volumetrically increased in order to compensate the subsequent sintering shrinkage (about 20%), and finally the block is shaped by computer-driven milling (CAM, computer aided manufacturing).

Typically the powder of 3Y- TZP used in the manufacture of the blocks contains a binder which makes it suitable for pressing process; it also contains about 2 vol % of hafnium oxide (HfO2) that is characteristically difficult to separate from the zirconia .

The powders consist of a particulate diameter of about 60μm and the blocks are formed by cold isostatic pressing . The binder is removed during the subsequent heat treatment of the "pre- sintering": This step is controlled very accurately by the producers as a major influence on the hardness and workability of the blocks.

1.5-The ceramic adhesion to the zirconia.

The interface core-veneer is one of the weakest points of these systems in fact delamination of the coating is possible as is observed clinically.

Most manufacturers provide the materials defined "compatible" as with a minimum mismatch between zirconia and glass ceramic with a coefficient of thermal expansion lower for the coating. The thermal expansion coefficient of zirconia is generally 10.5-11x 10_{-6} K_{-1}. This approach is applied to all systems, both with ceramic and metal supports.

The delamination of the glass ceramic during mastication indicates the presence of presumably tensional stress at the interface and perhaps are also involved modification of surface properties.

All manufacturers of ceramics for the zirconia-yttria supports are now providing "liners" to increase the bond with the ceramic as well as for aesthetic purposes (color/opalescence). These liners can improve the wettability or function as a chemical reducer of the possible interactions with zirconia.

The study of White SN et al. on the evaluation of the bending strength of the systems obtained by layering zirconia-ceramic (Lava System Frame and Lava Ceram veneer ceramic) by three-point bending test, although showing higher values systems alumina-ceramic (~650-750 MPa vs. 500 MPa) emerges the problem of failure of adhesion between these materials more than in other combinations as being due to the residual stresses resulting from sintering of zirconia, firing of the coating, finishing treatments.

Another important aspect coming from the stratification on the support of zirconia is the effect of the firing temperature of the glass ceramic: in fact coatings are fired at temperatures between 800 and 900°C and has been demonstrated that such heat treatments tend to reduce the resistance to bending of zirconia DC Zircon (DCS Dental AG) significantly. This system includes the modeling of yttria-zirconia substructures from that reached the final

degree of sintering.

The treatments of milling and finishing of zirconia induce the transformation t→m creating a state of compression sub-surface that can block the propagation of cracks that are produced; according to some authors this toughening produce a flexural strength up to 1500 MPa which is reduced to about 900 MPa after the heat treatments of the glass-ceramic cooking as they would promote the reverse mechanism of conversion m→t and the consequent contraction would unbend stress from compression, freeing the propagation of defects.

Regarding the adhesion values "core-veneer" reported in the literature on the fully ceramic systems, zirconia supports generally offer data that they adhere to under 30 MPa.
Al-Dohan HM et al. obtained by means of shear bond test the following values of the glass ceramic adhesion compatible with:

- 30.86 ± 6.47 MPa for media in lithium disilicate Empress II
- 28.03 ± 5.03 MPa for zirconia-glass ceramic Procera allZircon Core
- 27.9 ± 4.79 MPa for zirconia-glass ceramic DC Zircon
- 22.4 ± 2.4 MPa for alumina Procera Alumina Core AllCeram

The glass-ceramic was applied to simulate the traditional technique with three coats. From the optical microscopic observations of the separation surfaces resulted generally a mixed cohesive fracture in the veneer and an adhesive one between core and veneer; only the coupling between the glass-ceramic (lithium disilicate , Empress II) showed cohesive fracture in the core , while the alumina showed a prevalence of adhesive detachments.

Aboushelib et al. instead studied the adhesion force through "microtensile bond strength test." From a comparison study between zirconia and glass-ceramic,with substrates made by die-casting was obtained a value of adhesion of 29.1 ± 10.8 MPa for zirconia (Cercon ®, CTE 10.5 · 10^{-6} K^{-1}) and more than 90% of the samples showed adhesive fracture interface. The ceramic coating (Cercon ® Ceram S, feldspar, CTE 9.5 · 10^{-6} K^{-1}) was applied with a conventional technique by the interposition of a liner of feldspar ceramic selenium (CTE 9.5 · 10^{-6} K^{-1}) recommended by the manufacturers to mask the high opacity white zirconia and improve the bond with the coating.

From the tests without the liner authors got actually much lower adhesion values (16.9

± 4.8 MPa), although the SEM observations showed the presence of voids at the interface with its use.

The coupling instead with a ceramic coating with experimental coefficient of thermal expansion higher than the core (CTE 12.5 · 10_{-6} K_{-1}) caused the early and massive delamination in the samples already during their preparation. This solution was excluded from the experimentation. Since the zirconia showed adhesion values with the coating lower than in the other glass ceramic cores tested (close to 40 MPa), the authors conducted further experiments with different coatings and methods of production: it turned out that an improvement in adhesion strength (> 30MPa) happend with the application of glass ceramic through die-casting and in this case without the interposition of the liner, and if it is used it is recommended that further treatment of sandblasting and steam cleaning of the surface.

The application of glass ceramic involves a great deal of attention and technical skills: porosity and defects in the glass ceramic are in fact a major cause of failure, especially in reconstructions that provide minimal occlusal thickness, and the complexity of these systems must attract the attention of not only studies toward higher adhesion values but also on the type of fracture.

The application of glass-ceramic trough diecast obviously excludes the variable of manuality reducing the introduction of defects, and the standard result in the final properties of the ceramic glass provides better mechanical strength but lacks the aesthetic customization.

Have recently been proposed combined techniques of application of the first ceramic layer ("dentin") on the zirconia by die-casting to improve the binding and subsequent layering with a traditional technique to get the aesthetics. This technique appears promising and may be used in highly specialized laboratories, however, leads to the further restoration interface between materials of which you do not yet know the clinical behavior.

CHAPTER 2
Materials used for the implant prosthesis.

2.1-Introduction.

Often the prosthetic solution that comes to realize is not cemented directly on the stump, but onto implant solutions.

The effectiveness of the use of titanium for the implant construction is documented, but the same material for the construction of the abutment is heavily debated because of unsatisfactory results in the aesthetic zone. For the first tests was used mostly the alumina, which presented mechanical performance questionable having a very low tensile strength, insufficient for most clinical applications.

It was therefore suggested an abutment constituted by a metallic core covered by a structure aesthetically performant, which in some studies has given the best results, in the same way; however, zirconia, initially used as a layer to the aesthetic of above the titanium core, has been tested, thanks to the improvements of sintering, even as abutments integral, giving excellent results from the mechanical point of view.

In some studies (Stimmelmayr M. et al., 2013, Dundar M et al., 2007, Denry The IR and Kelly, 2008) the tests provided to verify how to combine the characteristics of zirconia with those of a second material which works as a dumper for mechanical shocks which, by construction, zirconia is not able to absorb.

It must be said that several clinical trials demonstrate the efficacy of using this material in the case of single-tooth prosthesis, especially in the anterior and premolar, also in the posterior have been demonstrated sufficient survival values; but the studies reported in the literature are based on relatively short periods, clinically speaking, in fact survival rates last one year from the implant. It should be considered in any case that the zirconia has mechanical characteristics very different to the titanium, in fact it presents a coefficient of hardness of about ten times compared to titanium and this difference in performance could lead to damage of the connection. This problem has been analyzed by several authors. In a study of Yuzugullu and Avci (Stimmelmayr M. et al . , 2013) was analyzed in the interface

between implant and abutment constructed with two different materials , in a case of alumina , in ' another titanium.

Observation to the scanning microscope the second group gave significantly better results as regards the gap after the load test.

A second study (Stimmelmayr M. et al., 2013) reported survival rates of restorations on implants with zirconia abutments cemented on titanium core, at 44 months were not observed fractures or other damage. A third study (Farbauten C. et al., 2013), more recent than the above mentioned, he tried to settle the issue by comparing the mechanical characteristics of fatigue resistance and mechanical stress of zirconia abutments instead of zirconia abutments with titanium core, also the samples after the test load were also analyzed by SEM. The strength of the abutments of the titanium core group was significantly higher than those in the comparison group; the average value of the fracture group made entirely in zirconia was sufficient to ensure acceptable clinical results in the anterior but not sufficient for the posterior. The resistance values are obviously not dependent on the construction of the abutment alone but also by constructive geometry, be it internal or external hexagon, highlighting, in the two groups different types of fractures. In summary, maximum was evidenced a statistically better fracture resistance in implant solutions that had a larger diameter and, with the same diameter, in those zirconia core with titanium.

It was not done the comparison with the solution clinically frequent, consisting of cemented zirconia abutments on titanium abutment attached to the implant. Furthermore, this study had the limitations of any in vitro study and not analyzed minimally the economic aspect, the construction of a core abutment with titanium has costs much more than a single material, and this aspect is not of secondary importance.

It should also be said that the zirconia, as seen before, has absorption characteristics of the forces applied to it much less compared to other composite materials, which opens up another discussion on what kind of solution can be used to combine the mechanical strength, the affordability and the absorption capacity of the occlusal stress.

2.2-The CAD/CAM.

The evolution from the metal-ceramic to fully ceramic seems to be oriented towards

technology-based digital design software CAD CAM, introduced on an industrial scale in the seventies, but only got to the dental field in the eighties because of the cost of machinery. The process of making prosthetic with this technique can be divided into three phases, can be summarized in: data capture through a digital scanner, processing the data and production of the artefact through different techniques.

The first stage consists in the acquisition of a digital model of the tooth or abutment that can be created thanks to the technology based on a laser scanner or a CCD camera. According to the company is preferred an alternative or the other, bringing out solutions with different characteristics but still valid for a clinical point of view as regards the marginal gap or the characteristics of boundary contour.

Similarly the reworking is developed by ad hoc softwares, which, in their diversity have pros and cons, but do not constitute a weakness.

It is the final step in fact, the creation of the object, that presents completely different solutions, there are several alternatives to the methods of implementation:

The methods for subtraction, in which one starts from a structure larger than what you want to achieve and then go to act with a series of cutters for shaping the desired project.

The method for addition that provides for a process of adding particles of material as a function of the requests of the software. Stereolithography in which a laser beam through a resin layer is made to pass from a liquid phase to a solid modeling, in a sort of 3D printing, the prosthesis.

The FDM, acronym that indicates the modeling technique to molten metal, which uses a principle similar to the method described above but in which the filler material is realized with a jet of molten material that creates a three-dimensional model due to movement on three axes of the support base.

The SEBM (Selective Electron Beam Melting) uses a beam of electrons, created in vacuum conditions, to increase the chemical energy of binding of a material to take it to a solid state in selected areas.

The SLM has a laser beam impacting on pulverized material that modifies the characteristics of the chemical bond.

The CAD CAM method has proved its worth in the dental field the first time in 1998, where the American Dental Association, which in previous years had established minimum specifications considered for clinical application of the products, said that the artifact so

produced satisfy the request of a marginal fit of less than 50 μm.

There are numerous studies comparing prosthetic products manufactured by this method with products created using traditional methods, in particular, seek comparisons with regard to certain solutions, such as crowns.

The crowns are in fact a method frequently used in the restoration of individual teeth fixed prosthetic treatment, in a study for the three-year survival crowns fabricated with metal-free techniques have overlapping rates to those formed in metal ceramic, the fracture of the ceramic crowns is obviously the most dangerous event for this type of prosthetic restorations.

Comparing crowns fabricated using CAD CAM made of lithium disilicate and crowns fabricated with zirconia with traditional technology, are evident optimal results for the first group; the reason is probably the absorption capacity of the occlusal stress.

Also interesting is the analysis of the which type of glass ceramic is best to use for the cover of zirconia. In some studies went out that, in a comparison of crowns produced by CAD CAM using three different techniques, the group built with traditional veneers technique gave results slightly superior to samples produced with overpressing technique, while the sintering technique has proven to be the most effective.

The overpressing technique starts from the abutment made following the initial scan, from there you make are made a number of constructive steps when initially applied a thin layer of liner, in accordance with Article IPS emax, which is in second place heat-treated at 960 ° .This product is then placed inside of a structure created in IPS PressVEST that is placed over the model after the technician has made in wax modeling of the finished structure. At this point, after pouring the wax, using a special ceramic, IPS emax ZirPress, that, having a coefficient of optimal thermal expansion than zirconia, is applied by pouring into an environment at a controlled pressure.

The samples are produced by sintering, the technique that has been proven the best in the prostehsis; it consists in the creation of a crown made of glass-ceramic created by CAD CAM in order to have a fit that can allow the insertion of a low viscosity fused ceramic. This crown is applied to the abutment and, after removing excess ceramic material, thermally treated at 850°C. This construction technique lead to the realization of models presenting a value of breaking load of approximately 6200 Newton, compared to 3700 achieved by the traditional technique of construction.

The materials used with the CAD CAM technology are different, the mechanical

properties are highly variable, in order to give a quick overview is attached graph obtained by Jordan Russel (Russel G., 2006).

It is interesting to observe the first two places, on the one hand can be found the zirconia material already described, on the other hand a nanoceramic material recently introduced and

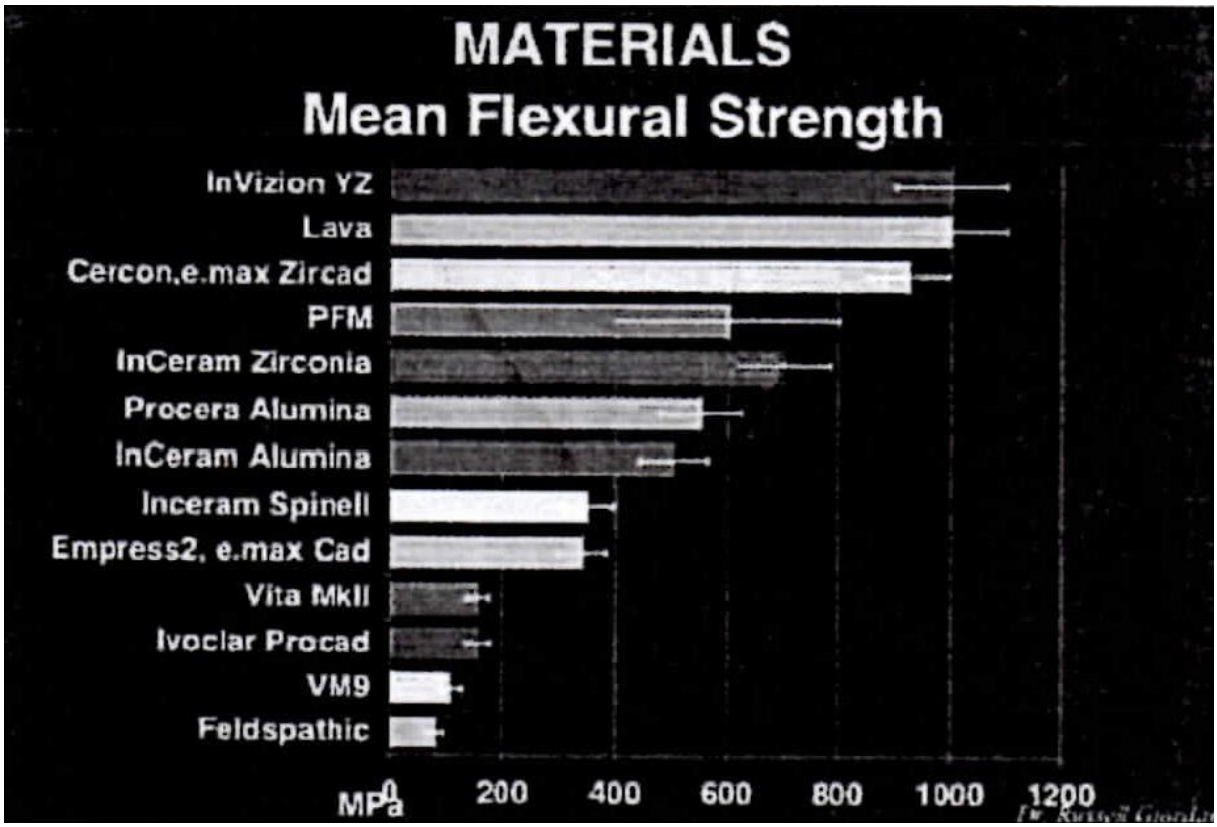

Figure 2.1: Graph obtained by Jordan Russel.

subject of the experimental part of this thesis.

2.3 Lava Ultimate.

Lava Ultimate is a nanoceramic material result of 3m research; it presents interesting aesthetic and mechanical characteristics. Lava Ultimate is on market and is recommended by the American agency for the design of different prosthesis on natural teeth or on implants.

This versatility of use is derived from the structural characteristics of the material: the atomic structure, of which it is composed, is based on the technology of nanomaterials; in particular it is a nanoceramic resin. This class of materials is able to combine the advantages

of ceramics based on nanotechnology and resins to high crosslinking.

On one hand there is the possibility of a processing typical of the resin, on the other hand the mechanical characteristics similar to ceramics; the aim that the company wants to achieve in the realization of this material is to take the best features from each component.

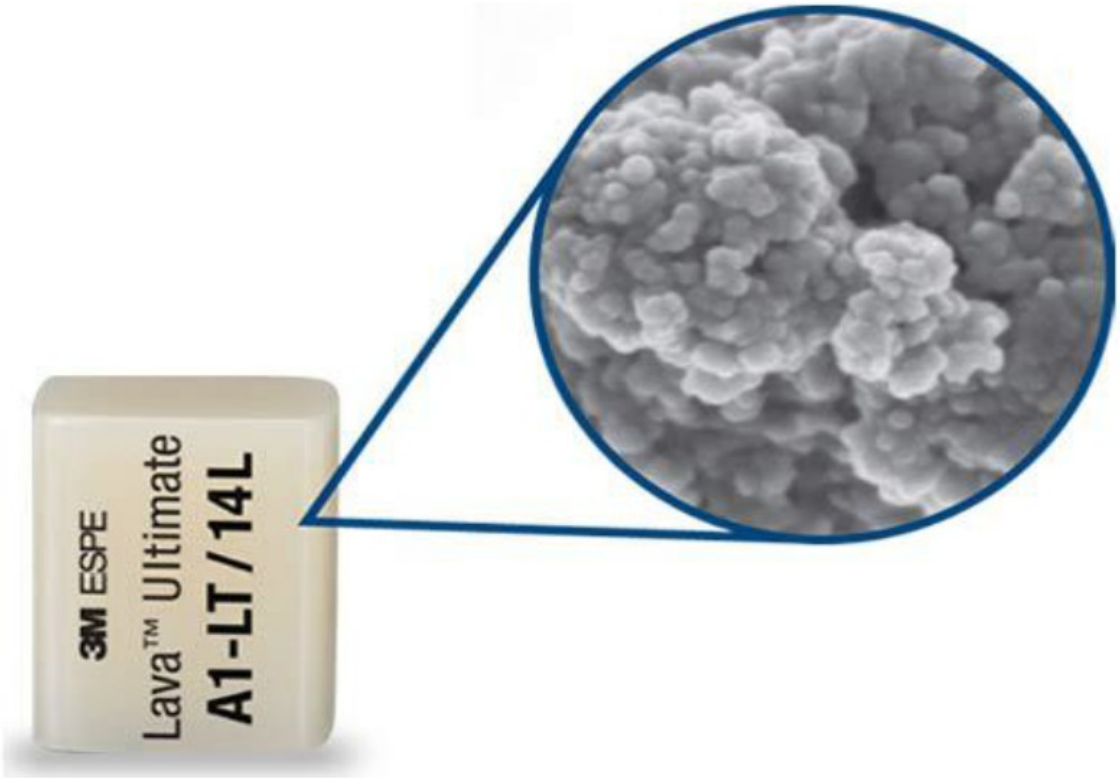

Figure 2.1: Lava Ultimate ready to work with CAD/CAM.

Lava Ultimate at the atomic level is comparable to a reticulate in which is alternated different materials, ordered and programmed to avoid the creation of points of possible fracture due to inadequate structural characteristics. It is composed of about 79% of modified surface nanoceramic particles. Such particles are composed of three different ceramic filler (silica and zirconium), from 4 to 20 nm, which reinforce the polymer matrix at high crosslinking.

The ceramic fillers are a combination of silica filler (no agglomeration/not aggregate, of 20 nm), fillers zirconium (not agglomerate/not aggregate, from 4 to 11 nm) and filler cluster of silica/zirconia (silica particles from 20 nm and particles of zirconium from 4 to 11 nm).

The monolithic restorations made with Lava Ultimate stand for their aesthetic with color and fluorescence very similar to natural teeth, the restoration can also be customized

according to the characteristics and the patient's subjective, thanks to a choice of colors and translucency based on eight shades and two levels of translucency.

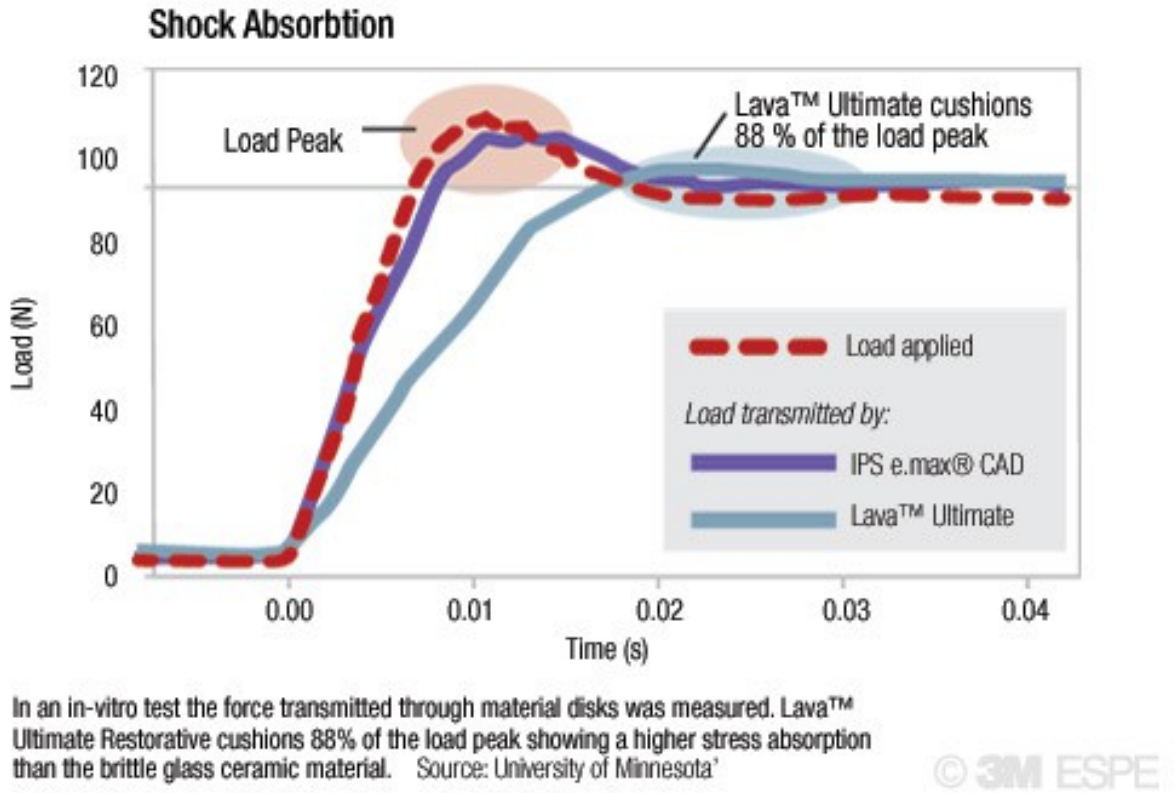

Figure 2.2: Shock absorption of Lava Ultimate compared with the load applied.

From the point of view of the mechanical characteristics, is noticeable the values that, as regards the abrasion, are compatible with the natural teeth and a modulus of elasticity comparable to dentin, which is a value particularly interesting, from the point of view of the capacity of absorption of shock and occlusal trauma (figure 2.3), whereas this material is often used for the construction of crowns of teeth previously treated endodontically that have mechanical characteristics considerably lower than the vital tooth, since the loss of hydration will inevitably lead to a considerable increase of the possibility of fracture.

The material also can be used for the construction of prosthetic piece adapted to be cemented on titanium abutments fixed on installations, in this case the importance of having an elastic modulus optimum appears evident: masticatory forces will be entirely on the plant to discharge and the ability to have a material that is able to absorb any trauma by acting as a shock absorber is a large added value to the use of Lava Ultimate in clinical practice.

It is worthwhile at this point to consider in depth the mechanical properties of this

material are useful in this regard graphs is detected by the producer test, both by independent studies.

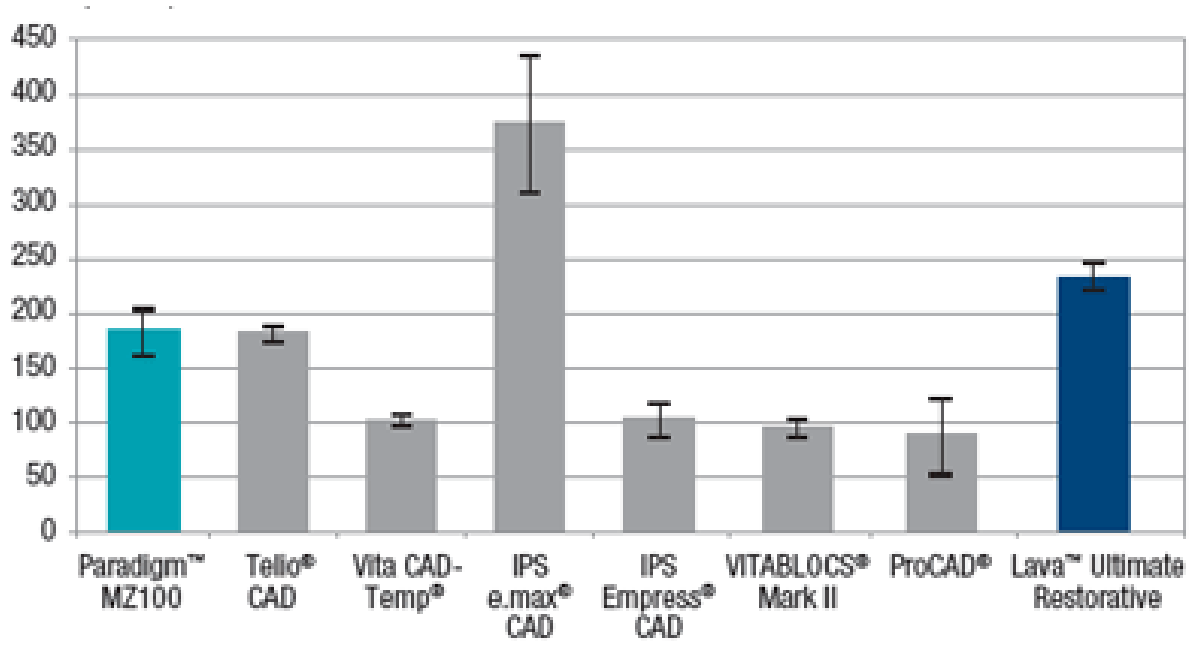

Figure 2.3.

In this graph (company data) is notable the resilience, I.e., the ability of a material to absorb mechanical energy by deforming elastically and then return to the original shape; in other words, the maximum amount of energy absorbed per unit volume. From the point of view of the flexural strength and flexural modulus observe that the flexural strength of Lava Ultimate is statistically superior to that of other comparable materials such as IPS Empress and eVITABLOCS Mark II, therefore more similar to that of the reported values for the human dentin.

A lower flexural modulus binds to a greater deformation under load, suggesting that Lava Ultimate is more prone to absorb stress compared to the glass-ceramics.

Furthermore, the combination of high strength and low modulus translates into a greater resilience. The fracture strength of Lava is completed statistically higher than that of IPS Empress and VITABLOCS Mark II, with the result of a greater long-term durability.

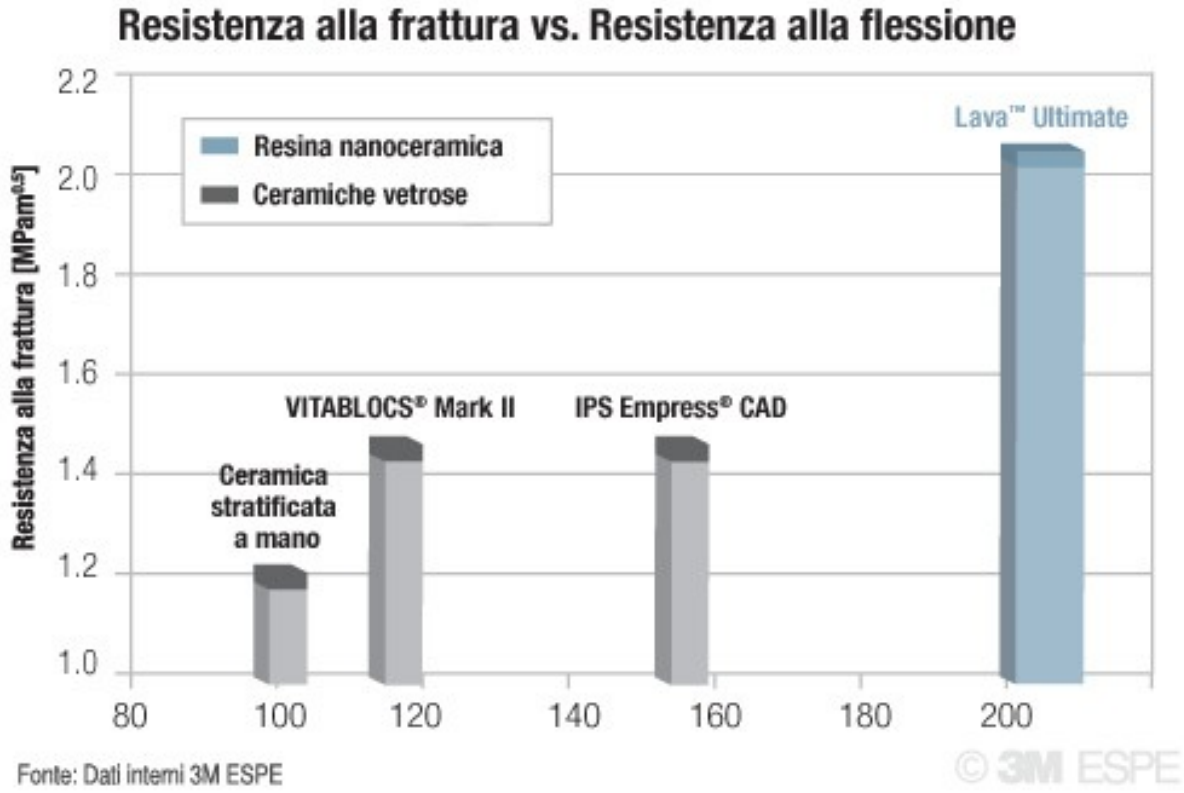

Figure 2.4: The graph describes the values of flexural strength of Lava Ultimate.

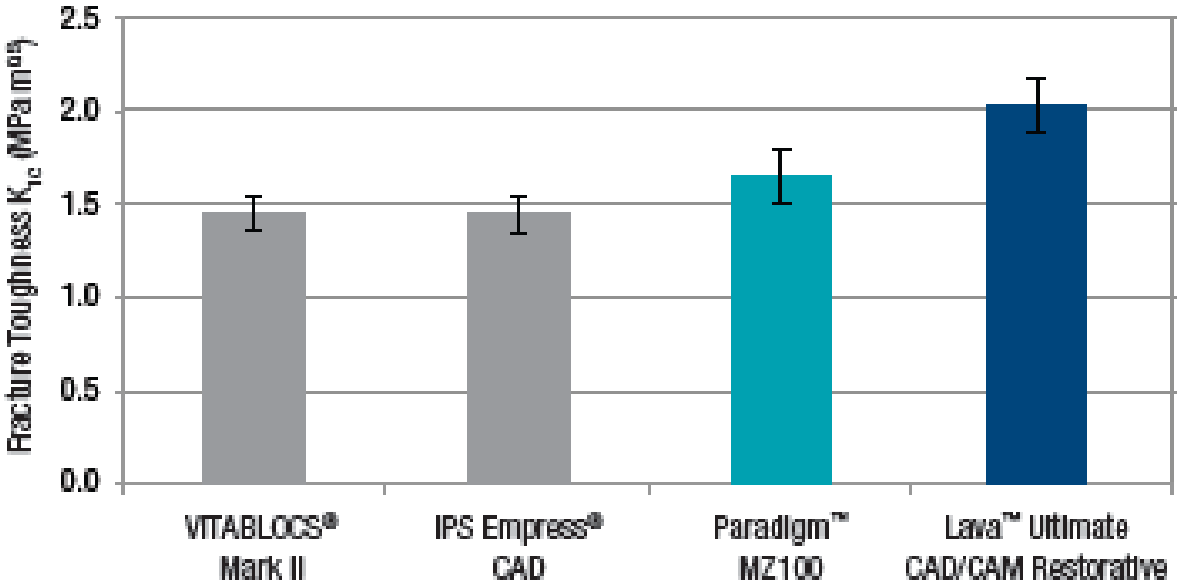

Figure 2.5: The graph shows the values of rupture of the samples subjected to the test load sketched on the figure, here we observe the excellent results obtained from the material.

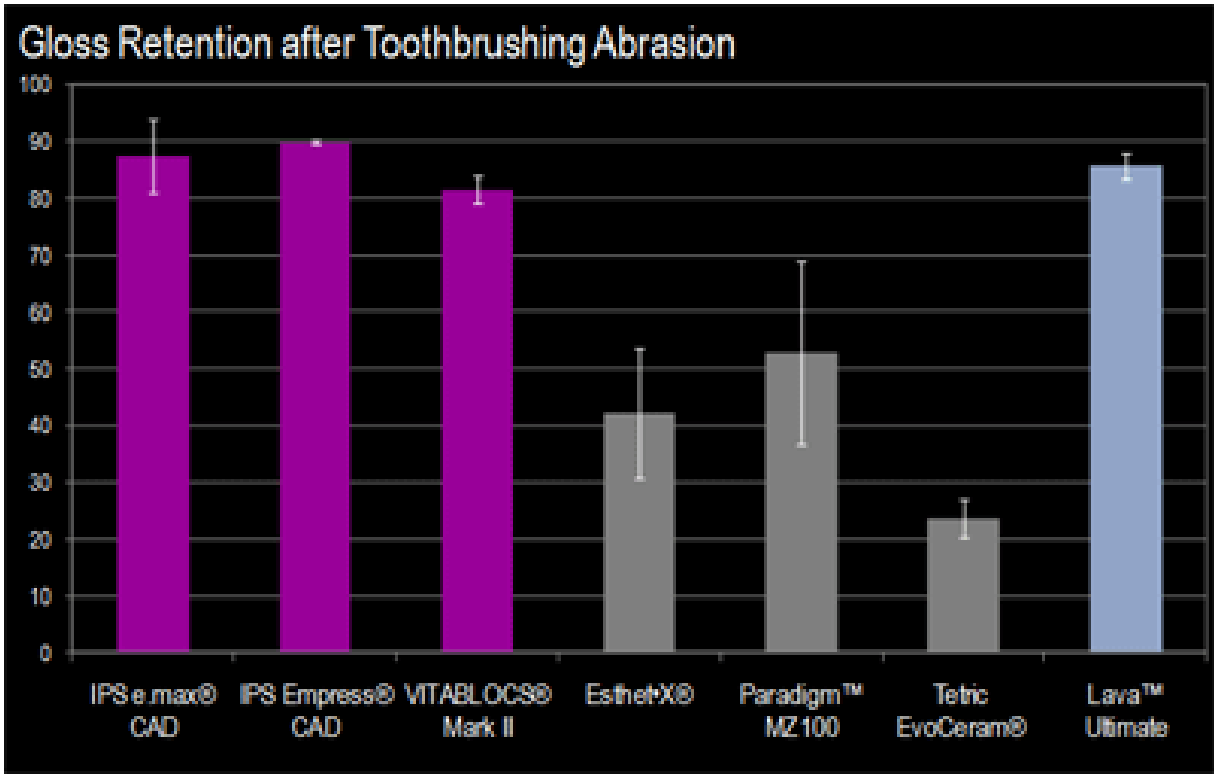

Figure 2.6: In this graph we see instead the values abrasion resistance, compared with other materials.

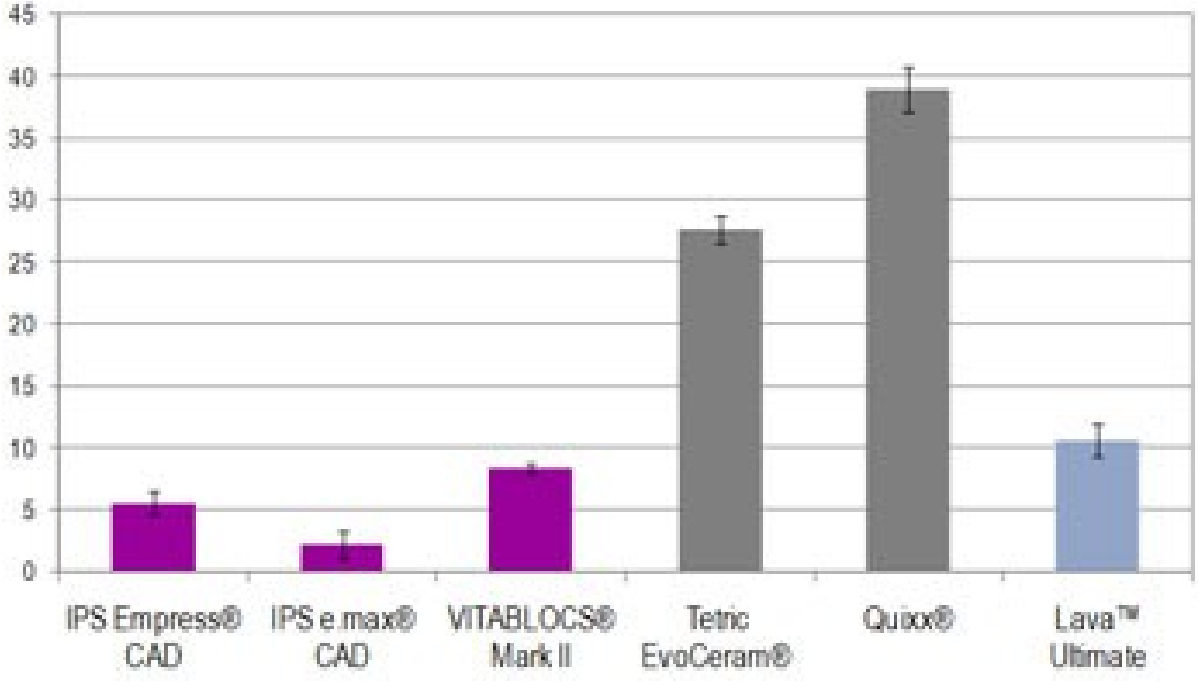

Figure 2.7: Stain resistance diagram.

Also interesting are the values observed in the previous graph, in which the material is subjected to an empirical test of resistance to staining, soaking the samples in red wine for 46 hours it was observed the color change of the various materials, giving a numerical value on the basis of the analysis to the colorimeter. Parameter rather important in the case of aesthetic restorations sectors.

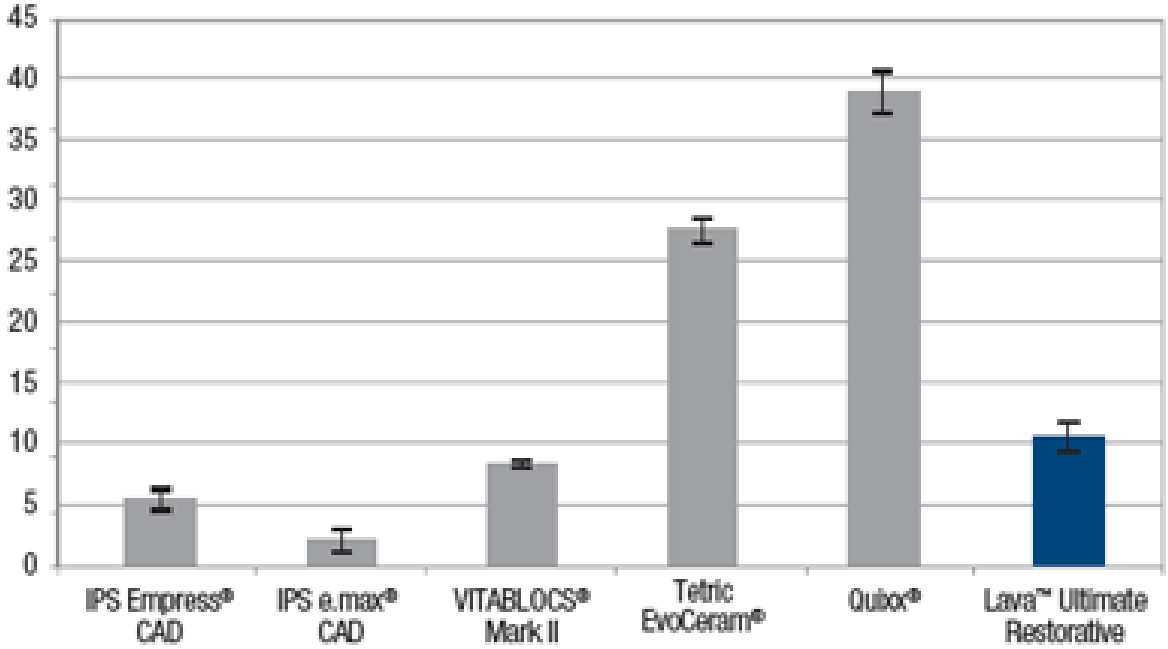

Figure 2.8: Bacterical resistance diagram.

Here can be seen the bond strength of the plate, the various materials, immersed in human saliva for 26 hours, were then analyzed under a microscope for the assessment of bacterial adhesion, give the results listed above.

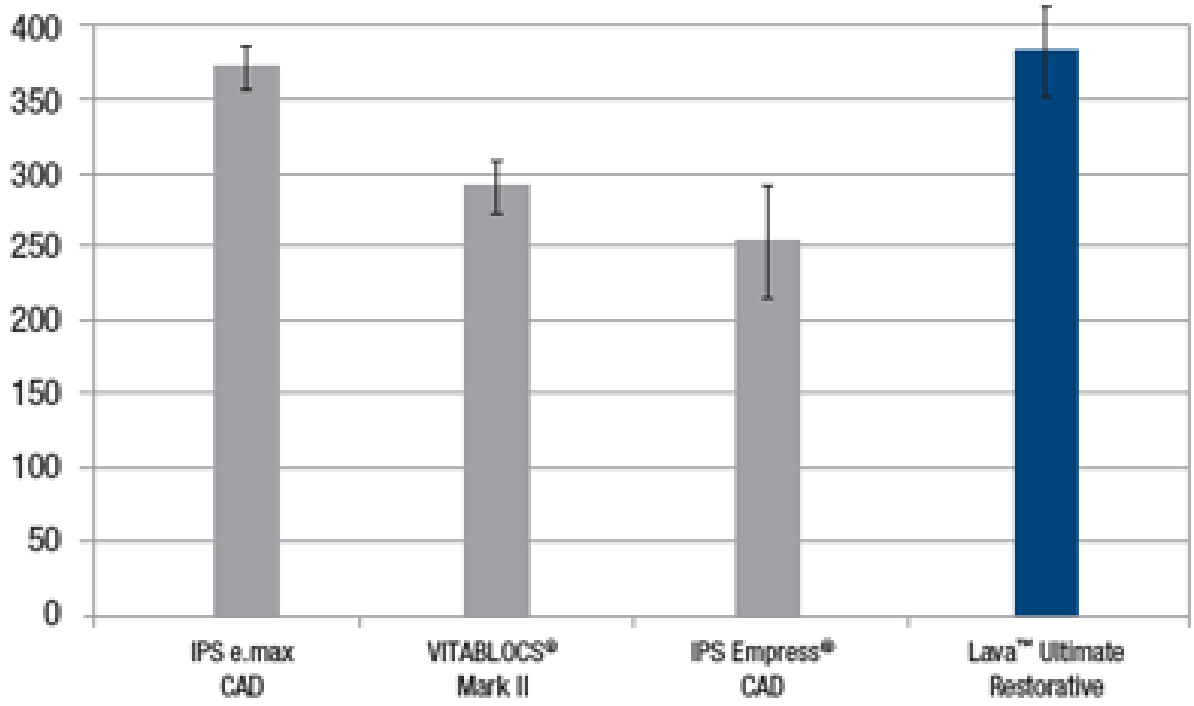

Figure 2.9: Compression strength in MPa.

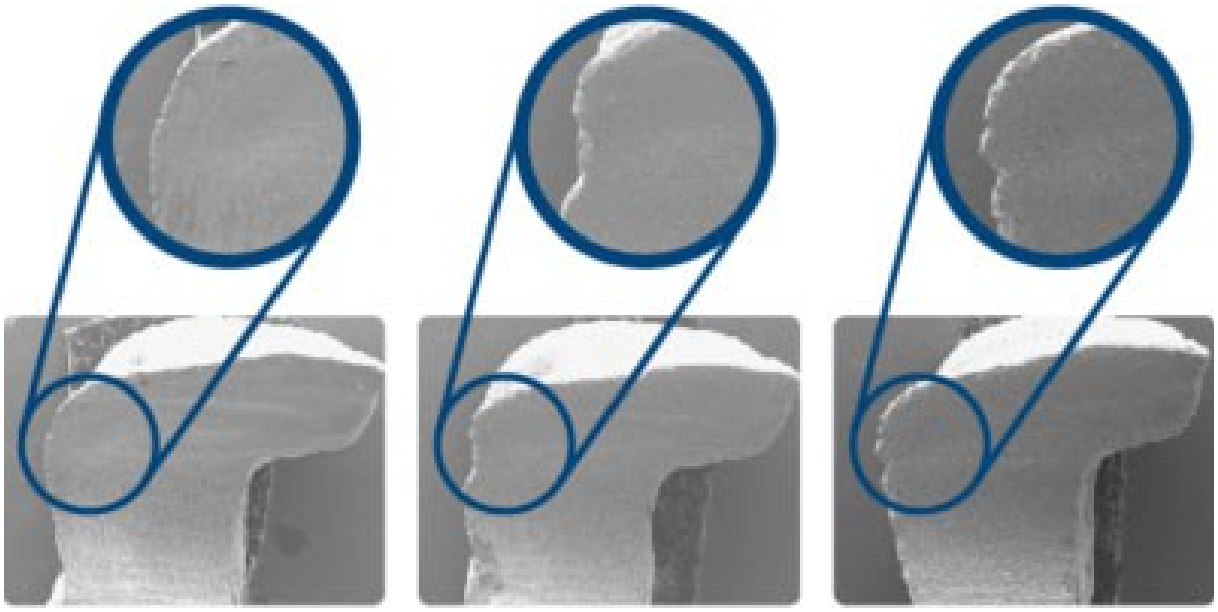

Figure 2.10: Surface enlargement of different material: Lava Ultimate, feldspathic and lithium disilicate.

In the figure 2.10 can be seen an enlarged section respectively: Lava Ultimate, feldspathic and lithium disilicate, appear evident surface characteristics are completely different.

This new material offers a greater resistance to bending and fracture with the result of a long-term durability.

The initial flexural strength of dry samples is the parameter most used to compare the resistance of the materials. However, the clinical use is always accompanied by the presence of humidity and mastication has dynamic nature. In the study from which it has taken the graph described here, has been explored the difference between the initial force in the dry and wet and the limit of flexural strength of the material with respect to feldspathic glass ceramic and glass-ceramic lithium disilicate. The nanoceramics resin was the only one of the tested materials that maintained its initial resistance in the passage from the condition of dry to wet. The initial strength of Lava Ultimate is superior to that of glass ceramic and feldspathic lower than lithium disilicate.

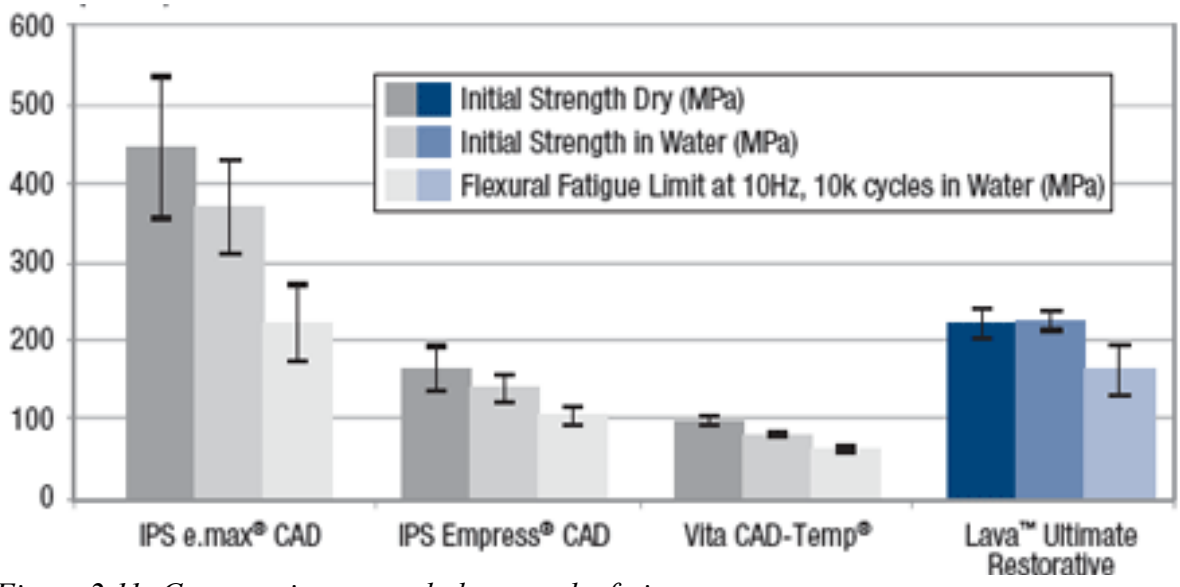

Figure 2.11: Compression strength decrease by fatigue.

All materials show a decrease in strength as a result of cyclic fatigue in water . The maximum flexural strength (FFL) of Lava Ultimate is at 74% of its initial resistance to dry, while the lithium disilicate remains at only 50%. The FFL feldspathic glass ceramic was 64% of the initial resistance to dry. It will be compared the mechanical characteristics of resistance to static and dynamic load of two prosthetic articles of similar shape and size built on an identical support implant, consisting of a titanium implant inserted inside a resin support, in which was screwed a titanium abutment that will be cemented the two prosthetic alternatives.

The first solution analyzed consists of a zirconia abutments created with CAD CAM technology which was cemented a crown nano ceramic resin also built with the same technique. The second prosthetic solution, identical in shape and size to the first, is instead constructed from a single block of resin nano ceramic, the same type used for crowns described above, directly cemented to the abutment. After making the mechanical tests are going to verify the characteristics of cementation by comparing the measured data to the tomograph before and after the test load dynamic interface between resin nano ceramic crowns and abutments in zirconia.

CHAPTER 3
Instrumentation.

3.1-MTS 858 MiniBionix.

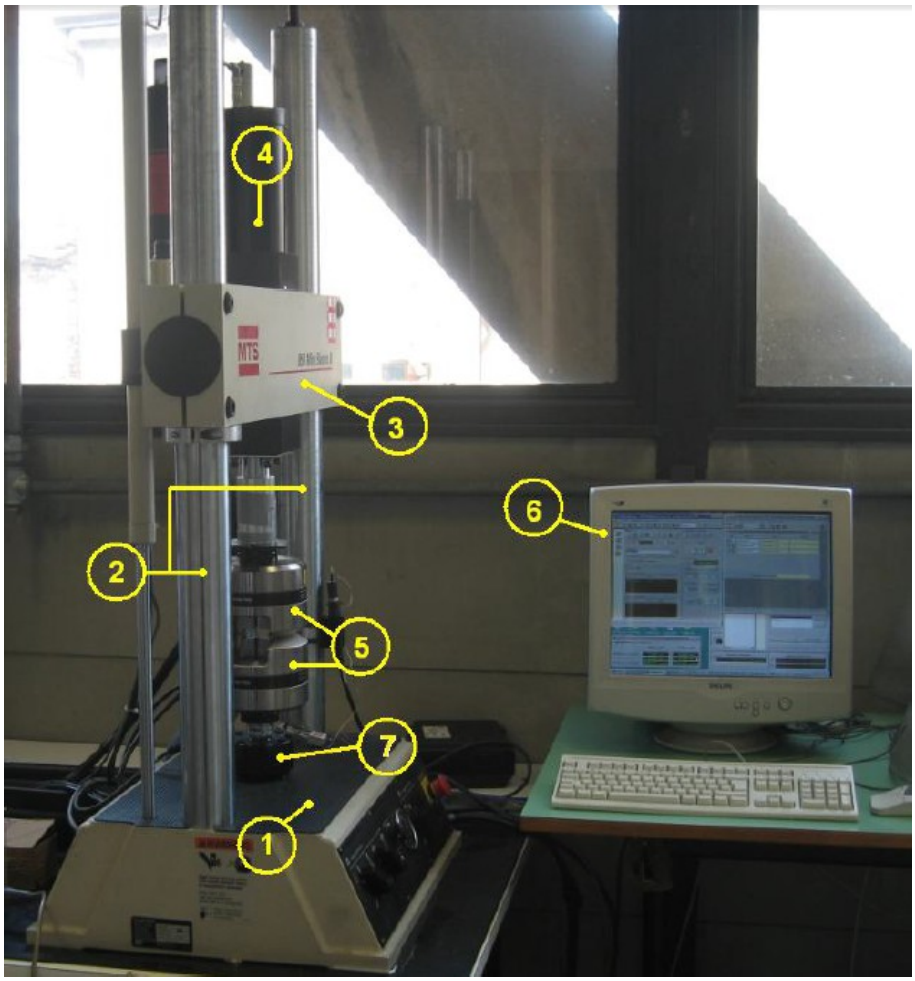

Figure 3.1: MTS 858 Minibionix.

The experimental tests were carried out using the testing machine MTS 858 Mini Bionix II equipped with a load cell of 15 kN with electronic Testar IIm. It is a standard hydraulic machine for tensile and compression.

The system is built of a base (1) on which are attached two vertical cylindrical guides (2) allowing the sliding of a horizontal cross member (3).

At the crossbar is connected to a double acting hydraulic piston (4) responsible approach and removal of clamps gripping (5).

The clamp is controlled by two commands on the base of the Minibionix; the gripping pressure can be regulated with a valve and near is placed a pressure gauge. Normally such pressure is about 100 MPa, but to not crush the support of the abutment it has been lowered as much as possible, that is about 40 MPa.

The punch through which the load was applied is made of an iron cylinder on which had been built a hemisphere of Filtek 3M made to adhere by the application of adhesive on the surface of the cylinder previously sandblasted. The load has been applied according to a specific protocol.

The resin support has been gripped laterally but, to avoid any form of slipping of the sample on the vertical axis is preferred to insert a support consisting of a iron cylinder as a "prolongation" for the resin base.

3.2-Load procedure.

- STATIC LOAD TEST

In the static load test the punch, consisting of a support incident on the occlusal surface of the tooth, it will apply an increasing force up to lead to breakage of the three samples subjected.

In particular, the force has been applied according to a protocol of loads, including an ascending preloading ramp set from zero to 50 N, this aims to make the punch to approach and brings it in contact with the occlusal surface.

Once the application of the load, the machine delayed for five seconds and then proceeded in increasing the force until the displacement of the punch would not exceed a threshold value of two millimeters, corresponding to the inevitable breakdown of the sample.

The apparatus was calibrated to achieve a maximum force of 3 kN and an data sampling frequency of 100Hz.

- FATIGUE TEST.

The load test has been performed with the help of a test machine that has imprinted the load by means of a cylinder constructed of the composite of seven mm diameter which was replaced for each test, in order to prevent “cone crack” fractures.

The fatigue tests which are more interesting, because they show the variation of the residual life of the specimen whether and how varies the modulus of elasticity of each implant.

For convenience cycles were taken at a distance greater than the intervals used during sampling. While the acquisition files presents 10 cycles sampled every 1000 starting from the first, in the results will be displayed instead 10 cycles every 10,000.

The initial loading protocol (sine load application with a constant frequency of 5 Hz) was thought to involve the following steps:

- 0 to -50 N 5000 cycles
- 0 to -400 N 25000 cycles
- 0 to -600 N 25000 cycles
- 0 to -800 N 25000 cycles
- 0 to -1000 N 25000 cycles
- 0 to -1200 N 25000 cycles
- 0 to -1400 N 25000 cycles

As described by P. Magne, the first part of the test simulates the normal range of use in the posterior areas, i.e., the 600 N load normally present in the masticatory as noted in the article by Bates; in the second part are simulated bruxism events or masticatory trauma as described by Gibbs.

Subsequently, the loading protocol was reviewed, because the detachment of the punch from the sample occurred, generating a hammering on the sample, when the cursor passed to the top dead centre.

The new loading protocol keeps the sine function shape and the 5Hz frequency) and it is:

- 0 to -50 N 5000 cycles
- -50 to -450 N 25000 cycles
- -50 to -650 N 25000 cycles
- -50 to -850 N 25000 cycles
- -50 to -1050 N 25000 cycles
- -50 to -1250 N 25000 cycles
- -50 to -1450 N 25000 cycles

The choice of this protocol is also supported by Article Kelly that identifies it as a compromise between incremental load test and durability test.

Figure 3.2: Specimen and puch gripped on the testing machine.

3.3-Industrial tomograph.

The Wenzel CT tomograph site at Unilab Laboratories Industriali Srl Monselice, is able to perform, on the internal and external structures of a component, geometric-dimensional reliefs, analysis of material defects (cracks, porosity cavities, inclusions,

variations in density) and three-dimensional reconstructions of the external and internal geometries.

Areas typically interested by this technology are that of the components made of light alloys (die casting, gravity casting, investment casting), plastic (injection molding process) or assembled in multimaterial is of interest for which a geometrical or non non-destructive defectologic survey.

The CT technology is useful for validation of numerical simulations of injection, filling and solidification in the field of plastics and light alloys.

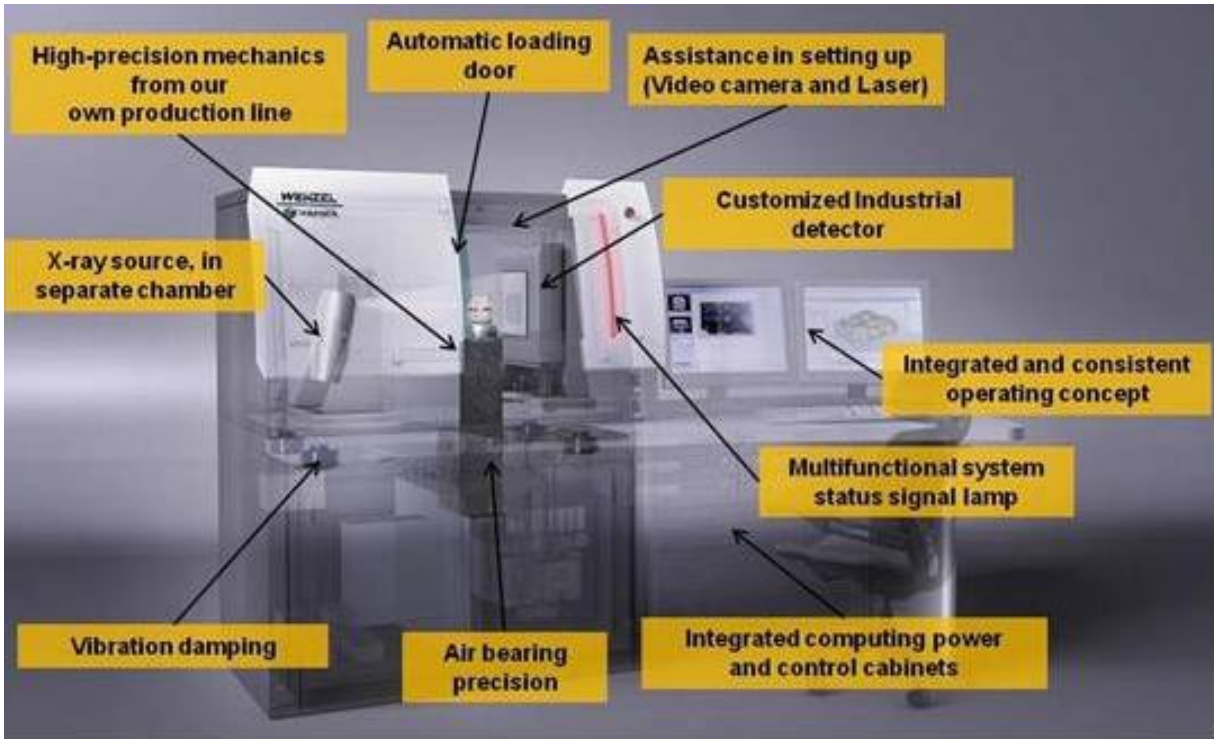

Figure 3.3

The tomographic reconstruction of an industrial product allows to:

- the display of the mode of coupling of the various components of an assembled product;
- the visualization of internal defects in terms of porosity, inclusions, cracks;
- the reconstruction of external and internal 3D-geometric parts;
- the comparison of a 3D CAD model with an actual piece, even for interior surfaces not in sight.

The ability to discriminate materials of different nature and density allows to isolate the internal components of an assembled virtually "pulling out" the entire component or analyze problems of coupling of two different materials (eg welding of two filaments, gluing surfaces, etc.) .

It also allows to study the plastic deformation of the body caused by mechanical coupling and to create virtual 3D models of the various constituents with an approach typical of the Reverse Engineering methodology.

The analysis of internal defects and potential of modern tomographic analysis software allows to observe the shape, size and distribution of the defects in the components, particularly critical to find areas where defects are concentrated, such that they can compromise the functionality of the product, support the designer in the early stages of industrialization of the product and in the stages of development and optimization of the production process.

The section in tomography of a mechanical component allows the analysis of the thickness compared to a reference CAD model while the chromatic map allows a local evaluation of the thickness variation across the three-dimensional volume of the component.

The analysis is particularly suitable for plastic components, made by injection molding, thermoforming or rotational molding, and metal components made from sheet metal by stamping or bending and shearing.

The following table (business data), please find attached the specifications of the machine we used for the purpose of the study sample:

Detail	**Units**	**Value**
Work piece diameter	(max) (mm)	250
Work piece height	(max) (mm)	300
X-Ray Source	Kv (max)	225
Number of Pixels	Megapixel	4.0
Pixel Size	Um (max)	45

CHAPTER 4
Materials and methods.

4.1- Manufacture procedure of the samples.

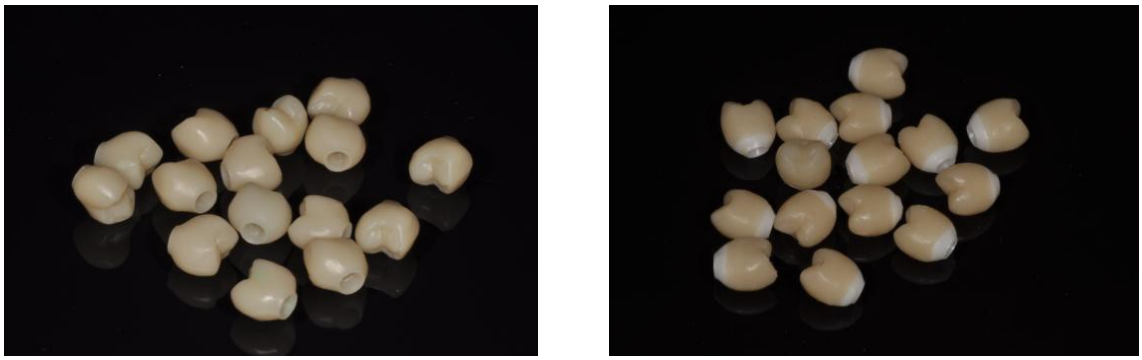

Figure 4.1: Two types of crowns; on the left the whole Lava crown and on the right Lava + Zirconia ones.

The 12 internal hex connection Aon Implant with a diameter of 4mm and length 11mm, were embedded in resin Palapress in a standardized way. The supports in the resin after being perforated with a drill given by the manufacturer, were subjected to tapping in order to allow the insertion of the implant through the use of a ratchet set to give a maximum 60 N of force; this limit was reached only in the final part of the screwing of a sample. To the 12 implants was fixed titanium castable abutment, which has been, once fixed to the structure, subjected to blasting with aluminum oxide of diameter less than 50 microns used in a pressure of about three atm.

The treatment was verified visually by controlling the loss of reflective properties of the material that is passed from one state to a glossy finish. From this common structure, we started the construction of the two sample groups.

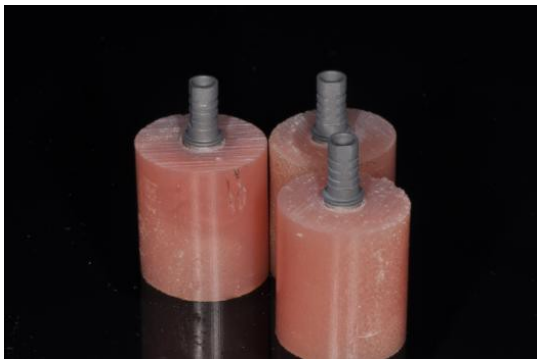

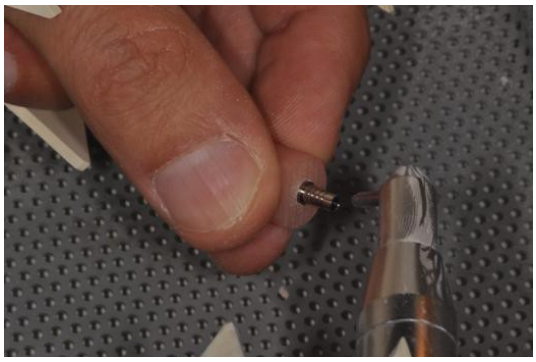

Figure 4.2: Resin supports with the implants.

- First group :

Figure 4.3: Example of Lava+Zirconia specimen.

The first group consists of six zirconia abutments made with CAD CAM technology and other six superstructures (crowns) in nano-ceramic resin nano.

As expected from the information provided by the manufacturer, for the cementation between the zirconia and the nano ceramic resin superstructure was used Relix Ultimate. The crowns were in Lava Ultimate and internally sandblasted with aluminum oxide and the same treatment was used for the pillar in Zirconia, both on the part that would have accepted the system and on the coronal part. Before cementation between crown and abutment has been applied a layer of adhesive Universal Scotchbond both on the inner surface of the crown and on the implant surface, which was then distributed through a compressed air jet to 3 bars.

Once is identified the correct direction of insertion of the crown was kept constant pressure on the structure while using spontaneous polymerization by Ultradent VALO lamp for forty seconds after removing any excess by micro-brush. The samples thus obtained were fixed on the titanium pin after treatment with Scotchbond Universal, cementation with RelyX Ultimate occurred which was then light-cured for forty seconds after removing the excesses of course.

- Second Group

Figure 4.4: Whole Lava specimen example.

The second group consists of six samples formed integrally of nanoceramic resin, starting from the same CAD project used for the samples of the first group. Lava Ultimate implants were placed directly on the pier after the standard titanium dioxide powder blasting with 30 micron aluminum (Cojet 3M) and the titanium abutment that the inside of the crown and the application to the bonding surface of the prosthesis by Relix Ceramic Primer following the instructions provided by the manufacturer. The cement was then performed using the resin cement RelyX Unicem.

After removing the excess photopolymerization was carried out using a special lamp (Ultradent Valo) for a total of 40 seconds around the prosthetic crown maintaining a constant pressure on the samples.

4.2-Manufacture method of the resin supports.

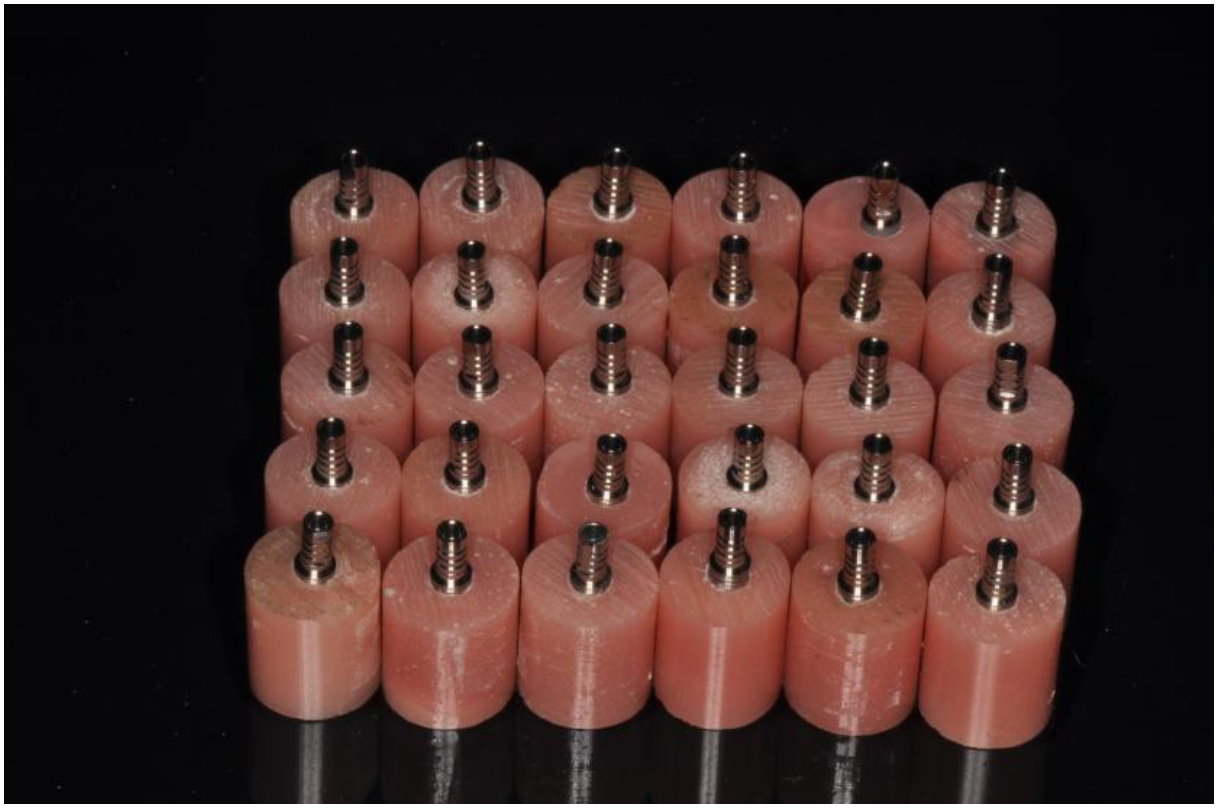

Figure 4.5: Resin supports.

The support in which the implants were inserted were made of resin Palapress, that is a resin for classical coatings or repairs of dentures, characterized by a pouring time of about 2 minutes and a processing time of up to 7 minutes. The choice of this resin was motivated by the mechanical characteristics of the same, in other studies in the literature (Magne P. et al, 2011) was used deeming mechanically comparable to bone.

It has the following characteristics: it is a cold-curing resin formed by two parts, one part of liquid consisting MMA 5-10% crosslinker, joint initiators such as copper chloride, additives, stabilizers and a portion of powder from the date that is PMMA copolymers with peroxides encapsulated, barbituric acid and pigments. Find its scope, normally in the production of dentures and repairs with a time of 7 minutes and work up to its polymerization.

For the realization of the supports resin has been used a hollow cylinder of plastic polymeric material of 12 mm diameter in which it was harden the resin casting; the walls, previously treated with a product that would limit the possibility of adhesion of the material, were characterized by a surface completely free of roughness, so as to remove easily the

cylinder material. Obtained the resinous cylinder with homogeneous characteristics, was sufficient to use a normal bench saw to create perfectly parallel cuts at the desired distance, in this case set to fifteen millimeters obtaining in this way the cylinders in which to allocate the implant structure. Then were garanteed the parallelism of the upper and lower surface and controlled the perpendicularity of the guide hole was using a bench lathe.

4.3- Manufacture of the punchs.

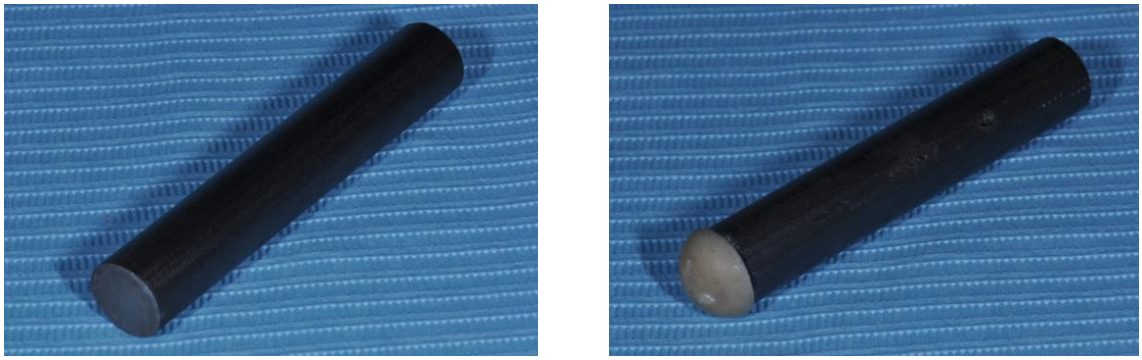

Figure 4.6: Punch.

The punch is made from an iron cylinder of diameter 10 mm and length 60 mm which was built in a hemisphere to a composite of the two ends.

The Filtek 3M has been made to adhere to the metal cylinder by means of a procedure consisting of a quote abrasive treatment with aluminum oxide of 50 um of particle diameter on the surface, and the subsequent application of the adhesive that, once uniformly distributed with compressed air and photopolymerized for five seconds by Valo lamp has been able to provide adequate support to the contribution of incremental ad hoc composite molded into the final shape through a die translucent.

The composite, as prescribed by the manufacturer was photopolymerized for twenty seconds.

4.4- Manufacture methods of the abutment in zirconia.

Figure 4.7: Abutment in Zirconia.

The zirconia abutment was created with CAD CAM technology from a wax model built by the engineer on the basis of the information techniques identified within the Magne 's article comparison, the scan of the model is then created in the pillar zirconia used in thesis.

In particular, from the constructive point of view, the pillar has been achieved in Lava Zirconia, starting from the scanning of the same device with a 3M optimized to give a good marginal fit.

The confirmation of compliance on the size and thickness of the artefact is given both by the CAD-CAM design, both from the control by CT.

4.5-Types of cements.

Ultimate Relix: RelyX™ Ultimate Adhesive Resin Cement is a cement self-photopolymerizable by 3M™ ESPE™ developed taking into account the specific needs of cementing the glass-ceramic. RelyX Ultimate has been designed for optimum performance in combination with Scotchbond™ Universal adhesive, which acts not only as adhesive self-etch or total-etch, but also as a primer for most of the surfaces of the restoration.

The formulation of the same RelyX Ultimate contains an activator for the auto-photopolymerization for Scotchbond Universal adhesive that eliminates the need to use a

separate activator and allows to avoid unnecessary operations.

Among the advantages of Scotchbond ™ Universal Adhesive there is the ability of adhesion total-etch and self-etch combined, integrated primer for glass-ceramic restorations, oxide-ceramic and metal, the bond strength to dentin etched constant wet and dry, and the virtually no postoperative sensitivity with total-etch and self-etch techniques .

Figure 4.8: Ultimate Relix.

The RelyX ™ Ultimate composite cement adhesive has instead as the advantages of being a cement self-photopolymerizable with the maximum bond strength, of presenting simplicity of use (self-photopolymerization activator integrated for Scotchbond Universal adhesive) and of having fluorescence similar to that of the natural tooth and high wear resistance.

Figure 4.9: Relix Unicem.

Relix Unicem: RelyX ™ Unicem Self-Adhesive Universal Resin Cement is a self-photopolymerizable suitable for the adhesive cementation of indirect restorations made of ceramic, composite or metal. With the use of RelyX Unicem is no longer necessary to perform the conditioning of the tooth and the subsequent application of the adhesive. The cement has a higher moisture tolerance with respect to the multi-step composite cements. RelyX Unicem cement releases fluoride ions and is available in various colors. Among its main features, there are high dimensional stability and tenacious adhesion to tooth structure. The resin matrix of RelyX Unicem is made from special multifunctional methacrylate monomers modified with phosphoric acid. These monomers provide a high degree of crosslinking of the matrix during the polymerization of the radicals. This leads to the high mechanical and dimensional stability of RelyX Unicem. Moreover, the phosphate groups of the monomers of methacrylic interact with the tooth surface, facilitating the autoadhesive process. The amount of inorganic filler contained in RelyX Unicem corresponds to approximately 70% of weight, the particle size (d [90] = 90% of filler) is less than 12.5 microns. The charge of the filler also ensures the radiopacity of the cement in all available colors. A portion of the filler is silanized and form a chemical bond with methacrylic monomers; another alkaline component (basic), neutralizes the phosphate groups residues of methacrylic monomers. This means that in the course of the polymerization reaction of the cement occurs adhesion to dentin and enamel, the increase of pH to a neutral value and the fluoride release. RelyX ™ Unicem Self-Adhesive Universal Resin Cement in the Clicker™ Dispenser is indicated for the permanent cementation of inlays, onlays, crowns, bridges, pins, pins in stumps and screws in ceramic, composite or metal.

4.6-Types of omplants and abutments.

The equipment, supplied by the company Aon, are titanium with hex connection internal diameter of 4 mm and length 11.5 nPOP E INT, while the zirconia abutment is to not rot. eight mm high.

Figure 4.10: Titanium abutment.

4.7-Project overview.

INDEPENDENT VARIABLES

The main indipendent variable are geometry solutions: Lava ultimate crown and Lava Ultimate crown with Zirconia abutment

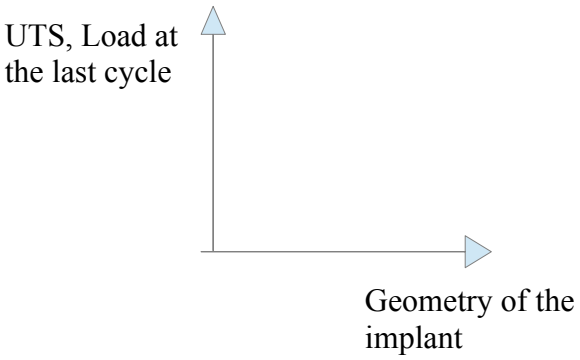

DEPENDENT VARIABLE

The main variable to be quantified is the Ultimate Tensile Stress and last load step in fatigue; because, because for reasons of complexity of shape is not possible to calculate a net section and an initial length to calculate stress and strain.

The specimens are in total 12; 6 for static tests and 6 for fatigue tests; each test has three specimen for every implant geometry.

CHAPTER 5

Results and data analysis.

5.1-Static tensile test.

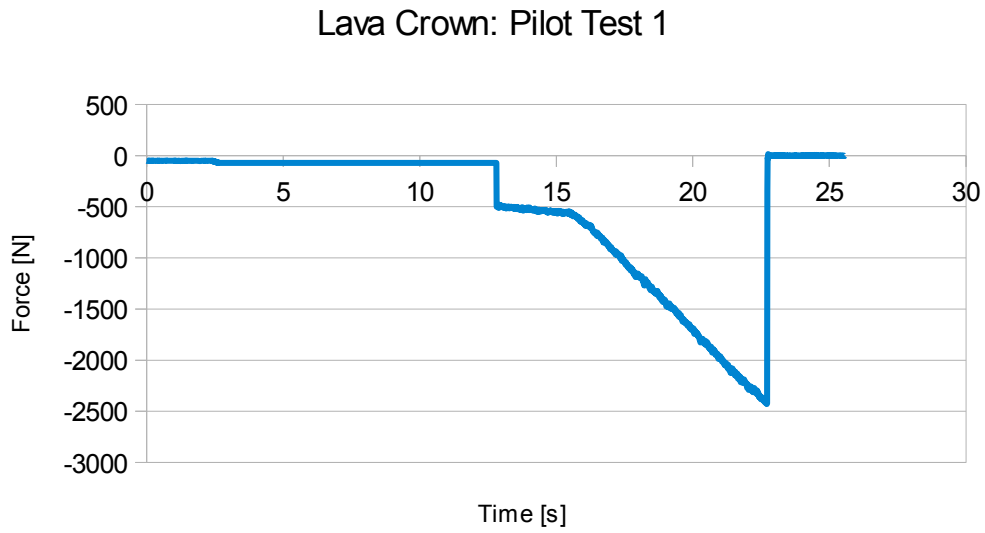

Figure 5.1.

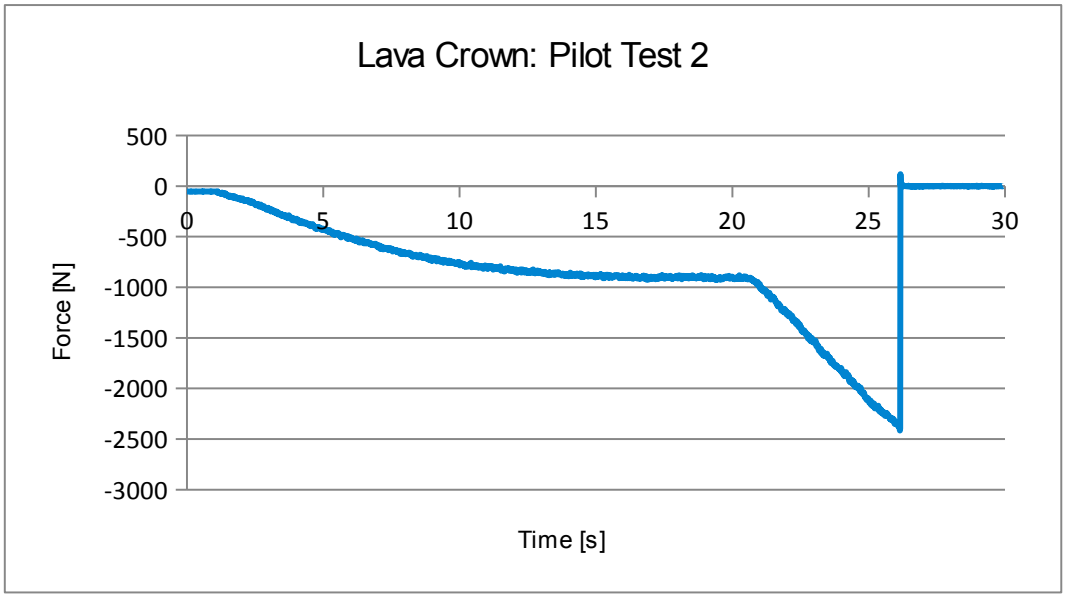

Figure 5.2.

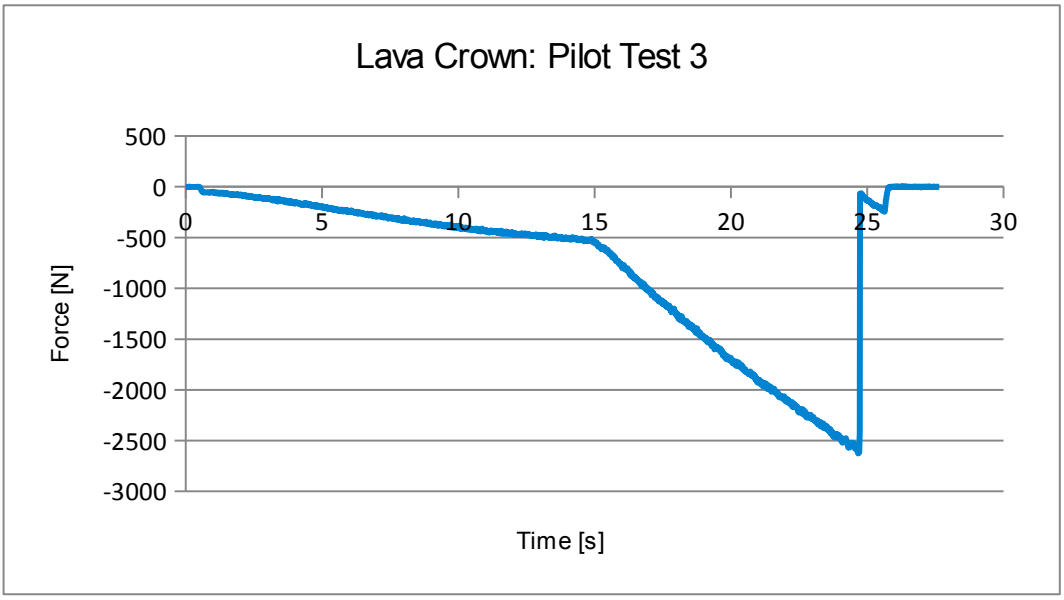

Figure 5.3.

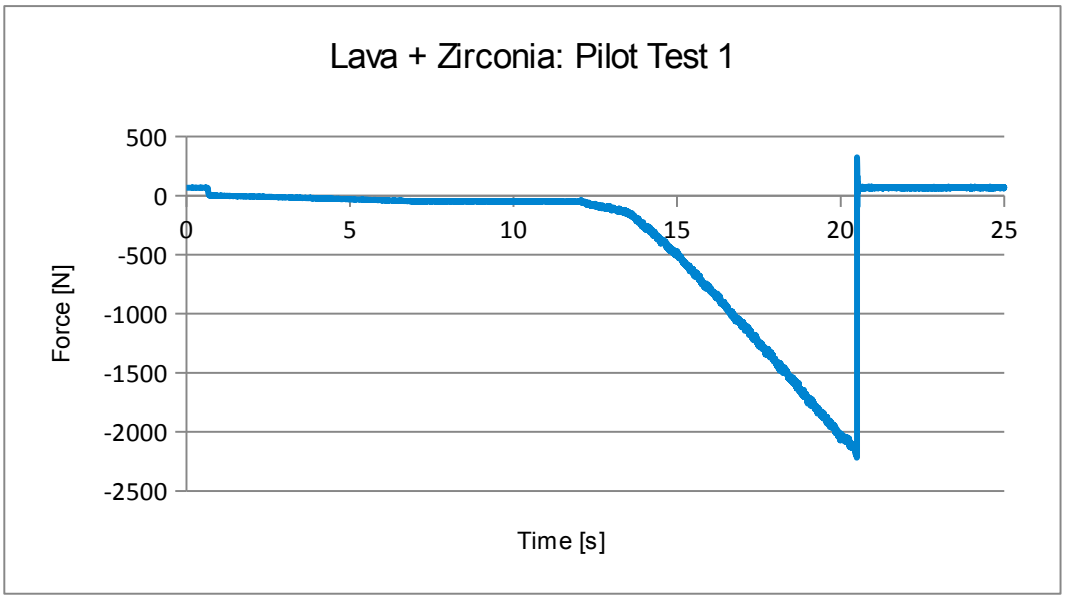

Figure 5.4.

Has been tested 6 sample for each geometry, and

Qualitatively the curves have the same trend. In fact, all have a first phase in which the MiniBionix impresses a contact load of approximately -50 N.

After the load increases and as can be seen each specimen responds differently, settling and adapting.

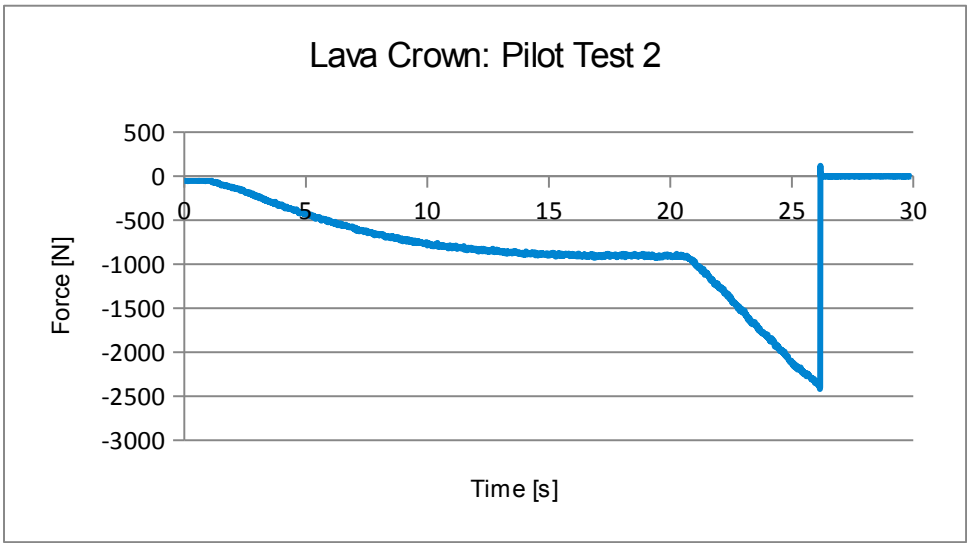

Figure 5.5.

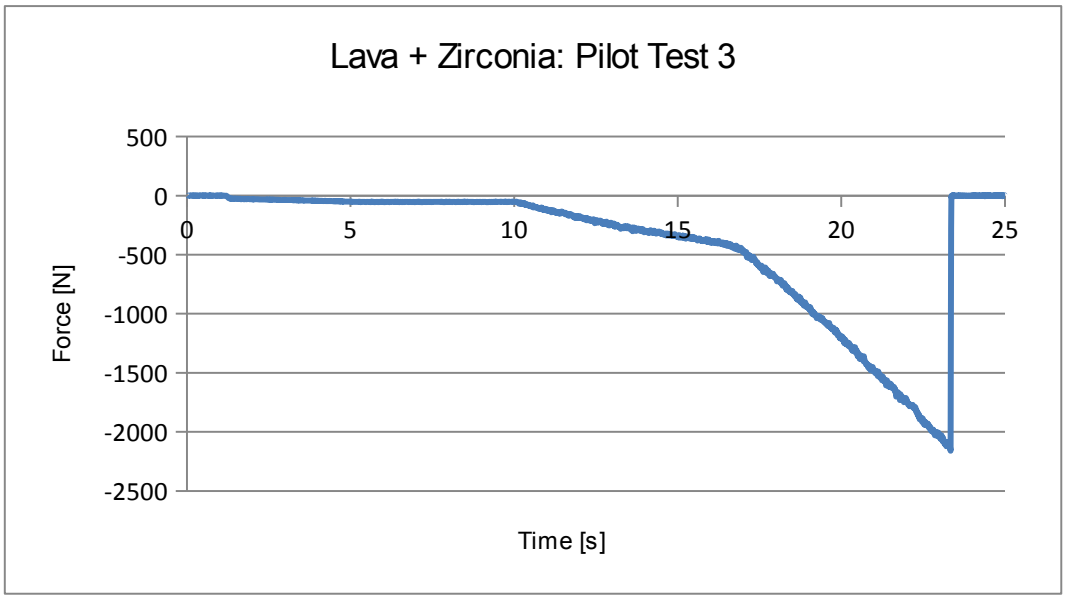

Figure 5.6.

All specimens have a final region of linear response, then occurs suddenly the brittle fracture of the samples.

Lava + Zirconia	-2429,5876 [N]	-2415,8201 [N]	-2625,853 [N]
Whole Lava	-2219,7847 [N]	-2301,9517 [N]	-2159,8777 [N]

Figure 5.7: Strength comparison of the two type of samples.

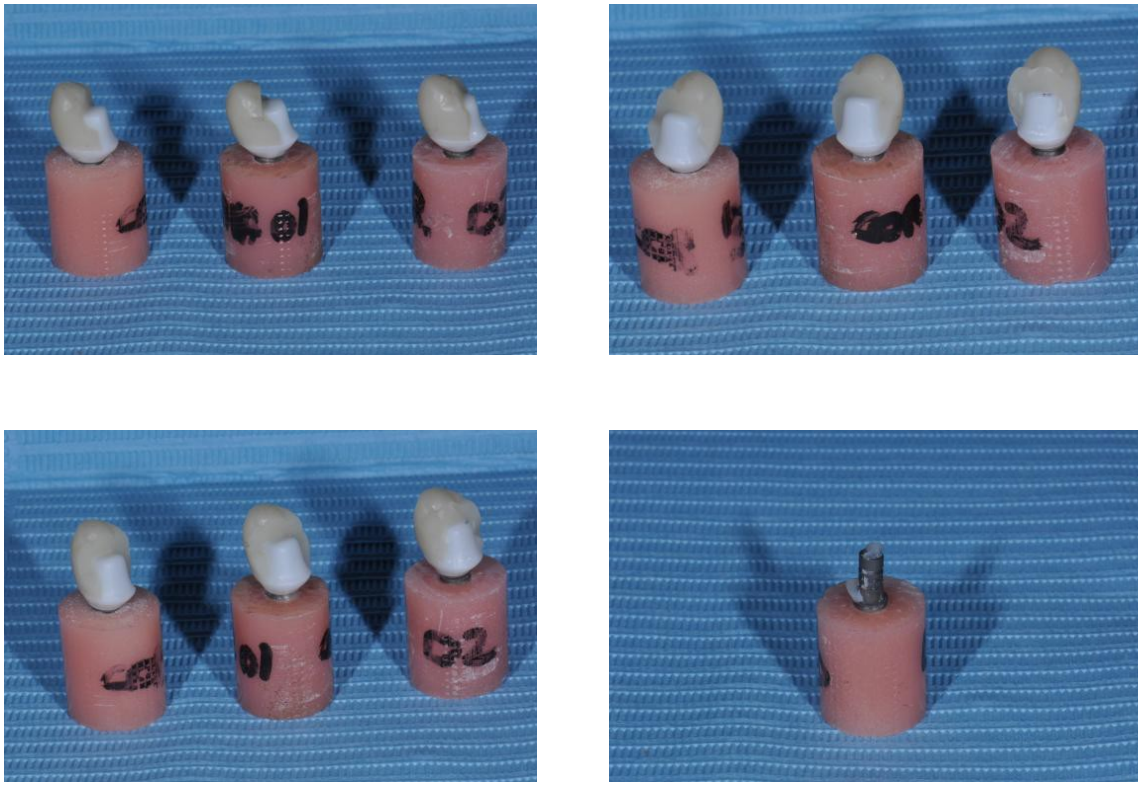

Figure 5.8: Note the lower left implant has no crown, because il was made just with Lava which bursted away after the rupture. In the first three picture are present the broken Lava + Zirconia samples.

As can be seen from the table the average value of rupture of the samples (Figure 5.7), consisting of zirconia abutment and superstructure Lava Ultimate is higher than the whole Lava group.

Should also be noted that the mode of fracture was substantially different; in the case of Lava Ultimate crowns fracture was partial in all cases and was not interested in the abutment in zirconia, in the case of samples consisting of a single material the fracture was always complete and happens like for glass.

5.2-Fatigue tests.

Skipping the first 5000 cycles of each specimen, which work just as adjustment, are highlighted the slopes of the force-displacement curves, that is representative of the modulus of elasticity.

With different colors are shown 10 cycles every 10000 and intuitively curves shifted to the right are those of subsequent cycles.

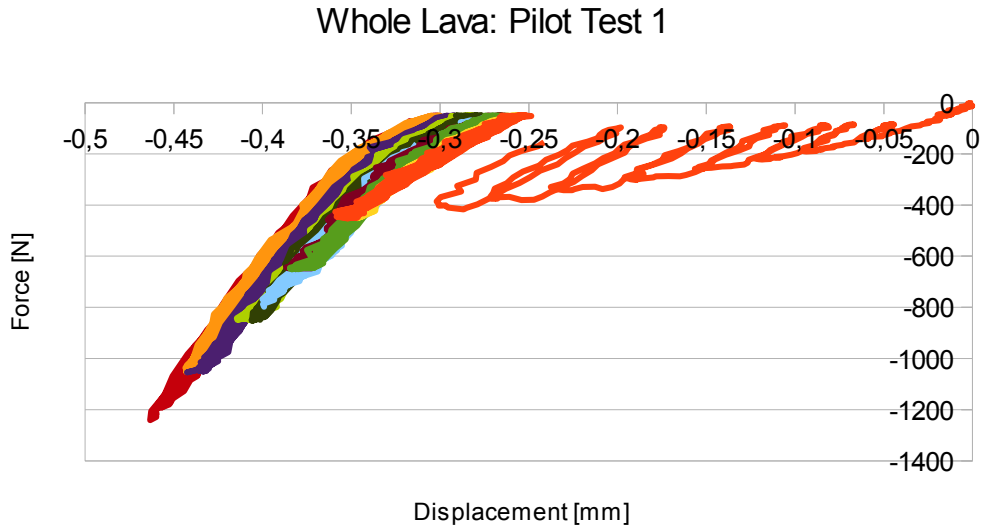

Figure 5.9: This sample broke in the early cycles of step 1250 N, then after the 109,000th cycle.

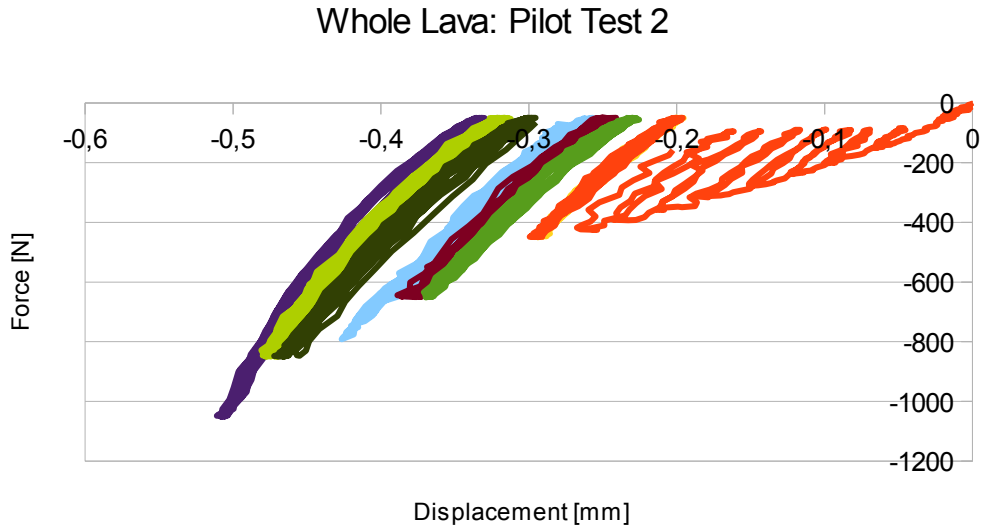

Figure 5.10: This specimen broke instead in the 1050 N step , the cycle after 91000.

Figure 5.11: This was the weakest of all the sample, it broke when subjected to a compression of 850 N after the 65000th cycle.

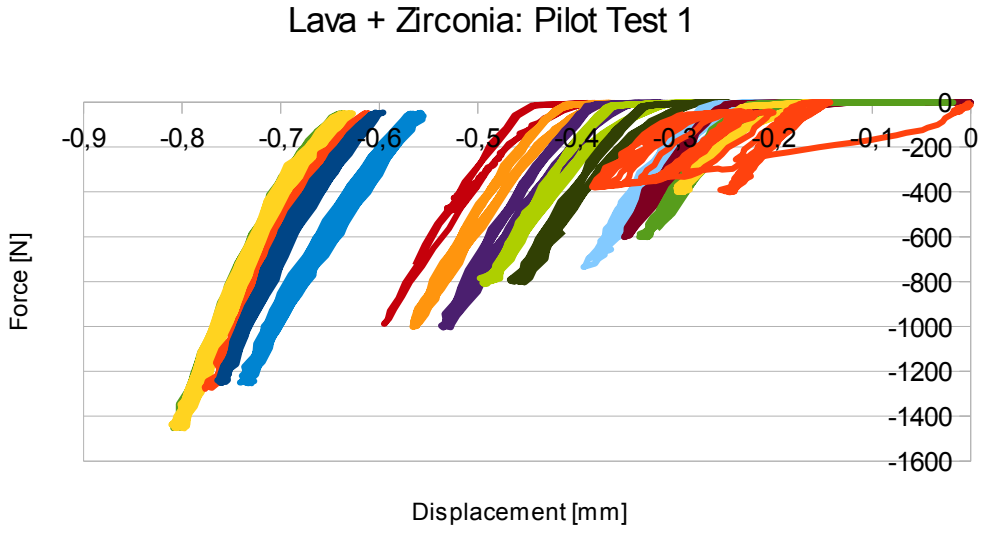

Figure 5.12: The first Lava + Zirconia specimen has been the subject of problems; the procedure was not appropriate and the values of the PID were not adequate. It can be immediately noted in the graph that the procedure has been interupted and besides, always in the graph, it is still more visible the hammering effect which manifests itself with a return to the point with coordinate (0 N; 0mm).While the punch is detached from the sample, the latter is then discharge and the load cell registers no load, instead the position sensor of the punch gets a large variaton of displacement.

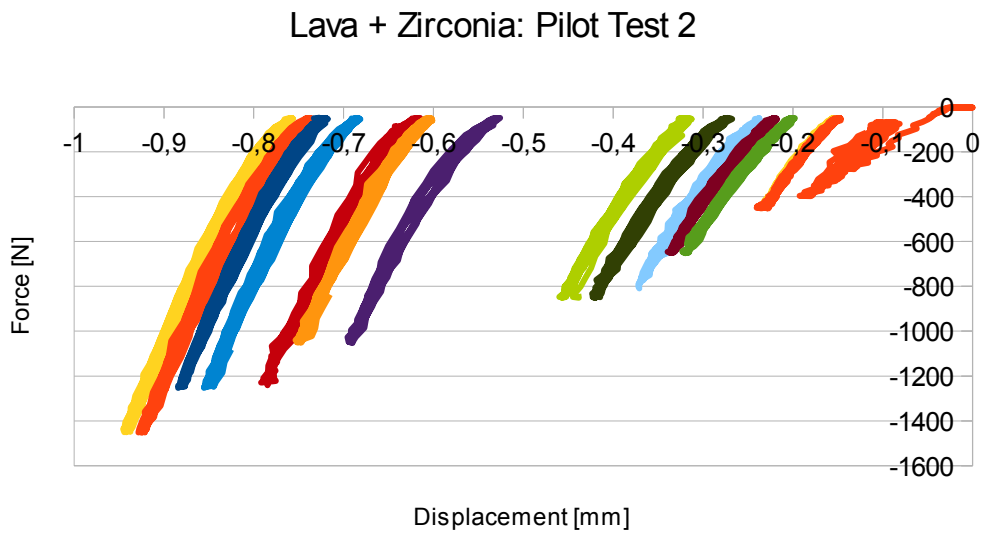

Figure 5.13: Here the specimen underwent to an obvious yielding, but has not led to serious consequences. Probably this is due to the base resin of the implant that may have had cavities porous and pliable. The implant has, however, responded with an adaptation without compromising the life of the specimen.

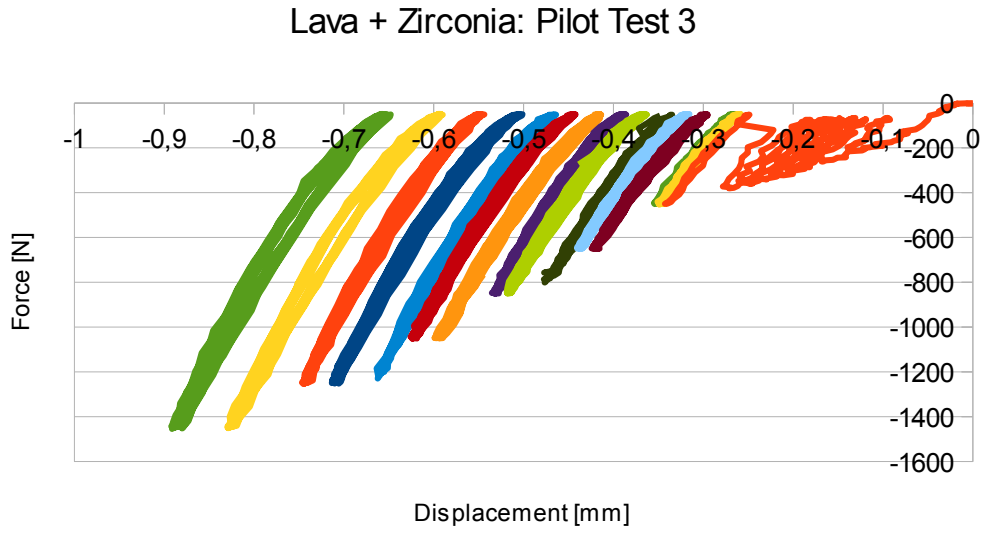

Figure 5.14.

5.3 Images and 3D models of the intact samples captured by tomography.

The images and 3D models captured by tomography, are useful to understand the geometry inside the specimen. Were reconstructed all geometries of all the components of the two types of specimens and emerges from the images of middle sections the reasons for which the whole Lava specimens have smaller life (in terms of number of cycles) and a UTS.

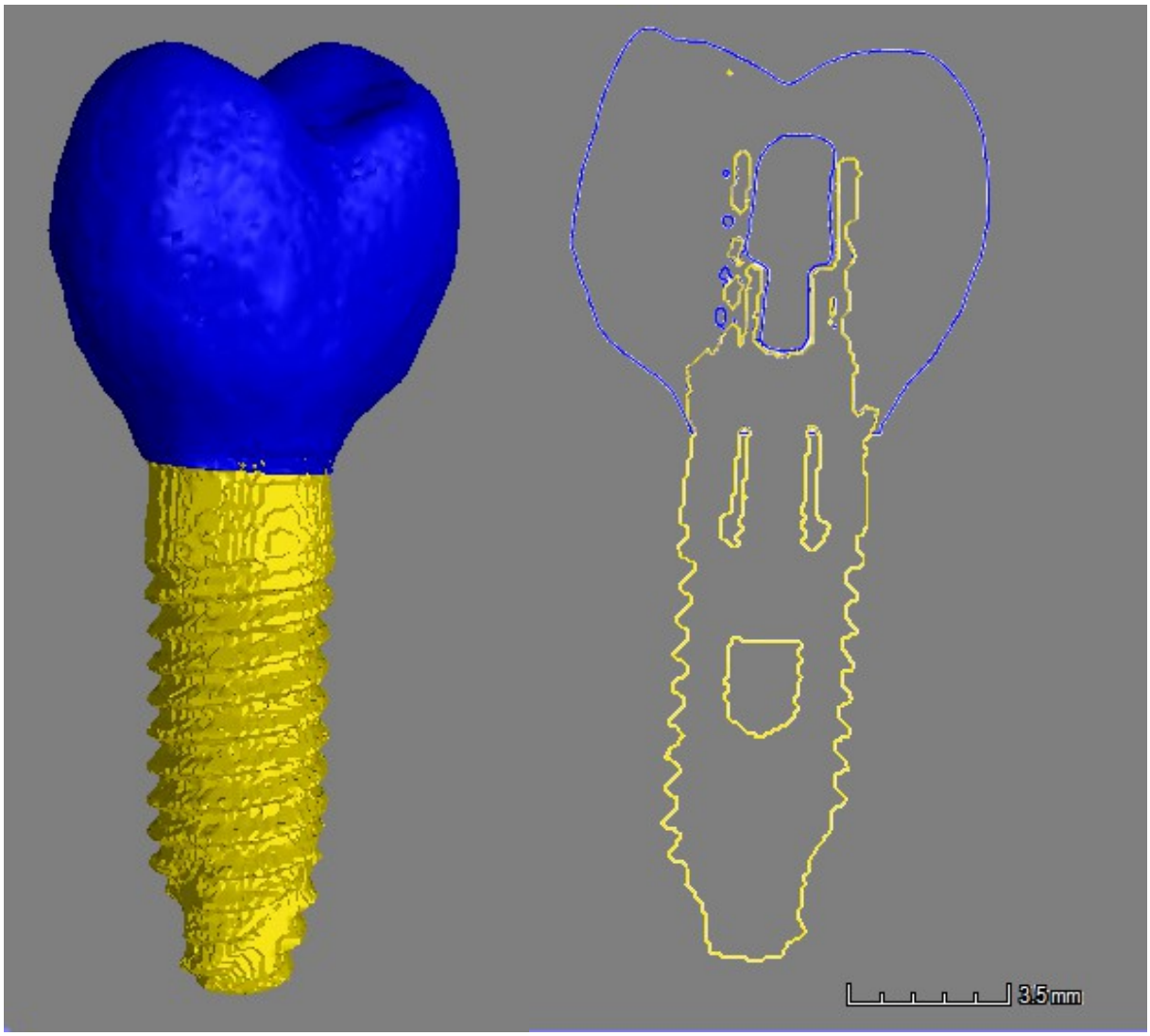

Figure 5.15: Lava sample tomography. The distance between the central fossa and the titanium implant is about 1,6 mm.

In this case the geometry is such as to generate local stress in Lava near titanium implant; these stress certainly are not felt in the early cycles of the head to fatigue, but beyond a certain limit after which the specimen was already fatigued by previous cycles, these stress are sufficient to generate cracks which then propagate to break the specimen.

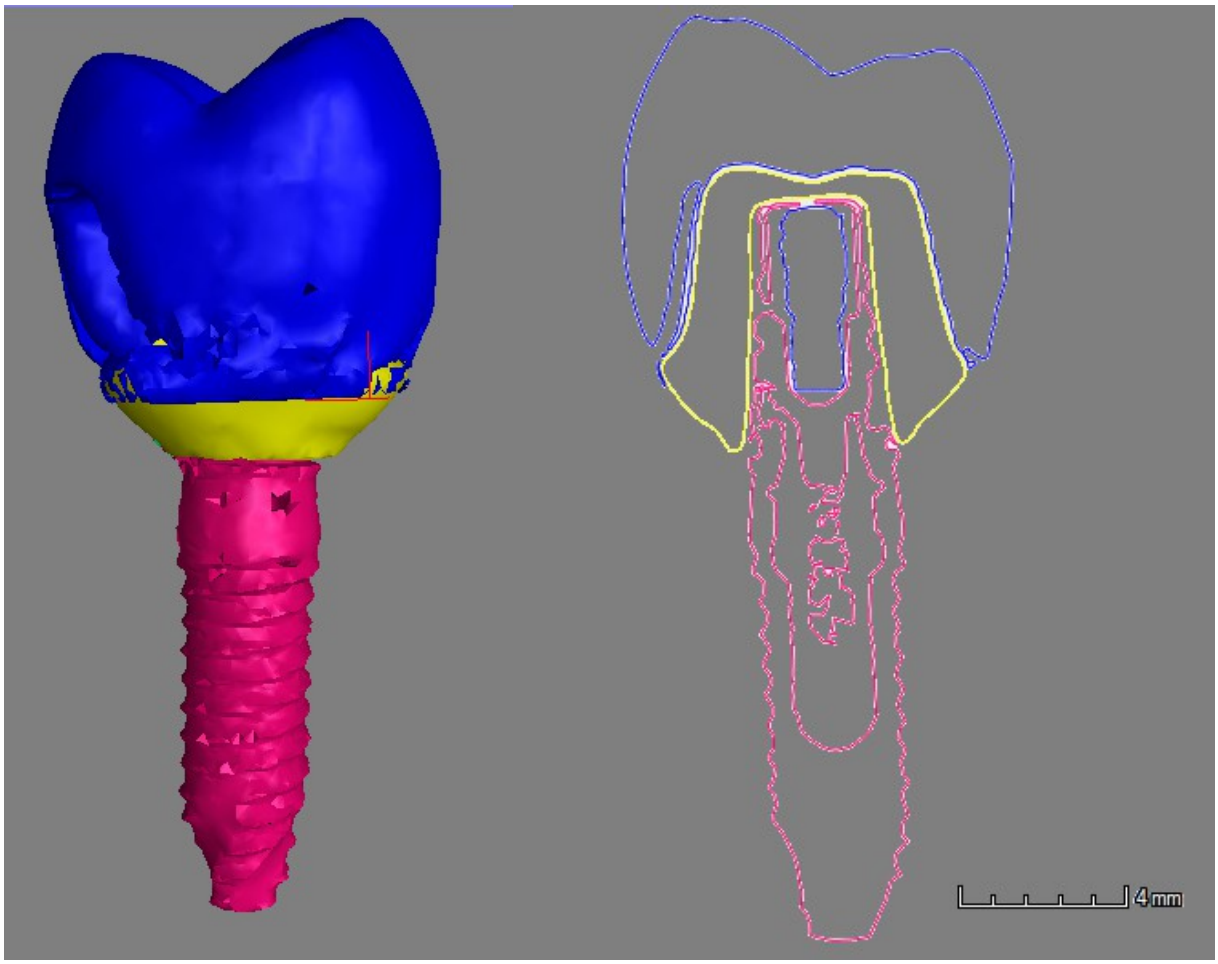

Figure 5.16: £d model of a Lava + Zirconia Specimen. Here is noticeable the zirconia abutment, which permit to unload the Lava from local stresses.

The zirconia abutment, interposed between Lava crown and titanium implant, makes the geometry slightly bigger. The distance of the central fossa from the titanium implant in fact is about 3.17 mm; so the stresses in the specimen have minor gradient, also because the load application point is farther from the implant.

Another effect makes the average life of this specimens geometry longer; the solution with two kind of material permit to unload the Lava one. The stress will be distribuited on a

larger interface area, instead for the solution with a direct contact of the Lava to the implant, where the latter act like a counterpunch, with sharp edges which make locally high stresses.

CONCLUSIONS

In the present study, the number of samples is not sufficient to make a statistical analysis of the survival rate of the fatigue tests.

With the limits dictated by the number of samples and the nature of the experiment can arrive at the conclusion that the initial choice of a prosthesis in two components is mechanically superior to that formed by a single material.

The samples made with the substructure Lava Zirconia, coated with Lava Ultimate have not presented macroscopic damage to the fatigue test, succeeding all, to get to the end of the protocol (180,000 cycles with increasing load up to a maximum value of 1400 Newton load).

None of the samples manufactured entirely in Lava Ultimate has instead led to the end of test fatigue stress. In fact, all the samples were broken at a load considerably lower compared to the maximum load resistance theoretical recorded in static test of breakage of the samples. The type of fracture observed is complete, type of glass and left completely exposed the titanium abutment.

The different behavior in the two groups of samples in the dynamic tests is essentially due to the geometric morphology of the two prosthetic.

In group one fact, thanks to the morphology of the zirconia, free of sharp edges, the applied forces are distributed evenly on the abutment and to them have been discharged vertically on implant, avoiding the formation and propagation of cracks in level of the superstructure.

Such morphological feature in the coupling of the parties, has led to a greater resistance to mechanical stress of the fatigue test.

In the second group the forces applied to the occlusal focused on the apex of the titanium abutment, which then acted as a wedge with respect to the crown in Lava Ultimate, strength agent was discharged in a non-optimal on titanium abutment, creating a mechanical condition that led to the creation of cracks which increased dimensionally during load cycles, until lead to rupture of the sample.

It is therefore the shape of the titanium abutment to determine the premature failure of

the samples and not the material itself, which as the static and dynamic tests have shown, are in line with data reported in other similar works published in scientific reading.

It remains interesting, for a future continuation of the work, hoe the analysis as the size and structural morphology of the titanium abutment affect the mechanical characteristics of the monomaterial samples and the possibility of studying a form that decreases the propagation of cracks in the prosthetic structure.

REFERENCES

- Liang-Ju Ning, Yi Zhang, Xiao-He Chen, Jing-Cong Luo, Xiu-Qun Li, Zhi-Ming Yang, Ting-Wu Qin; "Preparation and characterization of decellularized tendon slices for tendon tissue engineering"; Wiley Online Library; 2012-
- Shyam S. Raghavan, B.S., Colin Y.L. Woon, M.D., Armin Kraus, M.D., Kai Megerle, M.D., Matthew S.S. Choi, M.D., Brian C. Pridgen, B.S., Hung Pham, B.S., and James Chang, M.D; "Human Flexor Tendon Tissue Engineering: Decellularization of Human Flexor Tendons Reduces Immunogenicity In Vivo"; TISSUE ENGINEERING: Part A Volume 00, Number 00; 2011.
- J. M. R. Tilley • S. Chaudhury • O. Hakimi • A. J. Carr • J. T. Czernuszka; "Tenocyte proliferation on collagen scaffolds protects against degradation and improves scaffold properties"; Mater Med; 2011.
- Colin Y. L. Woon, M.D. Brian C. Pridgen, B.S. Armin Kraus, M.D. Sina Bari, M.D. Hung Pham, B.S. James Chang, M.D.; "Optimization of Human Tendon Tissue Engineering: Peracetic Acid Oxidation for Enhanced Reseeding of Acellularized Intrasynovial Tendon"; www.PRSJournal.com; 2010.
- Adapted by R. Lakes from D. Thelen and C. Decker; "Biomechanics Material Properties of Tendon"; U. Wisconsin; '09.
- Tishya A.L. Wren, Scott A. Yerby, Gary S. Beaupré, Dennis R. Carter; "Mechanical properties of the human achilles tendon"; www.elsevier.com/locate/clinbiomech; 2000.
- P. Kannus; "Structure of the tendon connective tissue"; Scandinavian Journal of Medicine & Science in Sports; 2000.
- Matteo Marchiori, Bruno Atzori, Nicola Petrone; Analisi strutturale di moderni metodi di fissazione nella ricostruzione del legamento crociato anteriore; Università degli studi di Padova; 2000-2001
- Stefano Tudini, Bruno Atzori, Nicola Petrone, Matteo Marchiori; "Analisi delle caratteristiche meccaniche di modelli biologici di trapianto e di materiali sintetici utilizzati nella ricostruzione del legamento crociato anteriore; Università degli studi di

Padova; 2001-2002.

- Davide Casarin Casarin, Marco Calabrese , Edoardo Stellini, Lorenzo Graiff, Roberto Meneghello; “Valutazione delle caratteristiche morfologiche di superficie e meccaniche di resistenza a fatica di una resina nanoceramica impiegatacome materiale da rivestimento su pilastri implnatari in zirconia”; Università degli studi di Padova; 2013.

ACKNOWLEDGEMENTS

Non poteva mancare una sezione dedicata al ringraziamento delle persone che mi hanno aiutato a percorrere questa strada lunga ed impegnativa.

Ringrazio in primis i miei genitori e mio fratello che mi ha aiutato e supportato fino in fondo anche nei momenti più difficili della mia carriera universitaria.

Ringrazio tutti gli amici e le persone dell'aula studio Pollaio di padova che nell'ultimo anno sono stati degli ottimi aiutanti per superare tutti gli ostacoli incontrati, ma soprattutto sono stati un'ottima compagnia di studio e di divertimento nella pause tra un libro ed un altro.

Un ringraziamento particolare anche al professore Nicola Petrone e a Tiziana Martinello che mi hanno aiutato nella stesura della tesi e mi hanno permesso quindi di puntare le mie energie su un argomento che mi affascinava molto.

Un ringraziamento finale ai colleghi del Laboratorio di ingegneria industriale di Padova, che, quando ho incontrato delle problematiche e dei dubbi, sono sempre stati disponibili ad aiutarmi a chiarire qualsiasi perplessità.

PROJECT TABLES

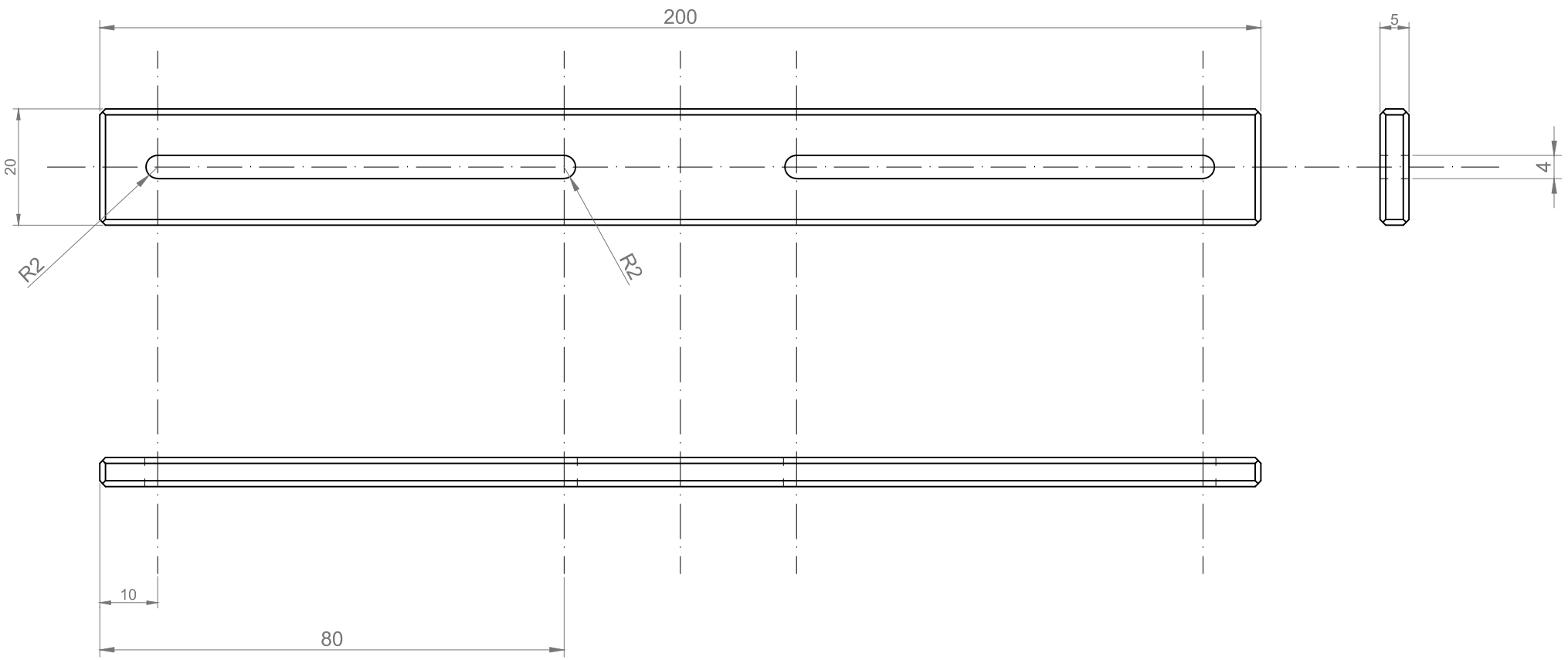

SMUSSI NON QUOTATI 1 X 45°

1:1						
ASTA DISTANZIATRICE						
				Alluminio 6082		

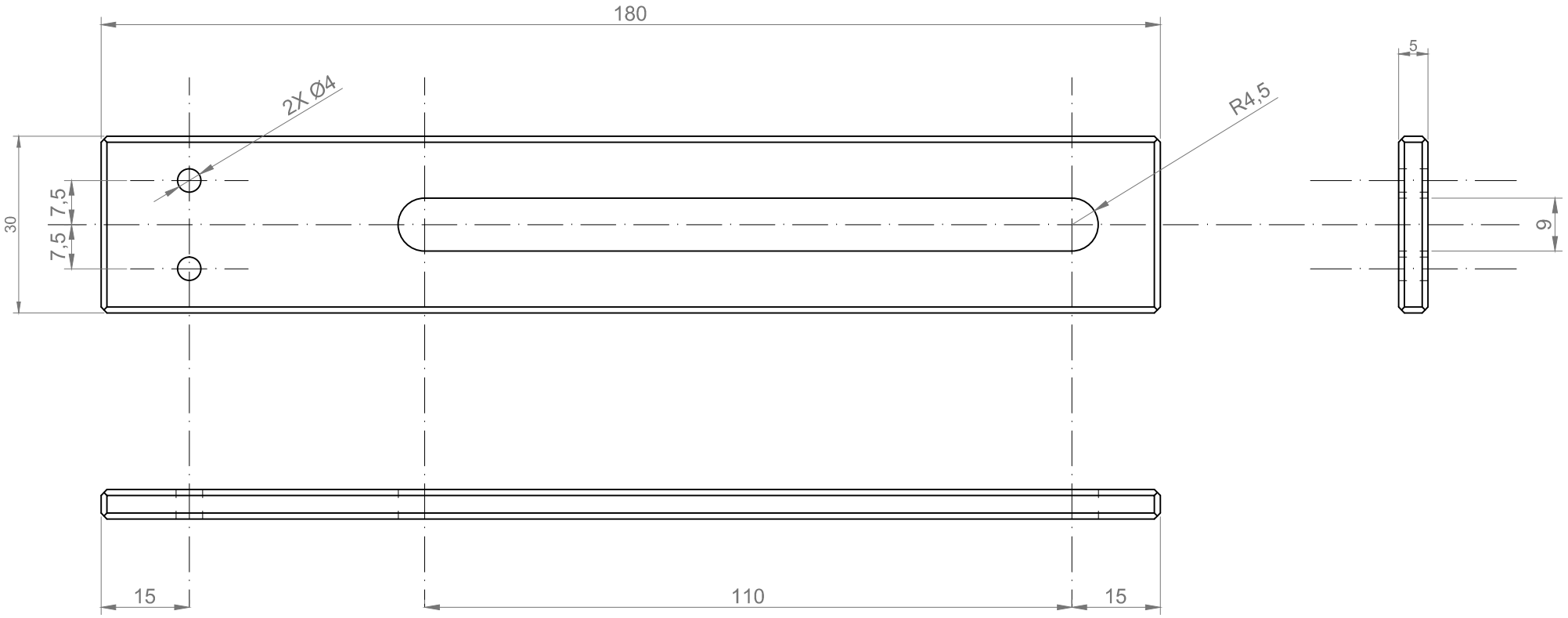

SMUSSI NON QUOTATI 1 X 45°

1:1						
ASTA PORTAPULEGGE						
				Alluminio 6082		

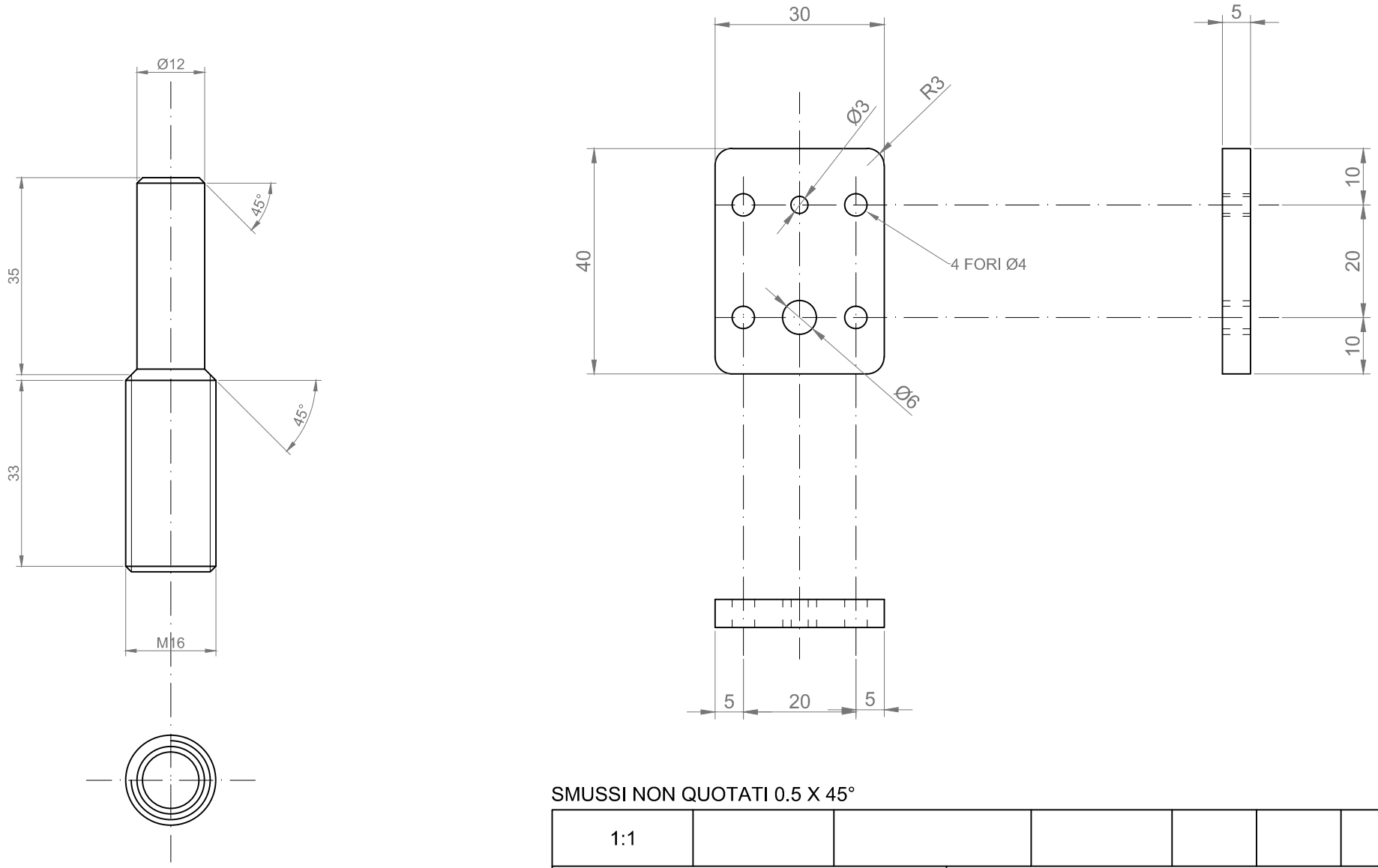

SMUSSI NON QUOTATI 0.5 X 45°

1:1						

CILINDRO DI SOSPENSIONE E COPERCHIO	
	Alluminio 6082

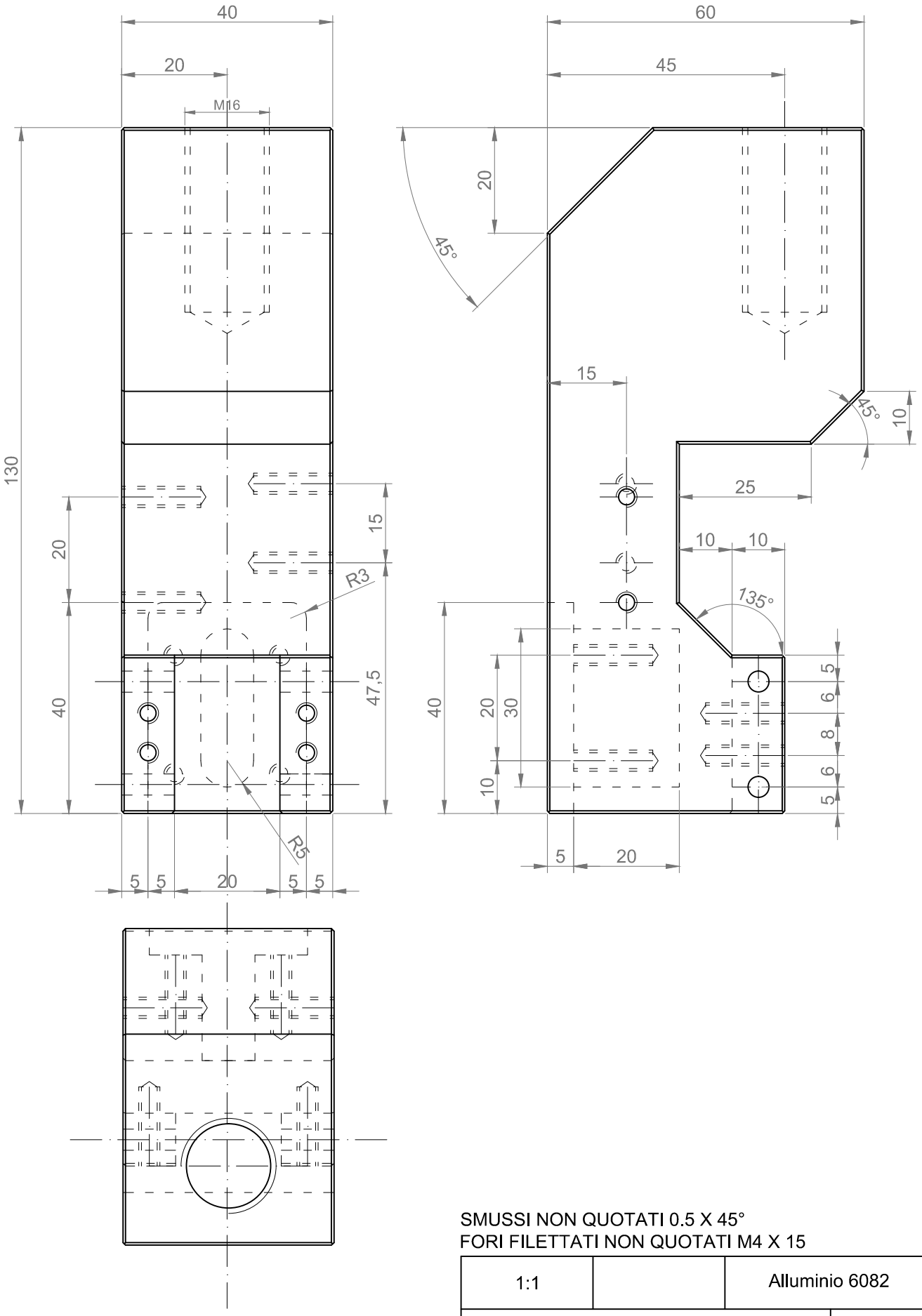

SMUSSI NON QUOTATI 0.5 X 45°
FORI FILETTATI NON QUOTATI M4 X 15

1:1		Alluminio 6082
CORPO CENTRALE		

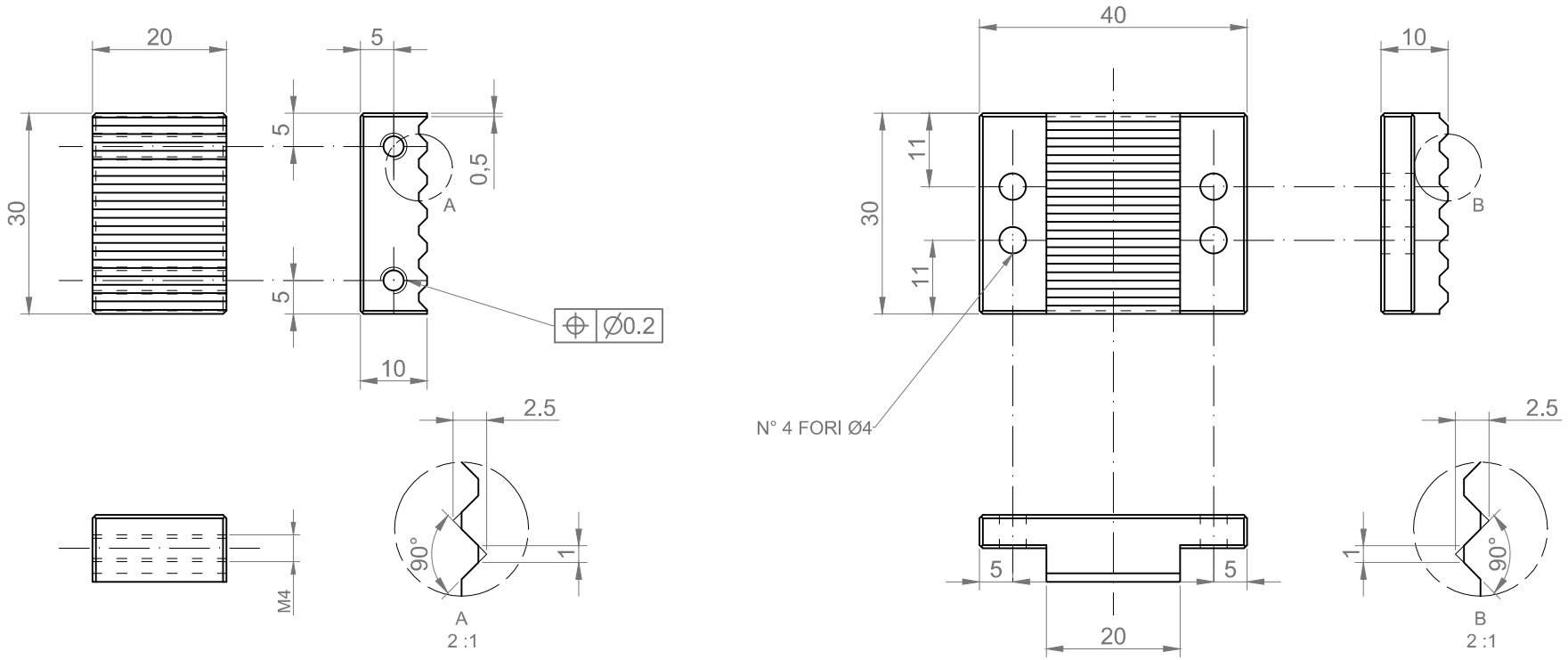

SMUSSI NON QUOTATI 0.5 X 45°

1:1						
PIASTRA FISSA E PIASTRA MOBILE						
				Alluminio 6082		

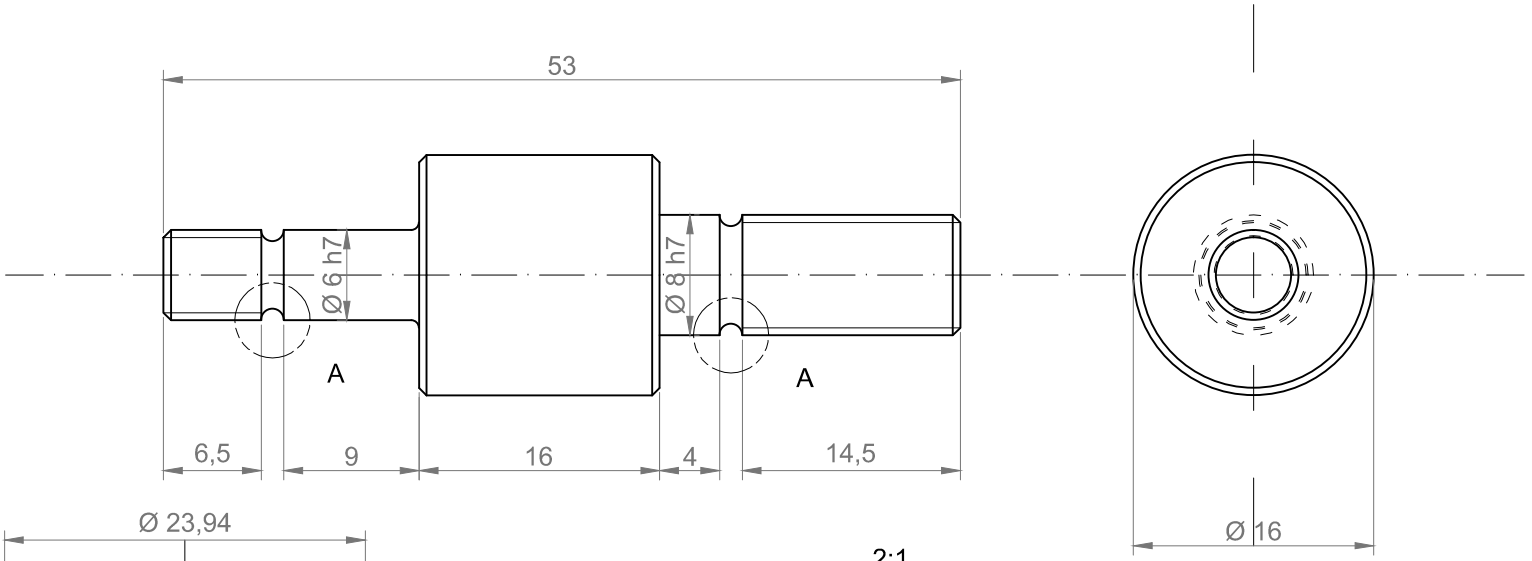

2:1
PERNO (C40)

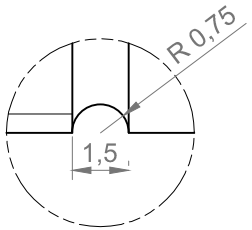

A
5:1

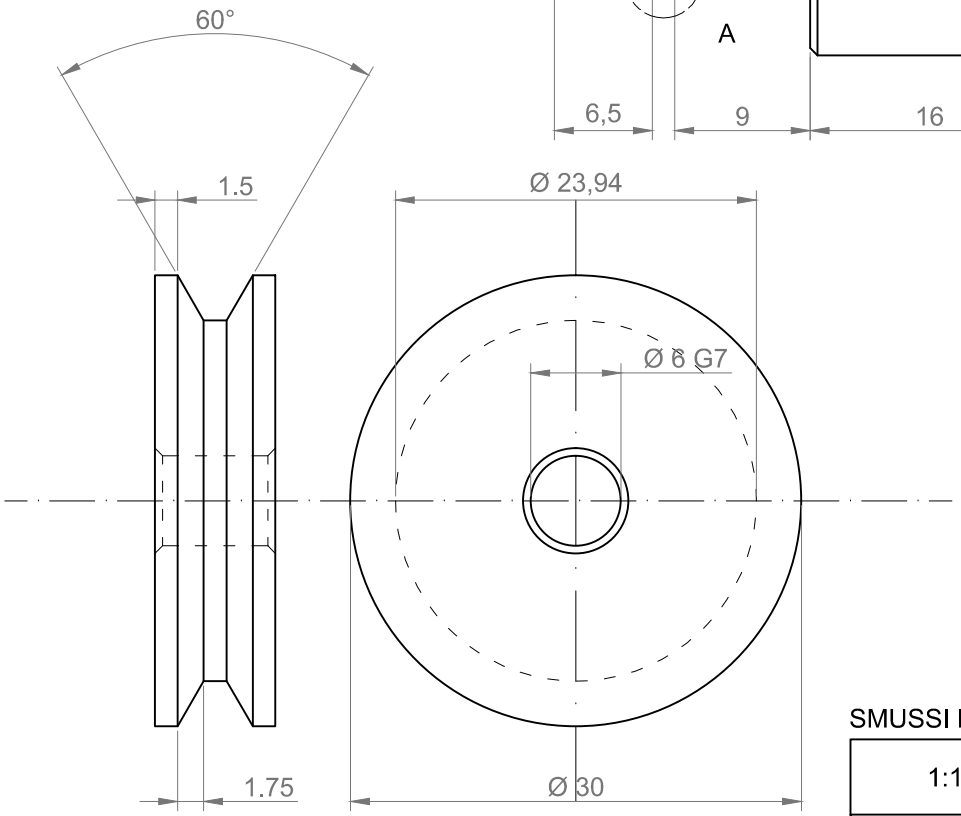

2:1
PULEGGIA (Allumino 6082)

SMUSSI NON QUOTATI 0.5 X 45°

1:1						
PULEGGE E PERNI						
				Alluminio 6082		